COMPARATIVE STUDY OF WIND GUSTS: DETECTION TECHNIQUES AND TERRAIN SPECIFIC FEATURES

Masters of Science Thesis

For obtaining the degree of Master of Science in Aerospace Engineering at Delft University of Technology

Nouman Zahoor Ahmed.

Date: November 30, 2015.

Wind Energy Research Group, Faculty of Aerospace Engineering, Delft University of Technology

DELFT UNIVERSITY OF TECHNOLOGY

FACULTY OF AEROSPACE ENGINEERING

The undersigned hereby certify that they have read and recommended to the Faculty of Aerospace Engineering for acceptance, the thesis titled “Comparative study of wind gusts: Detection techniques and terrain specific features” by Nouman Zahoor Ahmed for the fulfillment of the requirement for Master of Science Degree in Aerospace Engineering.

Date: November 30, 2015.

_____

Prof. Dr. G. J. W. Van Bussel
(Chairman, Head of the Dept.)

_____

Dr. Ir. W.A.A.M. Bierbooms
(Supervisor)

_____

Dr. Ir. M. I. Gerritsma
(Reader)

SUMMARY

In this research work, the phenomenon of extreme wind events or gusts has been studied in detail and different aspects related to the nature of gusts are explored.

In order to detect wind gusts from a stochastic time series different gust detection techniques collected from previous research works and literature studies were compiled, refined, verified and compared against each other. In addition some important insight is also given regarding the setting up of appropriate values for various gust defining parameters.

The gust detection techniques are developed into computational codes and applied over different data sets. A comparison between these techniques highlights the pros and cons of each one of them. The peak to peak method and the velocity increment method provides accurate information about the maximum wind speed acceleration within a small time interval. Other methods like peak over threshold and the acceleration over threshold methods are useful to detect specific type of wind gusts above a certain threshold.

Wind data sets sampled at high frequency resolution and from different geographical locations were obtained and analyzed through these gust detections algorithms. Among these locations are the offshore wind farm at Egmond aan Zee (OWEZ), IJmuiden and the Cabauw Experimental Site for Atmospheric Research (CESAR) which are a representative of a near offshore, far offshore and an onshore location respectively. By using a uniform gust threshold criteria for peak over threshold and acceleration over threshold methods, a comparison between different locations reveal that the maximum gusts were detected for IJmuiden which generally has higher wind speeds throughout the year.

For each location, the total number of gusts detected have been combined to obtain a mean gust shape. Furthermore, the maximum wind gusts are selected from each month and compared with the standard IEC gust shapes.

The available high resolution wind data is for a duration of 1 year only which is not sufficient for the prediction of a maximum 50 year gust. However two different approaches are discussed to demonstrate the procedure. A statistical approach involving the extrapolation of data to predict the amplitude of maximum 50 year gust highlights the need for the availability of long term wind data. The analytical approach involving the calculation of the return period of different gusts is also explained and the results presented within this report are promising to continue further research within this domain.

The techniques, findings and conclusions obtained through this research work can be further tested and eventually utilized to compliment or improve upon the existing extreme load cases of the wind turbine design standards.

ACKNOWLEDGEMENTS

I would like to thank my supervisor Dr. Wim Bierbooms for his time and help with arranging the meetings. I am also thankful to Prof Dr. G. J. W. Van Bussel and Dr. Mark Gerittsma for being a part of the assessment committee.

The completion of this research work required high resolution meteteorological mast data for different locations. I am thankful to PhD researchers Rene Bos and Maarten Holtslag for providing me with their assistance to acquire the data sets for Offshore Wind Farm Egmond aan Zee (OWEZ) and IJmuiden. The research work performed by Maarten Holtslag to incorporate tower shadow effects was extremely useful for the proper and accurate selection of wind data from the data sets.

I am highly grateful to Fred Bosveld from the Royal Dutch Meteorological Institute (KNMI) for providing me with high resolution sonic data from the Cabauw Experimental Site for Atmospheric Research (CESAR) database.

I would also like to thank my father for his immense financial support especially due to some unfortunate circumstances I had to endure during the completion of my graduate program. Finally I am thankful to all the people who have interacted with me in any capacity as they have helped me to become what I am today. I cherish the valuable knowledge and experiences gathered during my stay in Delft and consider this period as an important chapter among my life experiences.

Table of Contents

TABLE OF FIGURES

NOMENCLATURE

A: scale factor for weibull distribution

a: coefficient for defining the MCP variance method

b: coefficient for defining the MCP variance method

c: maximum gust variation

D_L: lapse time

D_{time}: dynamic component of a time series

D_t: gust rise time

DU: gust relative amplitude

d: duration threshold for the gust

d_{max}: maximum duration for the gust

F_{req}: minimum required sampling frequency (based on Nyquist rule)

$f_{Nyquist}$: maximum frequency that needs to be measured in the signal

f_η: return frequency

K: shape factor for weibull distribution

N: number of 10 minute (or hourly) observations

N_{time}: stochastic component of a time series

m_0: first order moment or variance

m_2: second order moment

T_η: return period

T_z: return period from the actual time series

U_{avg}: average value for 10 minute wind speed

u_{inst}: instantaneous wind speed (sum of the average and the fluctuating components)

u': longitudinal component of turbulent velocity fluctuations (in the direction of wind)

$u(z_1)$: known wind speed at the reference height z_1

$u(z_2)$: desired wind speed at the height z_2

v': lateral component of turbulent velocity fluctuations (normal to the average wind direction)

V_{ref}: reference wind speed

V_{50}: maximum 50 year gust

V_1: maximum annual gust

w': vertical component of turbulent velocity fluctuations

X: amplitude threshold for the gust

X_t: stochastic time series

$z_\circ$: surface roughness length

μ_r: mean wind speed at the reference site (MCP method).

μ_c: mean wind speed at the candidate site (MCP method).

σ_r: standard deviation at the reference site.

σ_c: standard deviation at the candidate site.

τ: characteristic time (time scale for a stochastic process

η: amplitude threshold on a time series.

1. INTRODUCTION

The field of wind meteorology has developed significantly over the last few decades. From the perspective of harvesting wind energy, the knowledge of wind and site conditions contributes toward a better understanding of the environments in which the wind turbines operate. It not only contributes towards better energy extraction from the wind, but also ensure the safe, efficient and economical design of the wind energy systems.

Wind turbines are subjected to a variety of loading situations during the course of their lifetime which they should be capable of withstanding for their effective and safe operations. These loading situations can be broadly classified as the fatigue load and the extreme load scenarios. A set of well-defined fatigue and extreme load cases are often included in the existing design standards for wind turbines. The most widely recognized and reputable of these standards are the IEC design standards 61400. Majority of the wind turbine manufacturers throughout the world comply with these standards to ensure the safety as well as the certification of their proposed designs.

Most of the current design standards (for example IEC 61400) defines the fatigue load cases using a real wind time series from the actual site data which incorporates the stochastic (random) properties of the atmospheric turbulence. However the extreme wind load cases are defined in a rather deterministic way which, in principle, is incorrect because the occurrence of extreme wind gusts is also stochastic (random) in nature.

Therefore, in order to understand the nature and occurrence of wind gusts, there is a strong requirement to come up with new innovative methods to extract maximum wind events from a long wind time series. These techniques would help to better evaluate the extreme wind load cases during the design phases of the wind turbines and wind farms.

The basic aim of this study is the development of different gust detection algorithms in the form of a programming code. Different gust detection methods identified during the literature study are programmed using Matlab and further refinements have been made as per requirements. A primary focus is made on the verification, reliability and validity of gust detection algorithms.

The phenomenon of gusts maybe defined differently depending upon the choice of criteria and application under consideration, hence the gust detection algorithms are programmed in a rather general way. The users (for e.g. a wind turbine or wind farm developers), depending upon their specific project requirements, would be able to re define the criteria of the extreme wind gusts and modify the algorithm accordingly. General guidelines have been provided for doing that in the user guide for the algorithms.

Furthermore, it remains an area of interest in the field of wind meteorology to compare different geographical terrains and analyze their potential for extracting wind energy. The wind speeds are significantly higher at offshore locations and the behavior in terms of seasonal and diurnal (daily/hourly) variations of the wind speeds is also different. Therefore, it is immensely important to explore how their gust patterns differ in comparison to the onshore locations.

In broader perspective, the ultimate objective is to provide different gust detection techniques for the accurate estimation of wind turbine load calculations and also identify and compare the pros and cons of each of these methods.

Although the basic motivation for this research is to correctly estimate the extreme wind gusts acting upon a wind turbine during the course of its life time but a better understanding of methods to detect wind gusts can be useful in a variety of other applications as well.

2. RESEARCH QUESTION, AIMS & OBJECTIVES

The primary objective of this research work is to detect the extreme wind events or gusts utilizing different gust detection techniques and to study and analyze the gust characteristics in detail for different geographical locations.

The research topic can be best described as, "A comparative study of the nature and characteristics of wind gusts at different geographical locations using various gust detection techniques for the estimation of wind turbine extreme load calculations."

Hence the main research question that needs to be answered is, "**What are the characteristics of wind gusts at different locations, and what are the unique findings, advantages and limitations of using different gust detection techniques?**"

In order to achieve a comprehensive answer to the above main research question, a number of sub questions would be dealt with.

1. What is the appropriate time scale for detecting wind gusts?
    a) What should be an appropriate autocorrelation function defining stochastic wind?
    b) What should be an appropriate time scale for different gust detection algorithms keeping in view the data set size and the computational resources? Or what should be the optimum sampling frequency for wind data.
2. What are the relevant gust parameters that can be detected through different gust detection algorithms?
    a) What is the pattern of different gust parameters like rising time, acceleration and duration etc. when detected through different gust algorithms?
    b) Which of these parameters are relevant to the load analysis of wind turbines? (optional)
3. Are the results of different gust detection methods reliable?
    a) Comparisons with a small test data set comprising of known gust values.
    b) Comparison with the similar previous study results if and whenever available.
    c) How reliable are different gust detection methods in terms of their accuracy when tested for different time duration or different gust criteria.
4. How to process and extract the relevant data from the given data set?
    a) Does the data acquisition system provides all the relevant data in the format desirable for gust detection algorithms? If not then what post processing and statistical techniques should be utilized?
5. What are the major differences between the offshore and onshore wind environments in terms of patterns of extreme wind gusts?

3. WIND MEASUREMENT AND INSTRUMENTATION

In order to perform the wind resource assessment at any location, detailed and accurate wind speed measurements are required for sufficient time duration. There is an additional requirement for a high sampling rate of wind data, if the study involves the analysis of wind gusts or any sudden fluctuations in the wind speed.

The details and accuracy of wind data is highly dependent upon the wind measuring instruments and the overall data acquisition system.

With reference to this particular research work, the data sets have been obtained from the meteorological masts installed at different locations. The met mast details are discussed in the next section along with site specific information for the reference data sets from Egmond aan Zee (OWEZ), IJmuiden and Cabauw.

The met masts at these locations are equipped with different wind measuring instruments. A basic knowledge of wind instruments is important for understanding the limitations of the wind data sets in general and it can further enable us to select the appropriate wind data from the data sets. A brief description is provided here about the working concept, accuracy and limitations of these wind measuring instruments.

3.1 Cup Anemometers

Cup anemometers are based on the principle of momentum transfer for measuring wind speeds. It consists of three or four cups placed on arms. The rotation of cups due to wind is directly proportional to the wind speed. The rate of rotation of cups can be measured either by mechanical counters registering the number of ticks, electrical signals (voltage changes) or via photoelectric switch counting the pulses generated due to the passage of the disc slots over a photocell.

The magnitude of variations in the cup rotational speed due to certain amount of change in wind speed is governed by the dimensions of the cups and the friction factors [1].

Resolution is the smallest unit of variable that is detectable by the sensor.

Limitations: Cup anemometers have limited resolution because rotations of the cups are measured by the data logger as "ticks". As it can only measure "ticks", so small values which could not produce complete rotations are not detected, thus limiting the resolution.

The accuracy of the cup anemometers is sometimes dependent upon the angle of attack and this instrument is also susceptible to the mechanical damage.

3.2 Sonic Anemometers

Sonic anemometers make use of ultrasonic sound waves to measure wind speeds and directions. Speed of the sonic pulses travelling between two transducers is directly related to the speed of wind. These anemometers can be used for measuring 1D, 2D and 3D wind speeds [2].

Advantages: Sonic anemometers are well suited for taking measurements at high frequency rates with a sampling rate up to 200 measurements per second. This makes them a much preferred choice for performing turbulence and gust studies. Furthermore they have no moving parts and there are no problems related to over speeding of the instrument.

Limitations: The downside of sonic anemometers is their higher cost and the dependency on temperature sensors which might affect the speed of sound.

3.3 Wind Vanes

Wind vanes are used for determining the wind directions during the measuring periods. Fig. [1] shows some pictures of these measuring instruments which are installed on the met masts at different locations studied during the scope of this project.

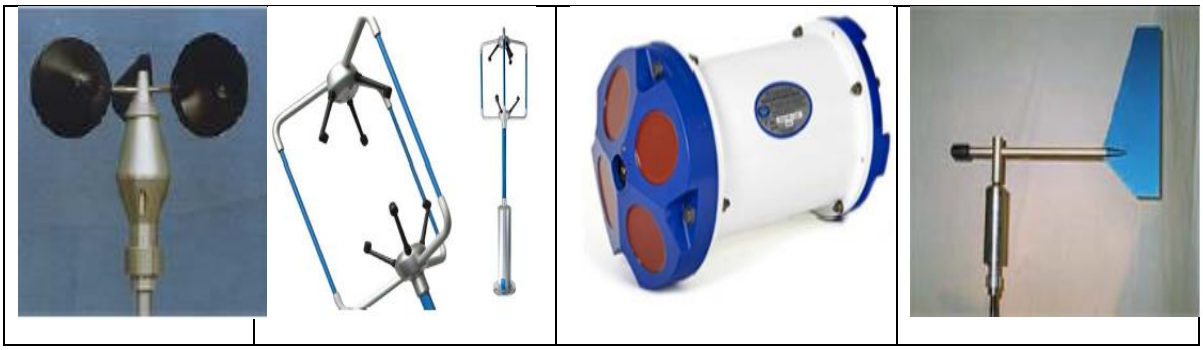

Figure 1: Wind Measuring Instruments. (From left to right) Cup anemometer, 3D sonic anemometer, ADCP, Wind vanes.

It should be noted that in terms of accuracy of wind measurements taken from different types of instruments, the availability of data for a longer period of time and the physical proximity of the source near the actual location is also equally important [3].

4. INTRODUCTION TO THE REFERENCE DATA SETS

Within the scope of this research, three different data sets have been used. All three of them comprises of meteorological masts data, representing onshore, offshore and far offshore locations respectively.

In the initial phase, the aim was to keep the gust detection algorithms flexible in a way so that the designed gust detection algorithms could modified during the execution of the programming code, depending upon the gust threshold criteria defined by the user. However, since the data sets used in this research work comes from different sources, the variations between their formats is quite significant. Therefore, any particular changes that needs to be incorporated into the gust detection algorithms for different data sets are mentioned in the user guide document for the assistance of the future users.

The data set obtained for near offshore location, Egmond aan Zee (OWEZ), is taken as reference data set for the initial setting up of gust detection algorithms and the explanation of met masts. Moreover, care has been taken to understand the specific features and limitations of all the data sets.

The OWEZ data set comprises of measurements taken over a period of one year starting from Jan 2008 till December 2008. Some of the specific details are discussed below.

4.1 OWEZ Site Information

The offshore wind farm Egmond aan Zee is located 10 to 18 km off the coast of Netherlands [4]. The wind farm comprises of 36 Vestas V90 turbines. The exact location of the met mast is in WGS 84 coordinates 52°36’22.9” N and 4°23’22.7” E, at the south western side of the wind farm as shown in the Fig [2].

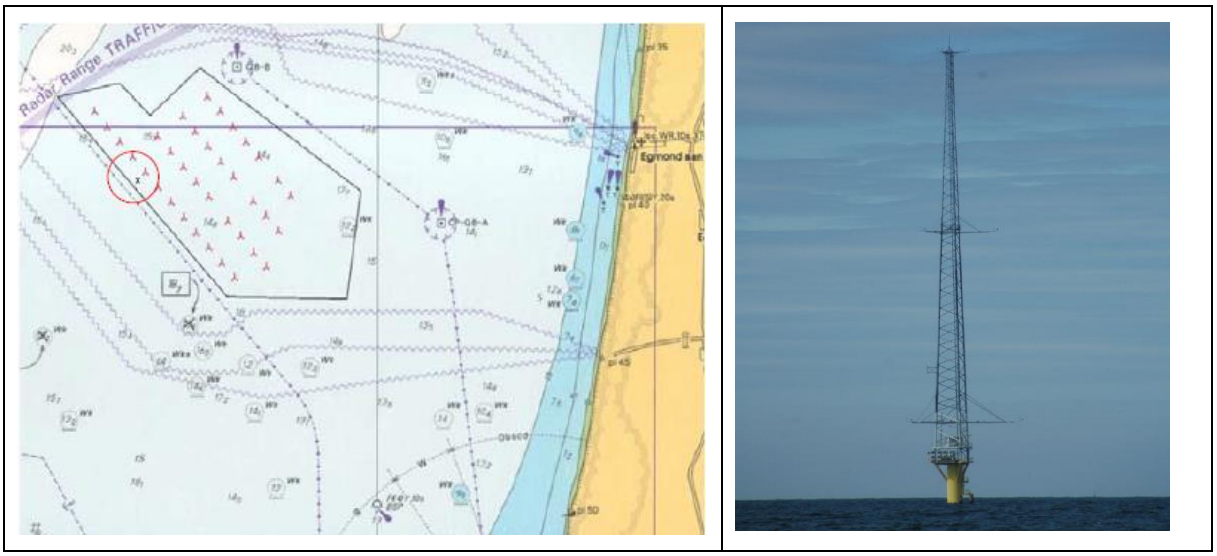

Figure 2: The OWEZ site location and the meteorological mast shown with a red circle on the map. Ref. [5]

The dominant wind direction is from south west. Fig [3] taken from a study conducted by Eecen [5] shows the distribution of wind rows during the measuring period from July 2005 to December 2007.

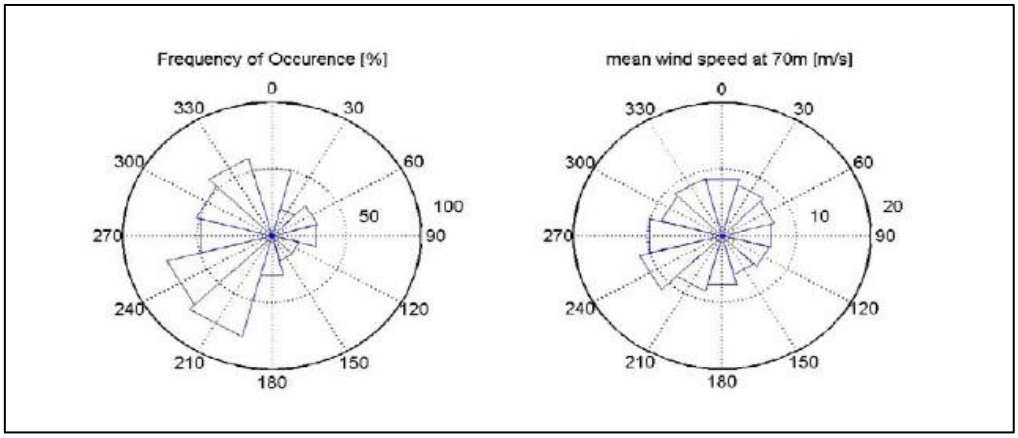

Figure 3: Overall wind speed frequency distribution at 70 m above MSL from July 2005 to December 2007. Ref [4]

The data for wind coming from this dominant direction could be chosen in different ways. Different factors needs to be considered in this regard. Based on the rough estimates such as the distribution of wind rows as shown in Fig. [3], the dominant wind direction may be chosen as **240 degrees** coming from south west. Later on detailed tower shadow effects can be implemented.

The Meteorological Mast and Instrumentation Details

The met mast at OWEZ is a lattice tower with measuring instruments installed at 3 different heights of **21.6 m**, **70 m** and **116 m** above the mean sea level (MSL). At each height, three booms are installed in the directions NE, S and NW at the following orientations.

Direction of the Boom	**Orientation (Degrees)**
North West (NW)	300
North East (NE)	60
South (S)	180

Table 1: The orientation of booms on OWEZ meteorological mast.

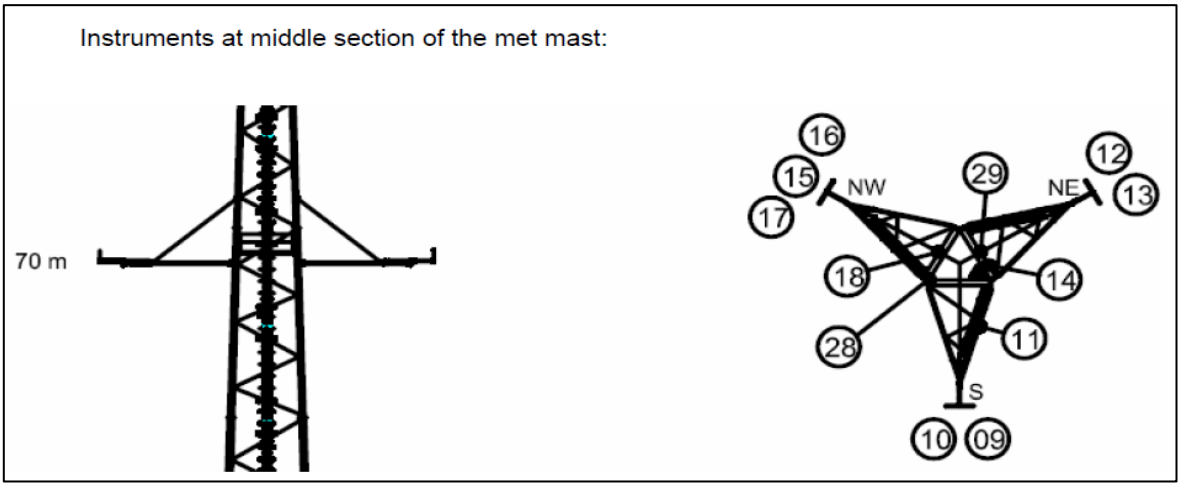

Figure 4: The orientation of booms at meteorological mast. Ref. [5]

Different types of measuring instruments are installed on the met mast. Table [2] provides a brief description of some of these devices which are important for studying wind gusts. The locations of these devices on the met mast are shown in Fig. [4] [5].

Signals from these measuring instruments are recorded into two parallel data loggers in the data acquisition system of the met mast. From there it is eventually sent to the shore via GSM cable. Data set of logger A is considered the leading dataset and is used for all the analysis.

A channel number is allocated to each instrument at a specific location as shown in Fig. [4]. There are **58 channels** in total, each of which correspond to a specific instrument code of Table [2]. It should be noted that the sonic anemometers are only installed at the NW boom of the met mast at OWEZ. Further details about the OWEZ site, the meteorological mast and instrumentation can be found from the references [4] [5] [6].

Instrument Type	**Location on Met Mast (XX/ Heights)**	**Instrument Specification**	**Instrument Code**
Cup Anemometers	NW,NE,S/ 21,70,116	KNMI anemometer model 018	WS 018/XX/height
Sonic Anemometers	NW/ 21,70,116	3 axis ultrasonic meteorological anemometer	3DWM4/XX/height
Wind Vanes	NW,NE,S/ 21,70,116	KNMI Wind vane model 524	WD 524/XX/height

Table 2: Brief descriptions of instruments installed at the met mast.

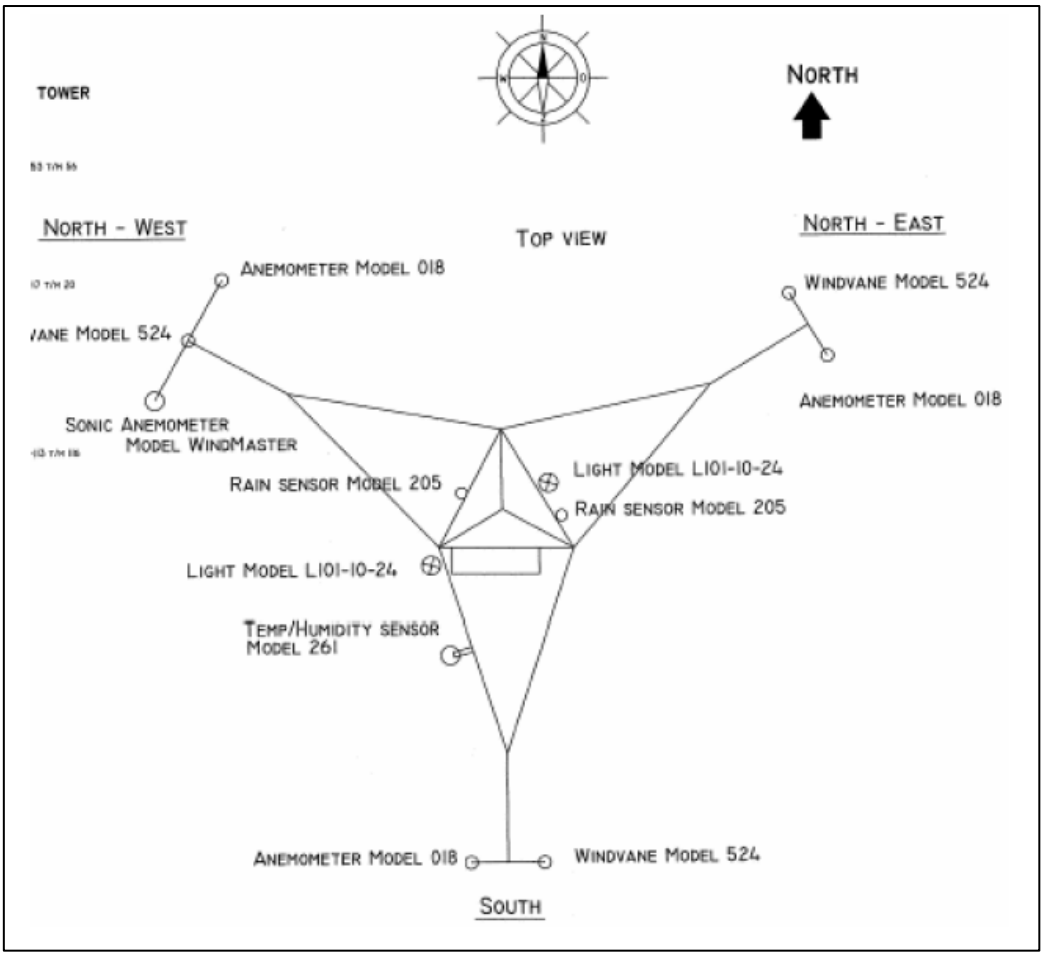

Figure 5: The locations of various wind measurement instruments on the met mast at OWEZ. Ref. [5]

Selection of Wind Measurement

For the selection of appropriate wind speeds from the data set, a careful analysis needs to be made considering a range of factors like dominant wind direction, availability of data, tower deflections and reliability of data to name a few. Ref [4] [5] provides details about the data availability and dominant wind direction etc. for OWEZ site. Two different methods are suggested here making this selection.

Method A

This method involves the selection of the dominant wind direction and the appropriate measuring height for the choice of wind data from the data set. The tower shading effects have not been considered at this stage.

Fig. [3] taken from Ref. [5] shows the wind rows for the OWEZ location during the measuring duration from July 2005 to December 2007. Based on the results, the dominant wind direction is chosen from south west at **240 degrees**. Fig. [6] from the same reference shows the detailed orientation of the booms on the triangular lattice tower.

Assumptions and Limitations.

Only the sonic anemometer data from the NW boom has been used because of its higher availability (around 98% of the time). Due to the underlying assumptions, this method is much simpler in terms of programming and it was used in the initial set up and verification of gust detection algorithms. For the detailed analysis, method B has been adopted.

Method B

This method involves the selection of dominant wind direction by incorporating some additional refinements and averaging rules considering the tower shadow effects and the orientation of the sensors on the booms.

To explain this method, let us consider the example when the incoming wind is from the dominant wind direction i.e. south west, at 240 degrees, as suggested in the previous studies [5] [7].

This implies that for accuracy, the contributions of wind speed measurements from the NW boom (inclined at 300 degrees) and the south boom (inclined at 180 degrees) should be average. If we divide the wind directions into six different zones, fig. [6] taken from ref. [5] indicates the dominant wind direction within **zone 5**, where an average of wind speeds from NW and S boom should be taken.

Table 2.3 *Detailed information to create the derived wind direction and wind speed based on wind direction.*

	Wind direction	Selected sensors
Derived wind direction	(1) 330 to 30 degree	average of wind vanes NW and NE boom
	(2) 30 to 90 degree	average of wind vanes S and NW boom
	(3) 90 to 150 degree	average of wind vanes S and NE boom
	(4) 150 to 210 degree	average of wind vanes NW and NE boom
	(5) 210 to 270 degree	average of wind vanes NW and S boom
	(6) 270 to 330 degree	average of wind vanes NE and S boom
Derived wind speed	0 to 120 degree	cup anemometer in NE boom
	120 to 240 degree	cup anemometer in S boom
	240 to 360 degree	cup anemometer in NW boom

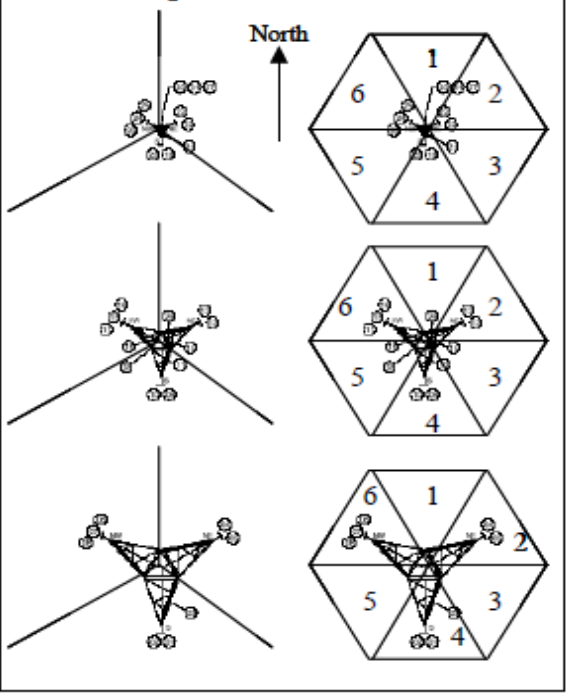

Figure 6: Wind Directions with reference to the different orientation of the booms.

The sonic anemometer data is available from the NW boom at 70 m height from channels 7 and 8 (instrument code: 3D WM4/NW/70). The data availability is around 98.8% of the measuring period. The velocity contribution from the NW boom "V_{NW}" is obtained from the average value of the horizontal and vertical velocities "V_H" and "V_V", obtained from channels 7 and 8 respectively as shown below,

$$V_{NW} = \sqrt{{V_H}^2 + {V_v}^2}$$

The cup anemometer data is available from both the NW and S boom at 70 m height. Channel number 12 for the NW boom (instrument code: WS 018/NW/70) has the data availability around 86% and channel number 14 for the southern boom (instrument code: WS 018/S/70) has data availability of 98.8% during the measuring period. The resultant velocity from the southern boom "V_s" is directly taken from channel number 14.

Hence in cases like these, where a combination of sensors from different booms is required, the resultant velocity "V_{res}" is calculated as the average of the two booms as shown below,

$$V_{res} = \frac{V_{NW} + V_S}{2}$$

It should be noted that depending upon the direction of the incoming wind, for example, wind directions falling within zone 6 of fig. [7], the velocity from only one boom i.e. NW may be taken.

At OWEZ, the distance between the tower and the measuring instruments is sufficient to limit the inaccuracy of wind speed measurements less than 5% [5]. Tower shading effects are discussed further in Ref [7]. The met masts strongly deflects the wind to the sides. Fig [7] taken from the same reference indicates these effects in the form of wind speed ratios at different heights.

The met masts strongly deflect the wind to the sides, hence the wind speed is strongly decreased directly behind the mast. In addition to that, the wind speeds at sensors upwind of the mast are also reduced. These effects are shown in fig. [7]. At a measuring height of 70 m and for wind speed orientation at 60 degrees, the ratio NW/S is approximately 1 whereas the ratio NW/NE is slightly greater than 1 while ratio NE/S is slightly smaller than 1 owing to the smaller wind speed values at NE. Therefore, the sensor which is located upwind of the met mast (NE sensors in this case), receives significantly lower wind speeds while the NW and S boom sensors (being equidistant from the dominant wind direction), receives equal contributions of wind speeds.

It should be noted that if the sensor was located exactly downwind of the met mast, it would receive very low wind speeds as shown in Fig. [7]. For a measuring height of 70 m and for wind speed orientation at 240 degrees, the ratio NW/NE is very large while ratio NE/S is very small indicating significantly smaller wind speed values at NE. The ratio NW/S remains equal to 1. Hence an average of NW and S boom sensors would be taken in that case as well.

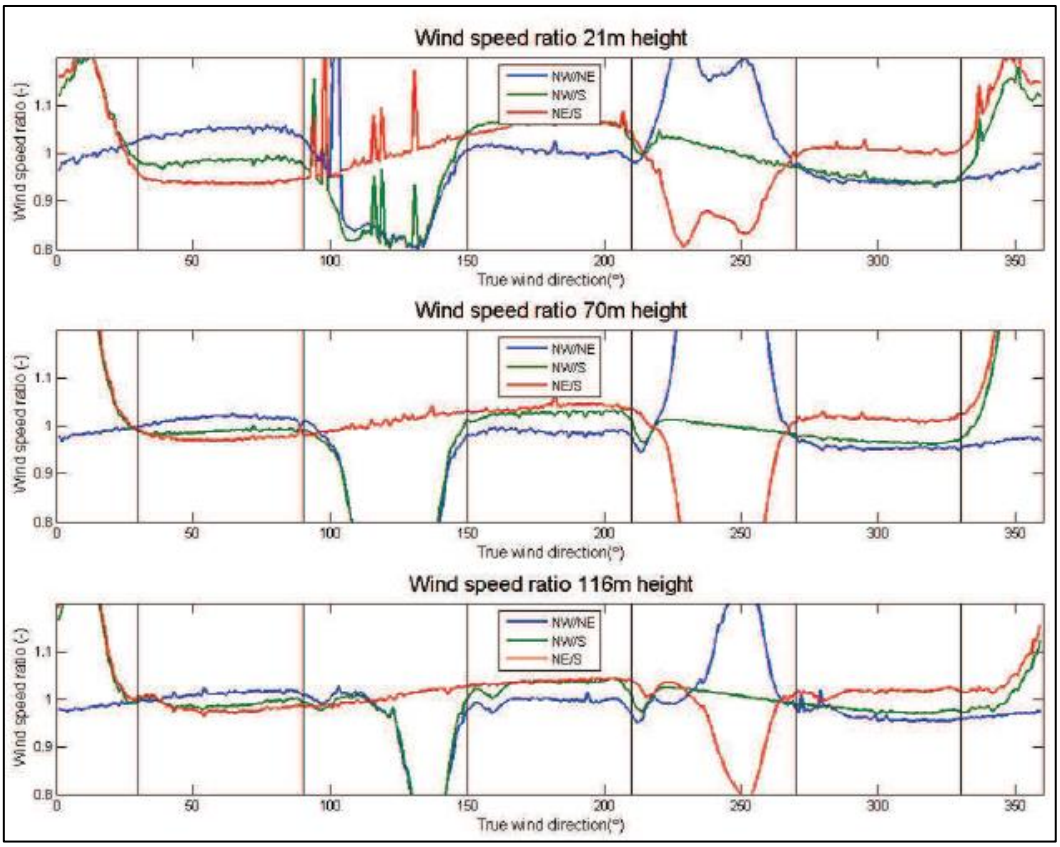

Figure 7: Wind speed ratios of sensors at NW, NE and S booms of the meteorological mast (OWEZ) at different measuring heights.

As it is evident from the discussion above, Method B is more detailed than Method A. However both methods rely on the assumption that vertical wind speeds are very small as compared to the horizontal wind speed measurements. It can be argued from the detailed inspection of the wind speed values that the contribution of vertical components are significantly smaller than their horizontal counterparts.

Therefore Method B has been used in the detailed gust analysis in the later sections of this report.

The measuring height of **70 m** above mean sea level has been chosen for gust analysis. This choice is made based on the following reasoning,

1. The availability of data is generally better at 70 m height as compared to the 116 m height, especially in case of sonic anemometers.
2. The turbines installed at OWEZ wind farm are Vestas V90 with a hub height of 70 m. Hence any gust analysis performed could be easily related to the actual wind farm conditions.
3. A height of 70 m is high enough to be unaffected by the effect of wind shear especially at the sea locations where the values of surface roughness length are typically low. Fig [7] from Ref. [7] highlights this issue for the wind speeds at 21 m height. These disturbances are most pronounced for wind directions between 90 and 150 degrees.
4. For the initial set up of gust detection algorithms, tentative estimates of turbulence intensity, sampling frequency, characteristic time and some other parameters have been made in the next sections. References [4] [5] [6] used for this purpose also provide much of the information at 70 m hub height.
5. The effect of “mast displacements” due to wind was also considered. If the mast top has large deflections, the wind speed measurements could be disturbed. According to a detailed analysis of the mast top displacements performed by Eecen and Branlard [6], the flow distortion due to the mast motion at 116 m height is nearly **3%** which can affect the wind speed measurements slightly. Hence the choice of 70 m height for wind measurements has been made to mitigate any inaccuracies.

Selection of the Measurement Period

The reference data set from OWEZ site comprises of wind speed measurements for one complete year (2008). Equal duration of wind data from onshore and far offshore locations (Cabauw and IJmuiden) will be used for comparisons in the detailed analysis. For this research work, a binding constraint is the duration for which the data was available from all three of these locations.

However it remains a subject of interest to define some “appropriate duration” of wind data which can be considered reliable enough for predicting the gust patterns at any particular location.

It is important to understand that the short term fluctuations of a stochastic climate variable like wind is in the order of seconds. Long term wind speed statistics are generally available in the form of 10 minute (or sometimes hourly wind speeds statistics) and are not really useful for studying the wind gusts.

In order to find some sort of correlation between the long term wind speed averages and the short term wind speed fluctuations (gusts) some of the concepts like the standard statistical techniques of measure correlate and predict (MCP) and the wind power density were explored during the initial stages of this research work but the idea was dropped as it was outside the scope of the project.

Therefore, for this research work, the choice for 1 year high resolution wind speed data has been made randomly (or rather imposed) for performing the gust analysis at different locations. It is mainly restricted due to the availability of data.

4.2 IJMUIDEN Site Information

The offshore meteorological station is situated 85 km from the coast of IJmuiden. Its coordinates are N52’50.89” E3’26.14” and the average water depth is 28 m. The details about the instrumentation and the ECN data acquisition system installed at the IJmuiden location are given in the Ref [8].

Figure 8: The IJmuiden site location.

The height of the met mast is 92 m above LAT and the measuring instruments are installed at three different heights **25.5 m, 57 m** and **86.5 m**.

Figure 9: The meteorological mast located at the offshore site (IJmuiden). Ref. [8]

At each of these measuring height, three booms are installed. The orientation of different booms at each of the measuring height is shown in Fig. [10] which is taken from Ref. [8]. It should be noticed that the orientation of booms here at IJmuiden is slightly different as compared to the OWEZ met

mast. Here the North East boom of the met mast is oriented at 46.5 degrees with respect to the geographical North while the southern and the North West boom are oriented at 166.5 and 286.5 degrees with respect to North.

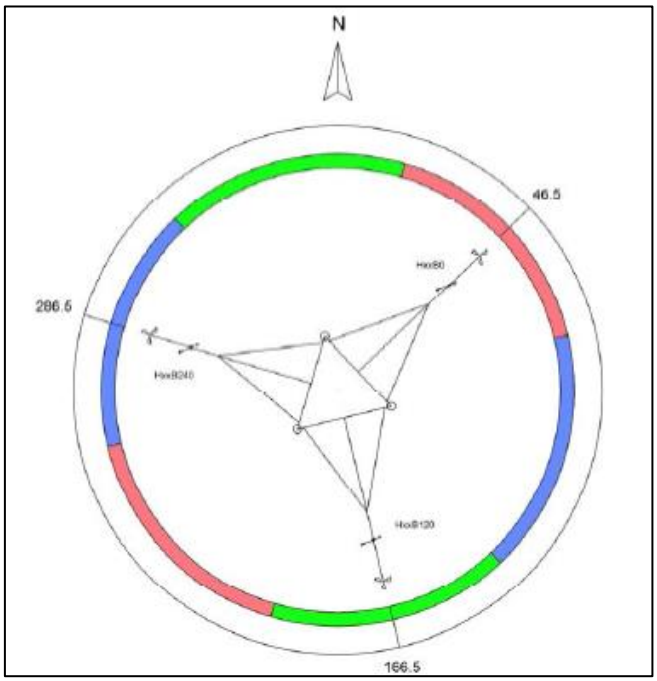

Figure 10: Orientation of booms on the met mast at Ijmuiden.

For the purpose of this research work, the sonic anemometer data available at the measuring height of 86.5 m with a sampling rate of 4 Hz has been used. The data has been scaled down to 70 m height using logarithmic wind profile laws. The details about the logarithmic wind profile can be found in any standard wind turbine hand book. In simple terms, if the wind speed is available at certain height, we can calculate the wind speed at other heights (within the surface layer) using the logarithmic wind profile assuming neutral atmospheric conditions.

$$u(z_2) = u(z_1) \times \frac{ln(z_2/z_0)}{ln(z_1/z_0)}$$

Where,

"$z_\circ$" is the surface roughness length whose value is taken as 0.0002 for the open water surface.

"$u(z_1)$" is the known wind speed at height z_1.

"$u(z_2)$" is the wind speed at the desired height of z_2.

It should be kept in consideration that the results and analysis conducted for the IJmuiden in the later sections, would be prone to the assumptions and limitations of logarithmic wind profile laws.

4.3 Cabauw Site Information

The Cabauw is an onshore site situated 50 km inland from the coast of North Sea. Its coordinates are 51.97 N and 4.93 E. It is a meteorological and experimental site of KNMI situated between the cities of Rotterdam and Utrecht. It is surrounded by the rural grasslands and represents flat and homogenous terrain conditions. The Cabauw Experimental Site for Atmospheric Research (CESAR) database [9] provides extensive meteorological data for scientific research purposes.

Figure 11: The Cabauw site location.

A 213 m tall meteorological tower has been erected at this location. The met mast is a tubular tower with a diameter of 2 m. Guy wires are attached at four different levels. From 20 m upwards, horizontal booms equipped with different measuring sensors are installed at every 20 m intervals. The booms are oriented at 10, 130 and 250 degrees relative to North. The SW and N booms are mostly used for wind velocity and wind direction measurements and the wind velocities are available at different measuring heights of 1.5, 10, 20, 40, 80, 140 and 200 m. Furthermore, wind speed data measured at a frequency of 10 Hz by Gill R3 sonic anemometers is available from the SE boom. This high resolution data is available at 60, 100 and 180 m heights.

For this research work, the 10 Hz data from the 60 m height has been used which is scaled up to 70 m using logarithmic wind profile laws. The surface roughness length value "z_o" is taken as 0.03 for the open land field.

The details about the Cabauw site location and instrumentation installed at the meteorological mast are available at the CESAR database [9] and also in other previous studies conducted at this meteorological site [10] [11]. Fig [12] shows the Cabauw met mast and the site landscape in general.

Figure 12: The site location and met mast at Cabauw.

5. CALCULATION OF CHARACTERISTIC TIME OF STOCHASTIC WIND FIELD

Before defining different gust detection algorithms, it is important to define some "time scale" related to a stochastic wind time series which can ensure the accurate detection of wind gusts from a turbulent wind field. Time scales, in general, gives an indication of the "memory" of the stochastic processes and they can be described in the form of either "characteristic time" or "decorrelation time". For this research work, characteristic time has been chosen as the preferred time scale. Details can be referred from ref [12].

5.1 Characteristic Time "τ"

Any stochastic time series X_t usually comprises of two components, a dynamically determined component D_{time} and a stochastic component N_{time}, such that,

$$x_t = D_{time} + N_{time}$$

Sometimes the dynamic component is evolving independently of the stochastic component. Such time series can be termed as "deterministic", for example, the annual cycle of the tidal motion. Such stochastic processes are fairly predictable.

However, in case of an interdependence of the dynamic component and the stochastic component, the process does not have any regularities. It only exhibit some "memory" in the sense that for example, if a series is positive, it will tend to stay positive for some time.

$$P\big((X_{t+\tau} > 0 | X_t > 0)\big) > 0.5$$

Where "τ" is known as the characteristic time, which is the time up to which the above expression holds true. For sufficiently long time lags i.e. if the time lag is greater than this characteristic time "τ", "there is no forecast skill". The characteristic time can be defined in other different ways as well.

In this research work, wind field will be treated as a stochastic process with interdependent dynamic and stochastic parts and a characteristic time "τ" defined as "the time for which the atmospheric turbulence is correlated".

5.2 Atmospheric Turbulence Criteria

Different values of "τ" can be used for turbulence study and wind gusts. Typically some of the factors that needs to be considered are the nature of the climate variable i.e. wind speed, atmospheric turbulence and the local wind conditions.

THE ORIGIN OF THE ATMOSPHERIC TURBULENCE

The origin of the atmospheric turbulence can be attributed to two mechanisms. First one is the mechanical (wind shear) and the other one is the convective or thermal effects.

The mechanical cause of turbulence is due to the roughness of the surface and the mixing of the turbulence. For example, if we consider an air parcel at a certain height above the ground, it is subjected to unequal shear forces because the wind speeds above the parcel are higher than the wind speeds below it. The deformation of this air parcel within this region of sharp velocity gradient is demonstrated in Fig [13]. Due to the unequal velocities on both sides, a net pressure force would act on the fluid parcel which would amplify the disturbance or turbulence. Thus a shear layer is unstable and tends to curl up and finally coils up into vortices.

The vortices in one direction are stretched. The area becomes smaller and just to maintain the circulation, the vorticity goes up. This phenomenon is in accordance with Kelvin's Law which states

that the circulation around a closed surface remains constant. Therefore, the vorticity increases and hence the turbulence gets stronger.

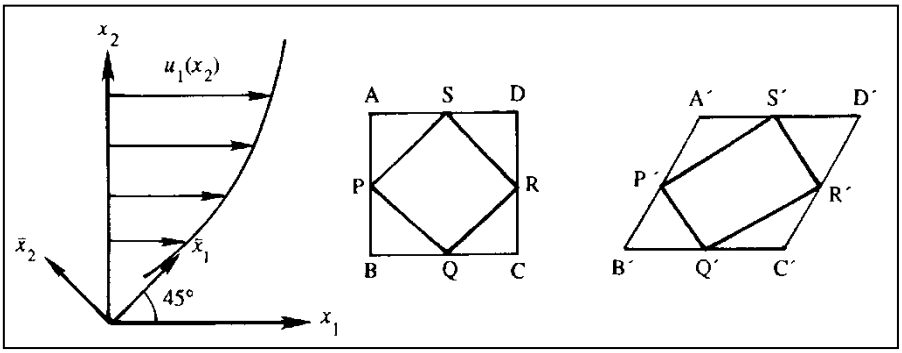

Figure 13: The mechanical deformation of the fluid (air) parcel in the atmosphere.

It can further be argued that the wind shear (i.e. sudden change in direction of wind) is caused by turbulence and the same is true vice versa.

The second mechanism of turbulence generation is due to the convection (thermal) effects. The convective (thermal) effect is due to the motion of the air because the hot air is rising. Due to the unstable atmosphere, i.e. the difference between the environment and surface temperatures, there is some heat flux (the amount of heat passing through per unit area per unit time) either in the upward or downward direction. With more heat flux, there is more mixing and the kinetic energy of the turbulence will increase.

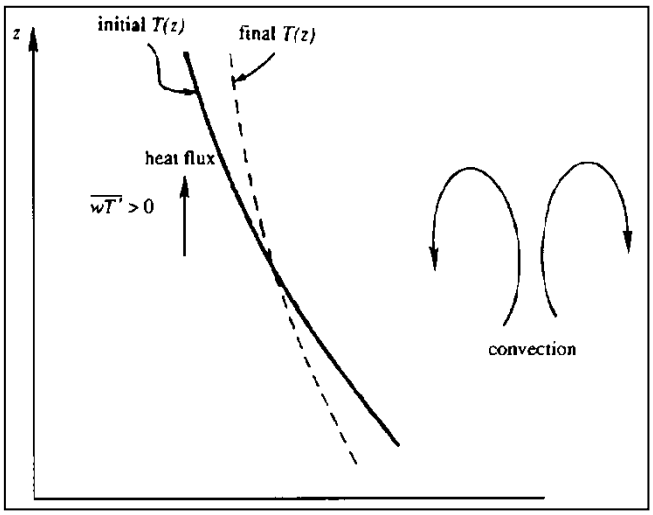

Figure 14: The turbulence mixing due to the convective (thermal) effects.

The stochastic nature of the turbulent flows has been discussed in various reference books under the domain of fluid mechanics [12] [13]. Wind turbulence can be defined as random wind speed fluctuations imposed on the mean wind speed. It is caused by the dissipation of the wind's kinetic energy into thermal energy via the creation and destruction of eddies.

The small velocity fluctuations occur in all three directions. For example, if u, v and w are the average values of longitudinal (in the direction of wind), lateral (perpendicular to the average wind) and vertical components of wind speed, then u', v' and w' are their respective turbulent fluctuating parts. Hence the instantaneous wind speed in any particular direction, for instance longitudinal direction is given by,

$$u_{inst} = u + u'$$

These fluctuations, as compared to the mean velocities, can produce large changes in overall stresses which can be shown in the form of additional Reynolds stress terms within the momentum equations

of fluid flow. Hence for the analytical description of turbulence phenomenon, the Navier Stokes Equation of fluid flow are modified with an addition of nine extra Reynolds stress terms. These Reynolds stress terms can also be represented by Reynolds Stress Tensor which is of the form,

$$\begin{matrix} u^2 & uv & uw \\ uv & v^2 & vw \\ uw & vw & w^2 \end{matrix}$$

The longitudinal, lateral and vertical components of the turbulent fluctuations at two neighbouring points within a flow field are different. However, they are not completely independent. For any given time series, as long as the average values of product terms “uv”, “uw” or “vw” remains non zero, the turbulence is correlated. The duration of this time for which the turbulence remains correlated can be taken as a characteristic time for the algorithm.

An example of some anisotropic turbulence is shown in the time series given in Fig [15]. It can be seen that when there is maximum value of u, there is some maximum value for w, hence the two velocity components are somewhat correlated and the average of product term “uw” is not zero.

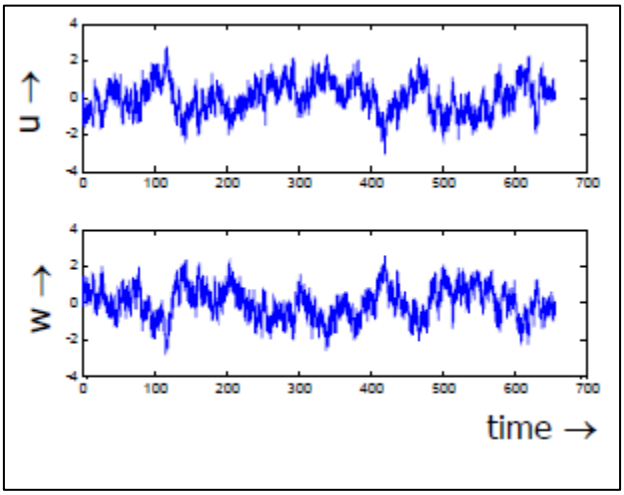

Figure 15: Time series with velocity components correlated.

It should be noted that in order to consider the correlation as zero, the terms u^2, v^2 and w^2 are not necessarily required to be zero in the Reynolds stress tensor. This is simply because in real atmosphere, the turbulence is mostly anisotropic in nature. Only on very small scale, it may be isotropic which can be neglected [12].

5.3 Covariance and Autocorrelation Function

In order to determine the interdependence of fluctuations of velocity components u, v and w, in a turbulent wind field, different statistical parameters may be used like “**covariance**” and the **autocorrelation function (ACF)**.

Covariance is simply a measure of how much two variables vary together. Mathematically, the covariance between velocity components u and v is given by,

$$Covariance\ (uv) = \frac{\sum uv}{n} - (\bar{u})(\bar{v})$$

Where n is the total number of observations and ($\bar{u}$) and ($\bar{v}$) represents the average values of the velocity components u and v respectively.

The correlation function is a more precise measure to define the relationship between two stochastic variables as it takes into account the effect of the variance of the individual variables as well. For example, the correlation function between velocity components u and v is given by,

$$R_{uv} = \frac{covariance(uv)}{\sqrt{var(u)}\sqrt{var(v)}}$$

When the correlation function is defined for the values of the same variable at two different time instants, it becomes autocorrelation function which may be given as,

$$ACF(\tau) = \overline{u(t_1).u(t_2)}$$
$$ACF(\tau) = \overline{u(t).u(t+\tau)}$$

The value of the autocorrelation function varies between 0 and 1. A value of 1 represents a perfect correlation of the turbulent fluctuations at that point. A negative value on the other hand shows that the velocities at that point are out of phase. A zero value shows that the velocity fluctuations are not related anymore.

Bierbooms et al. [14] have discussed in detail, the analytical formulations of the autocorrelation function for the stochastic wind field. The formulae requires the values of turbulent intensity, velocity at hub height and the standard deviation. Matlab routines based on ref [14] are available at the Wind Energy research group of Delft University of Technology which can be utilized to compute the autocorrelation function for any stochastic time series.

Using the available Matlab routines, a sensitivity analysis is carried out to determine a suitable characteristic time "τ" for which there is strong correlation.

Fig. [16a] shows the sensitivity analysis carried out at different hub heights. It should be noted that with the increasing height, the logarithmic wind profile becomes steeper and there is no significant impact of the surface roughness effects. For example, the variation of ACF with "τ" was more or less similar when the analysis was carried out 70 m and 116 m heights.

Fig. [16b] shows the effect of different velocity at the hub height of 70 m. The original Matlab code were written for auto covariance which needs to be normalized for calculating the autocorrelation function by dividing it with the variance. Alternatively, a standard deviation value of 1 can be taken.

The time duration for which the ACF remains closer to 1 (greater than 0.75) shows the time for which the turbulence remains correlated. The maximum time for which the turbulence remains correlated can be taken as the characteristic time for the algorithm.

Therefore an appropriate characteristic time, which can accurately capture the effect of random fluctuations of turbulent wind time series, is taken as 1 second because the ACF associated with values greater than 1, did not show strong correlation.

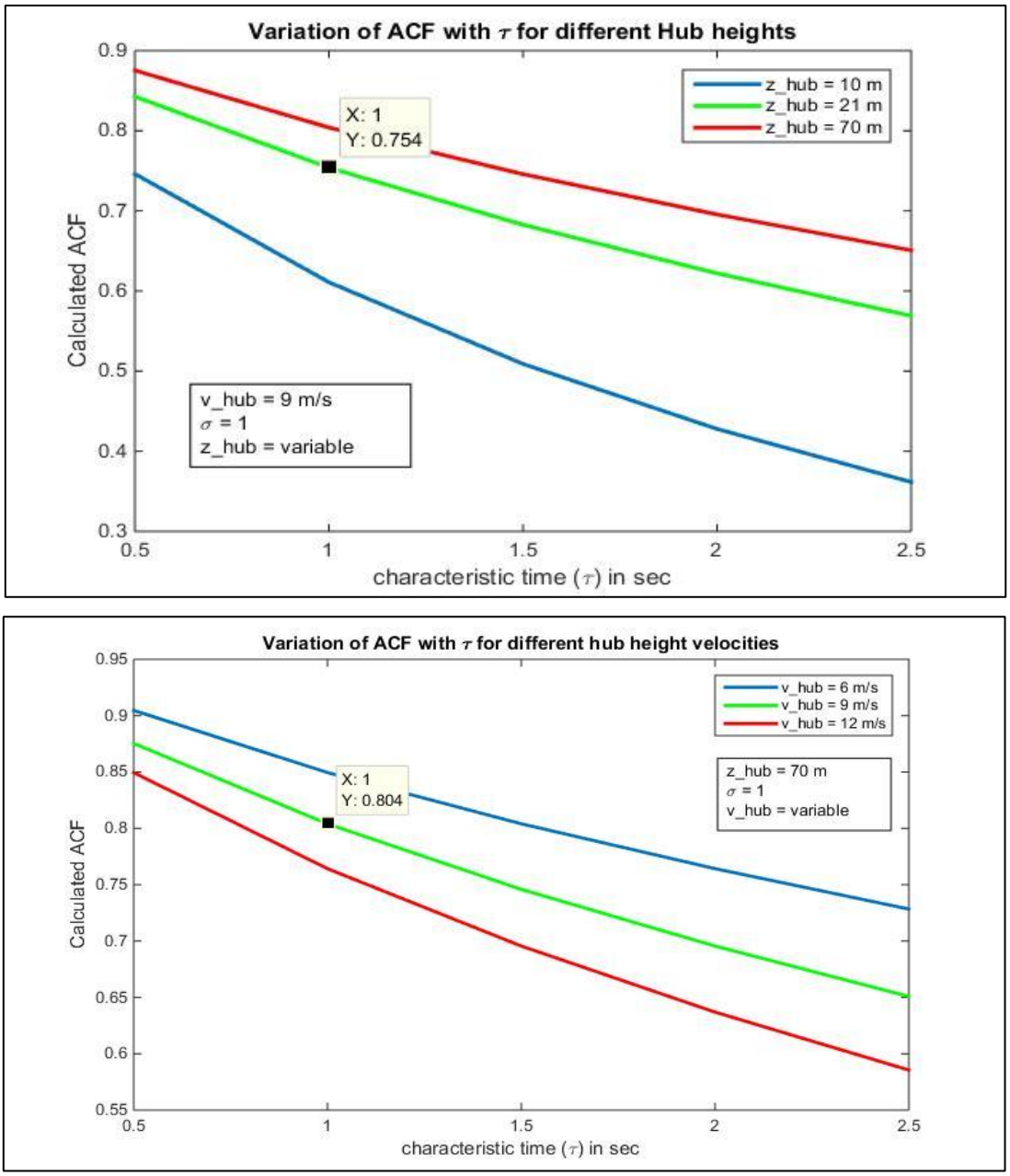

Figure 16: Variation of Autocorrelation function with characteristic time "τ".

5.4 Concept of a Moving Window

From the programming perspective, the characteristic time is incorporated into the gust detection algorithms as a "moving window", which is basically a moving time step which detects the wind gusts as it scans over the turbulent wind time series. Fig [17] shows the concept of a moving window on a stochastic wind time series.

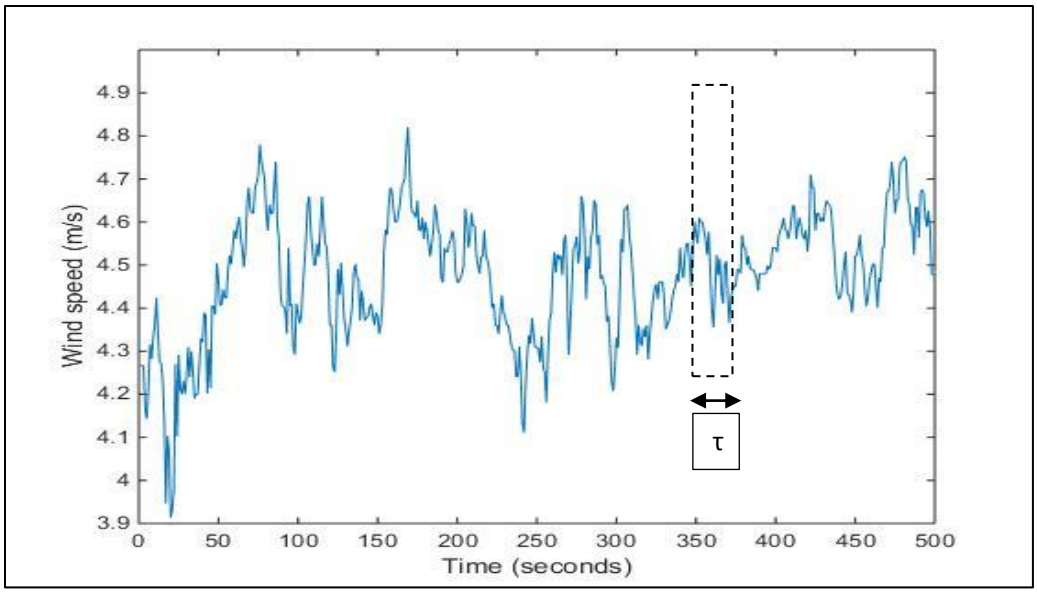

Figure 17: A moving time window on a stochastic wind time series.

It should be noted that the gust detection algorithms used in this research work have been programmed to let the users define their own criteria for the duration of characteristic time, depending their specific wind and site conditions.

6. CALCULATION OF APPROPRIATE SAMPLING FREQUENCY

The most commonly available form of wind data is in the form of hourly wind speeds. 10 minute average values are also commonly available from various meteorological websites and databases.

However, for detecting wind gusts, the availability of raw wind data with high sampling rate is important. Therefore, an appropriate choice for the sampling rate is considered here which can ensure the detection of small scale gusts with the most efficient use of computational time. The following factors can be considered for deciding the minimum sampling frequency required for gust analysis.

6.1 Characteristic Time for Algorithm

The characteristic time for algorithm "τ" is based on the integral time for which the atmospheric turbulence is correlated. This value has been calculated by performing a detailed sensitivity analysis of the autocorrelation function for the turbulent wind series in section [5] of this report.

Minimum Frequency rule:

Based on the optimum value of characteristic time for this study (τ=1 sec), the corresponding frequency is 1 Hz. This frequency can be taken as the **Nyquist** frequency, which represents half of minimum required sampling frequency such that,

$$f_{req} = 2f_{Nyquist}$$

The required sampling frequency should be twice of the maximum frequency of the signal (Nyquist frequency) because this is the requirement for regenerating the original time domain signal from the frequency domain signal ref. [15].

A sampling frequency lesser than this value would result in an error called as the **aliasing error** which is a condition when we cannot regenerate the original time series by converting it back from the frequency domain. Another way to avoid aliasing error is to incorporate anti-aliasing filter in the controller design. This factor may be considered during the selection of the data acquisition system of the wind turbine which is out of the domain of this study.

Therefore, for the purpose of this research work, the required sampling rate should be at least **2 Hz** based on the minimum frequency rule and for the characteristic time of 1 second.

6.2 Dynamic Characteristics of Wind Turbine

The dynamic characteristics of wind turbine due to the "excitation frequencies" of the moving parts have also been considered to discuss the suitability of sampling frequency for studying wind gusts. This is especially important because the turbulent fluctuations of wind speed are perceived differently by a rotating observer. If a rotating part sees turbulent fluctuations at certain frequencies then it also receives forces at these frequencies. The wind turbines are subjected to different types of loads [1].

The **resonance induced loads** depend upon the natural frequencies of the turbine components. These are limited by ensuring a proper design.

The **steady loads** should not affect the sampling rate in any way as they are constant.

The **transient** and **stochastic loads** depends upon the external factors (for example gusts) and cannot be well estimated for the pre selection of sampling rate for detecting wind gusts.

The **cyclic loads** are repeated specific number of times per cycle or revolution. These loads are typically denoted by multiples of "per revolution" load, like 1P, 2P or 3P etc. The rotor frequency "1P" and the blade passing frequency "3P" (in case of a 3 Bladed turbine) are most critical for the design of wind turbines.

A sensitivity analysis has been performed to study the effect of change in rotor size on the cyclic frequency of wind turbines. Fig. [18] summarizes the results.

An upper limit can be imposed by considering the maximum tip speed ratio of 80 m/s. This value has been used for calculating the rpm and hence the cyclic frequency of moving parts in a wind turbine.

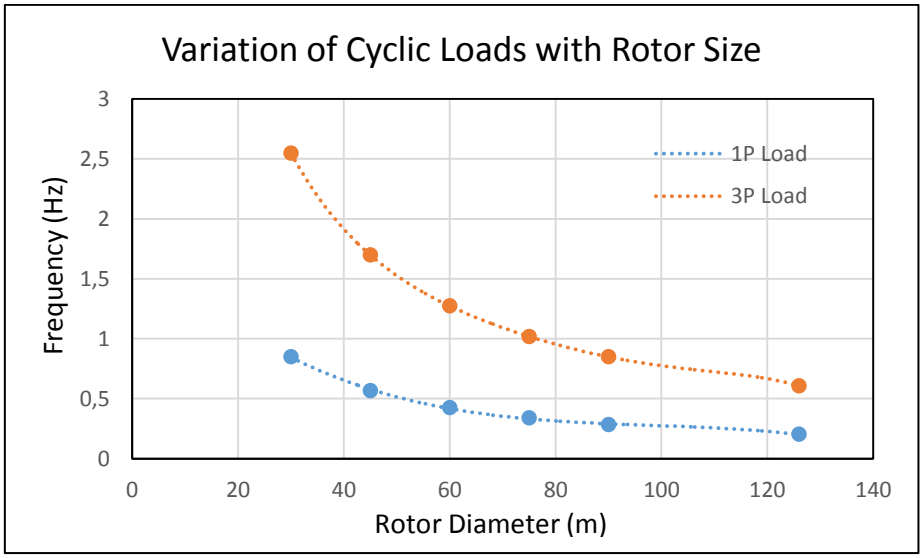

Figure 18: Dynamic characteristics of a wind turbine

From Fig. [18], it can be inferred that for small size rotors or with higher number of blades, there is a requirement for a higher sampling rate. Furthermore, with large size rotors operating at lower rpm, a lesser sampling rate would suffice.

As an example, the turbines installed at OWEZ are Vestas V 90 which have a rotor diameter of 90 m. The corresponding maximum cyclic frequency is around 0.8 Hz for 3P loads. This frequency represents the Nyquist frequency. Hence, by applying the Nyquist rule, the required sampling frequency should be at least **1.6 Hz**. Moreover, it can be argued that with an increasing trend towards larger wind turbines for offshore locations and for a hub height of 70 m, any wind turbine installed would at least have a rotor diameter greater than 40 m.

6.3 Met Mast Considerations

Just as the dynamic characteristics of wind turbine have been discussed here, it is important to do the same for the met mast because the data is acquired through the instrumentation installed at the onsite met mast. A study performed for the analysis of mast top displacement by Eecen [6] shows that the maximum frequency of oscillations of the met mast is **0.4 Hz**.

The reference data set available from OWEZ site is sampled at **4 Hz**. which satisfies all the above requirements for an optimum sampling frequency in order to study wind gusts. Moreover, the gust detection algorithms allows the user to adjust the sampling frequency which means that the gust analysis can be performed for any other frequency (maximum 4 Hz as it is the limit of the data set). A lesser sampling frequency may be set to perform faster calculations. This can be done by using various techniques for example, by skipping the alternate values or the subsequent 3 values after each recorded value from the dataset. This aspect will be dealt in much detail in section [10] for Cabauw data set.

It is recommended on the basis of the above mentioned considerations to keep the sampling frequency at least **2 Hz** or higher depending upon the sampling rate of the data set.

7. GUST DEFINITIONS AND CHARACTERISTICS

Some of the important definitions and gust related parameters are briefly described in this section. Details maybe referred from wind energy handbooks ref [1] [16] and the IEC design standards 61400 for wind turbine [17].

Gust: A wind gust can be defined as a short term speed variation within a turbulent wind field [16]. Various standards for defining a wind gust can be found from different sources which sometimes also depends upon the application under consideration.

American Meteorological Society [18] has defined gust as a “Sudden brief increase in the speed of wind”. According to U.S. weather observing practice, gusts are reported when the peak wind speed reaches at least 16 knots (8.23 m/s) and the variation in wind speed between the peaks and lulls is at least 9 knots (4.63 m/s). The duration of a gust is usually less than 20 seconds.

Gust Shapes: Depending upon the amplitude criteria defined for the gust and also from its shape (by plotting wind speed against time), duration and other characteristics, different standard forms of wind gusts have been defined in Ref. [16] [17] which are as follows,

1. Extreme Operating Gusts (EOG)
2. Extreme Direction Change (EDC)
3. Extreme Coherent Gust (ECG)
4. Extreme Coherent Gust with Direction Change (ECD)
5. Extreme Wind Shear (EWS)

The most commonly used gust shape in the wind turbine standards is the extreme operating gust which typically has a Mexican hat shape as shown in Fig. [19]. However, in reality the detected gusts may have any different shape which will be investigated in the detailed analysis section of this research work.

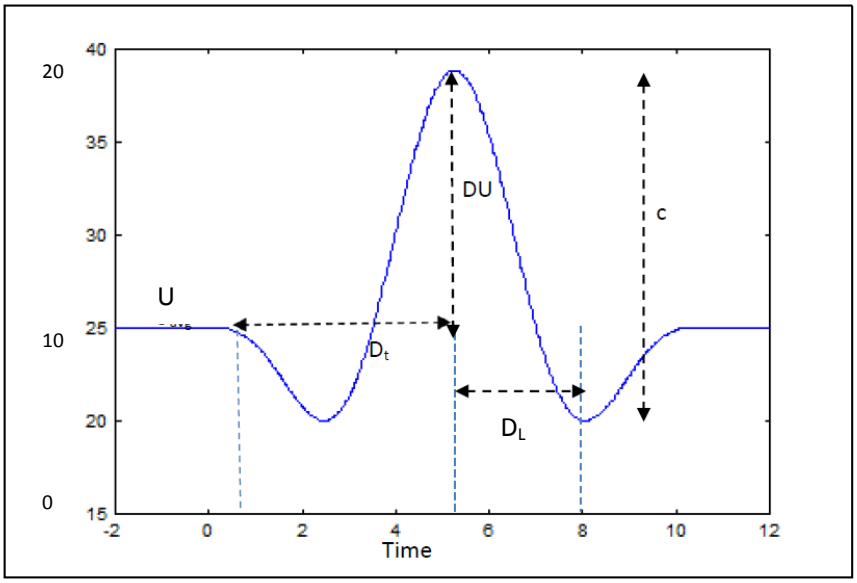

Figure 19: Different Gust parameters defined on a typical Extreme Operating Gust.

Gust Parameters: Each type of gust represents a unique set of characteristics and has a specific form when plotted on a time series. In ref [1] [16] various important parameters have been defined in order to describe a wind gust. Fig. [19] shows some of these parameters where U: Average wind speed, D_t; gust rise time, DU; gust relative amplitude, c; Maximum gust variation, D_L; lapse time.

Gust Front: The cases when the gust is characterised by the sudden acceleration of its amplitude (small rise time) are known as fronts.

Squall: The cases when the gust higher wind speeds are sustained for comparatively longer period of time (longer total duration) are known as squalls.

8. GUST DETECTION METHODS

Various types of algorithms can be created for the detection of wind gusts. Different gust detection methods were identified from the previous research works and literature studies. Ref [14] [19] [20] contains useful information about these techniques along with their proper implementation on the actual wind data for specific site locations. Detailed findings have been included in the literature study report preceding this research work.

It has been identified that the previous studies for gust detection methods have focused on a specific statistical technique and mostly concentrated upon a particular operational mode for wind turbines. Most importantly, these studies were limited to a specific geographical location only. Branlard [21] has summarized most of these gust detection techniques for the research work conducted at ECN test site at Wieringermeer in which the behaviour and characteristics of wind gusts (as detected by different gust detection methods) has been discussed in detail. However the results need to be validated for their consistency and applicability over different geographical terrains.

In this current research, different gust detection methods identified during the literature study and along with further adjustments and improvements are explained in detail. These methods have been developed into computer programs using Matlab.

It is important to recognize that any of these methods could produce completely different results, even when applied on the same wind data set which depends upon how we define the gust criteria based upon various gust parameters discussed in section [7] of this report.

Moreover, since the phenomenon of gusts maybe defined differently depending upon the application under consideration, the gust detection algorithms are programmed in a rather general way. The users (for e.g. a wind turbine or wind farm developer) would be able to define the criteria of the extreme winds, according to their specific project requirements and the code can be modified accordingly. In terms of general flexibility and the broad applicability of these algorithms, some of their salient features that need to be mentioned are,

- User defined sampling frequency (for reducing the simulations steps if desired).
- User defined characteristic time of the algorithm.
- User defined gust criteria (for the duration and amplitude threshold of the gust).

In this present section, the theoretical description, accuracy and limitations of each algorithm has been discussed. Appendix A contains programming pseudo codes and flow charts for each method.

In the next section, the testing and verification procedures for these algorithms would be elaborated. Finally in section [10] of this report, these gust detection algorithms would be utilized to identify wind gusts at different locations for which the high frequency wind data is available.

The following four methods are explained below in order to perform the detailed gust analysis. The first two methods, are based on “moving window” technique on a time series.

8.1 Peak-peak procedure

The peak to peak procedure, is based on the moving window technique. A time window of a suitable time length “τ” (the characteristic time of an algorithm) is defined. The basic considerations for defining this characteristic time have been discussed in section [5] of this report.

This time window moves through all the data values present in the time series. Fig [20] demonstrates the concept of the “moving window” and the application of peak-peak procedure.

At any given point of time, this window includes a set of values. The number of values within this set depends upon the characteristic time “τ” and the sampling frequency “f”. The difference between the local minimum and the local maximum is noted. This difference can be considered as the local gust for that step.

After each step, this moving window shifts one value forward on the time series. As the window moves from left to right, we can find the local maximum and local minimum for each step. The step for which this difference is maximum is selected and that difference is taken as extreme gust for the 10 minute sample.

$$\Delta U_{max} = max\,\{U_{\max}(t) - U_{min}(t)\}/t \;\in 10\ \min sample$$

$U_{max}(t)$ is the local maximum within the time window “τ”.

$U_{min}(t)$ is the local minimum within the time window “τ”.

ΔU_{max} is the maximum difference between the local maximum and local minimum for all the steps taken within the 10 min or 1 hour time sample.

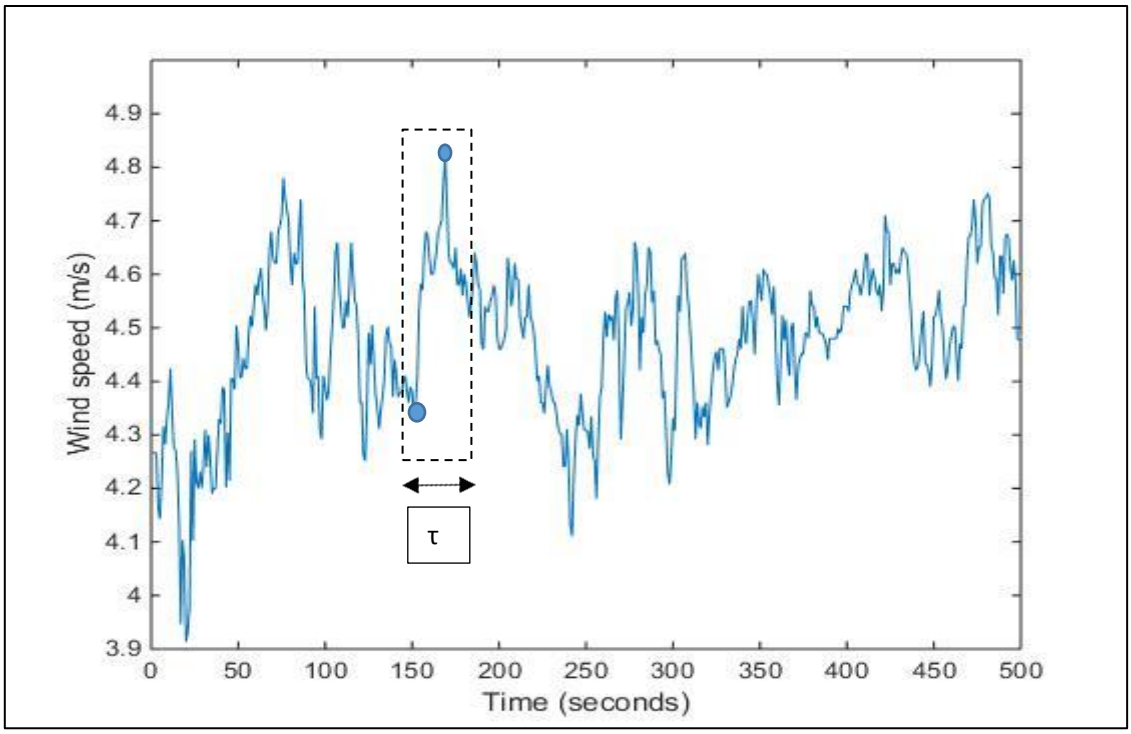

Figure 20: Peak to peak method utilizing moving window technique.

Advantages

1. This method is particularly suitable for detecting sudden variations within a very short span of time defined by the size of the moving window.

Disadvantages

1. Only maximum gusts are selected and many important gusts are forgotten.
2. The no. of gusts detected would be the same as the number of 10 minute samples.
3. With each step, the window moves one value forward on the time series and hence entire calculation needs to be performed once again. This makes the method is very time consuming.

It is important to mention that significant improvements in reducing the processing time of this code have been made by using different vectorization techniques.

Role of User Defined Frequency

As mentioned earlier, the user could specify the sampling frequency during the execution of the program. This could also reduce the processing time of the code.

For instance, if the user species a sampling rate of 2 Hz and the wind data set contains data sampled at 4 Hz, this effect is incorporated into the moving window technique as well. The window moves two values forward (instead of one) skipping every alternate value. Hence the overall number of steps is reduced to half of the previous scenario.

8.2 Velocity Increment Procedure

The velocity increment procedure is also based on the “moving window” technique just like the peak to peak procedure. However, the only difference is in the way, the local gust is measured for each step of moving window.

Here for each step, only the velocity at the first point and the velocity at the last point within the window frame is considered. The difference between these two values is noted and it is considered as the local gust for that step.

The step for which this difference is maximum is selected and that difference is taken as extreme gust for the 10 minute sample.

$$\Delta U = \max(\{u(t+\tau) - u(t)\}) \,/\, t \;\in\; 10\,\min\, sample$$

Where u (t) is the velocity at the start of the time window and u(t+τ) is the velocity at the end of the time window. Fig [21] demonstrate the principle of velocity increment procedure.

Advantages

1. The processing time of this code is comparatively faster as compared to the peak to peak procedure since this method utilizes only the first and the last value for each step.
2. The method is much easier in terms of coding and can be easily vectorized.

Disadvantages

1. Like peak to peak method, the velocity increment method is also based on the moving window technique, hence it is subjected to the same limitations.
2. The method is less accurate than peak to peak method because sudden variations within a very short span of time could be skipped when only the first and the last value for each window step are taken.

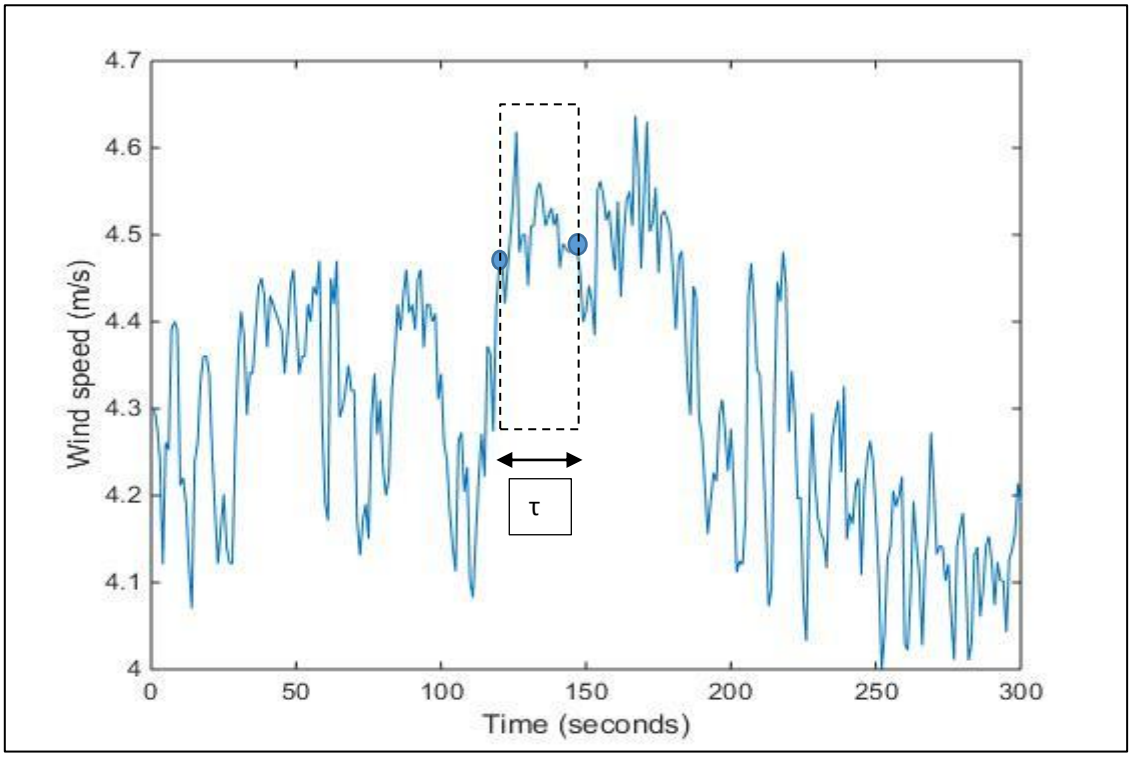

Figure 21: Velocity increment method utilizing moving window technique.

8.3 Peak-over Threshold Procedure (POT)

In this method, a wind gust is defined in a more precise way. An absolute amplitude threshold "x" is defined for wind speed and a minimum duration "d" is specified to neglect small scale fluctuations. A gust is identified whenever the following criteria are satisfied,

1. The velocity increases above the defined amplitude threshold "x".

2. The velocity remains above the defined amplitude threshold “x” for at least sufficient time i.e. greater than or equal to “d”.

In case the velocity drops below “x” quickly before completing the duration “d”, no gust is detected. As the phenomenon of gust is associated with short term wind speed fluctuations an additional criteria “d_{max}” may also be defined for the maximum gust duration. In other words, if the wind speeds remains above the value “x” for time greater than “d_{max}”, the gust will not be counted. Figure [22] demonstrates the peak over threshold method on a time series. Here three peaks are detected (x=4.6, d= 1 second).

Advantages

1. The peak over threshold method is a good choice for processes where only the peak values i.e. the extreme wind speeds exceeding a certain threshold are of importance.
2. The method is easier in terms of programming and it is found to be much faster as compared to the velocity increment or peak to peak method since it does not rely on the moving window technique.

Disadvantages

1. This method is not suitable for identifying sudden velocity fluctuations within a short span of time as defined by the size of the moving window or the characteristic time of the algorithm.
2. For wind turbine loading when the dynamic character of loading is often vital, other methods should also be used in conjunction with peak over threshold method.
3. Just like peak to peak procedure, the peak over threshold method also assumes stationary time series and hence de trending may be required for better accuracy.

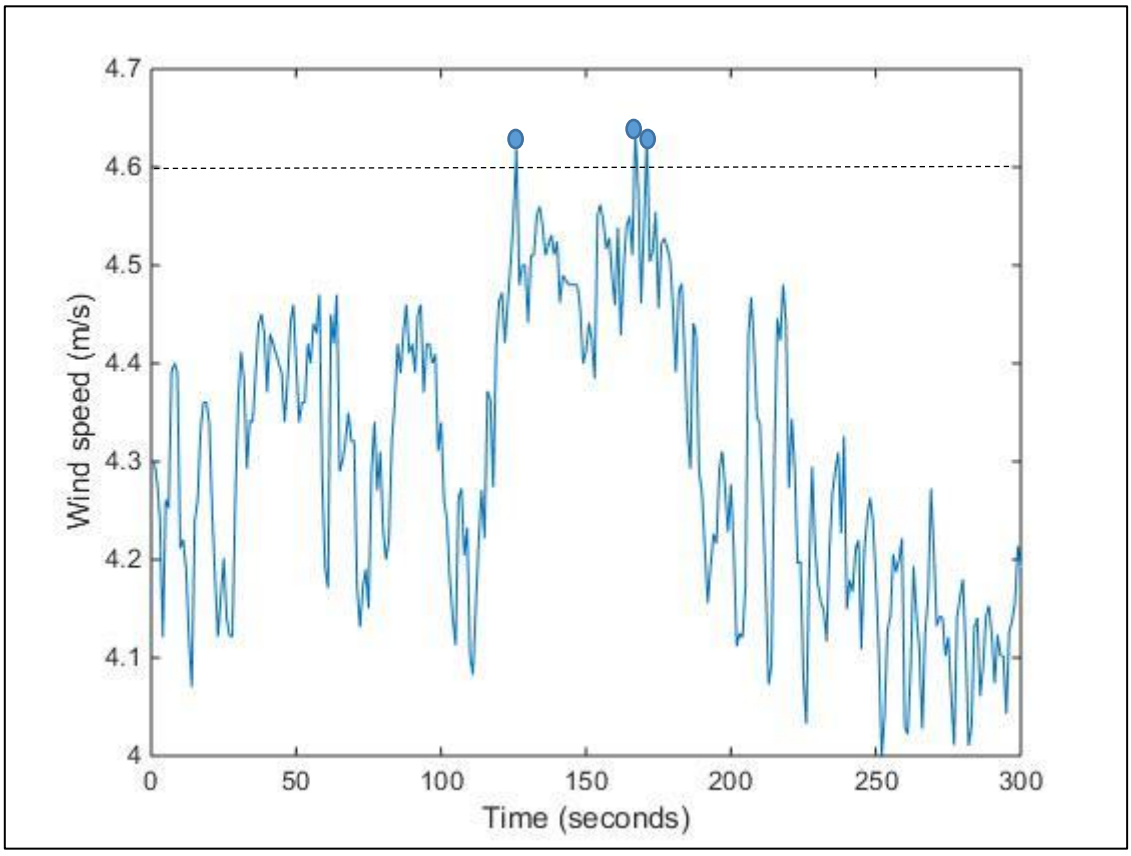

Figure 22: Peak over threshold method.

8.4 Acceleration over Threshold Procedure (AOT)

This method is a further extension of the peak over threshold method. Just like peak over threshold method, the gust criteria are precisely specified in terms of an amplitude threshold "x" and the minimum duration threshold "d". However in this case an additional acceleration criteria is introduced. A gust is identified whenever the following criteria are satisfied,

1. The velocity increases above the defined amplitude threshold "x".
2. The velocity remains above the defined amplitude threshold "x" for at least sufficient time i.e. greater than or equal to "d".
3. The increase in velocity is accompanied by the acceleration value greater than the acceleration threshold "a_t".

The acceleration value is computed in the algorithm code with the help of change in velocity value "ΔV" computed over specific time such as "τ" as shown in the equation below.

$$Acceleration = \frac{u(t_0) - u(t_o - \tau)}{\tau}$$

It should be noted that while "τ" is the characteristic time length of the moving window, the change in velocity is determined differently as compared to the velocity increment method because here $u(t_o)$ is the velocity at point where the amplitude threshold "x" is exceeded while $u(t_o - \tau)$ is the velocity at point preceding it depending upon the value of "τ".

A gust is counted only when the above calculated value for acceleration is greater than the acceleration threshold "a_t". The size of this moving window "τ" can be well defined as discussed in the previous sections of this report but the choice of the cut off threshold for acceleration (to be used as a defining criteria for gust) remains arbitrary as far as this research work is concerned.

As expected, by increasing the acceleration threshold criteria "a_t", the number of detected gusts would be reduced.

Fig [23] demonstrate the acceleration over threshold method. Comparing it with the peak over threshold method which could detect three gusts (x=4.6 m/s, d=1 second), the AOT method only detects one gust due to the additional acceleration criteria (a_t=0.05m/s^2).

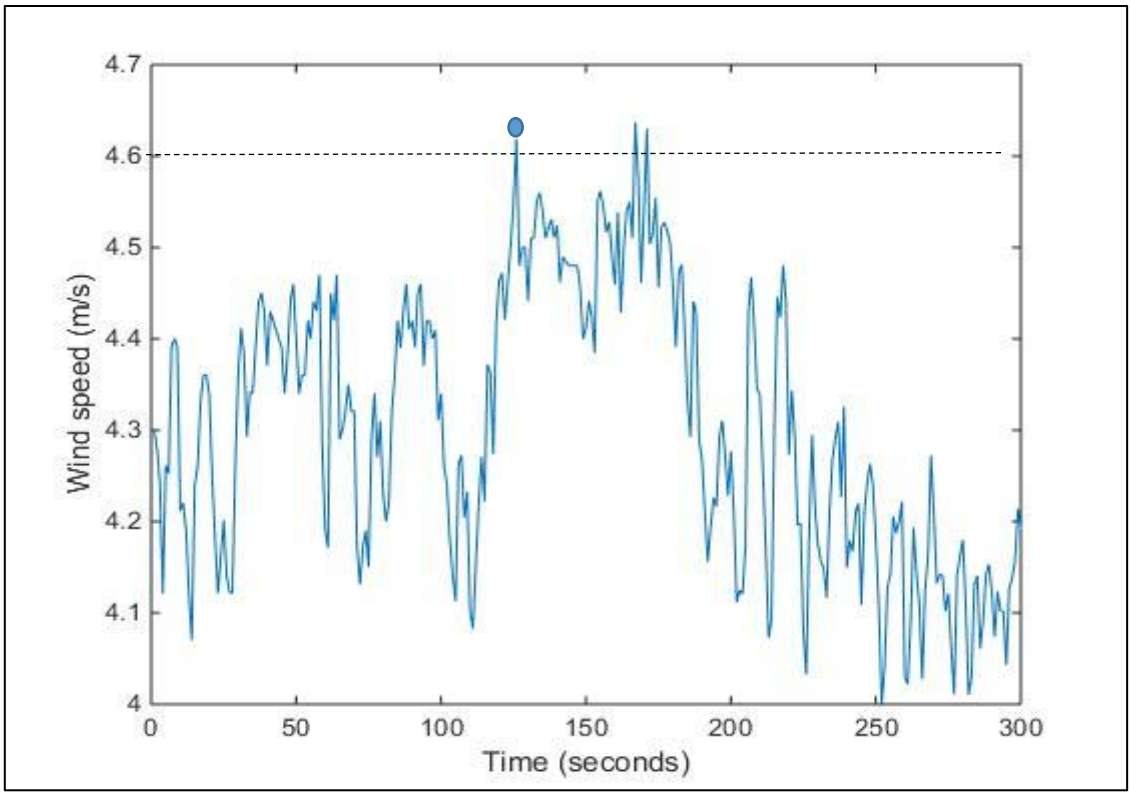

Figure 23: Acceleration over threshold method.

Advantages:

1. This method successfully detects gusts fronts. Hence it is particularly useful for determining dynamic loading characteristics of wind turbines.
2. Unlike the peak over threshold method, this method is suitable for detecting sudden fluctuations within a short span of time.

Disadvantages:

1. This method incorporates an extra condition imposed due to acceleration, therefore it may not detect extreme wind peaks encountered in time series if they are not accompanied by any significant acceleration. Furthermore, the acceleration criteria remains arbitrary.
2. This method imposes additional criteria on the detection of wind gusts. Hence fewer wind gusts are detected. Moreover the simulation time is also slightly increased as compared to the peak over threshold method because of the evaluation of additional acceleration condition.

9. VERIFICATION OF GUST DETECTION ALGORITHMS

Different gust detection methods explained in the previous section are programmed in the form of computer codes using Matlab. Effort is made to keep the coding structure simple. An user manual is prepared to guide the future users for running and modifying these codes. These codes will be available at the Wind Energy research group at TU Delft.

It needs to be mentioned here that while the results from some previous gust detection studies were consulted at the start of this research work, no specific computer codes were available. Hence significant time is spent on the development of the codes, there testing, refinement and verification etc. The verification of the gust detection codes has been ensured in the following ways,

1. Verification through test data set

2. Verification through different programming techniques
3. Treatment of missing data values
4. Tower shadow effects
5. Unreliable data values

9.1 Verification through Test Data Set.

The test data set comprises of two separate csv files. Each file contains wind speed values in longitudinal (dominant wind direction), lateral and horizontal directions. There are 300 data points (corresponding to wind speed values) in each of these directions. The csv (comma separated values) format was chosen because wind data acquired from the actual data acquisition systems is usually provided in this format.

This test data set, which represents a stochastic wind time series, has been further modified to ensure that the gust peaks are prominently visible. This would help in comparison of the results and different aspects of the gust detection algorithms can be evaluated easily.

Fig. [24] shows a single file made after combining the unidirectional (longitudinal) wind speed values from both of these csv files. The idea of "combining only the relevant data from all separate sample files" into a single file is utilized here. This is particularly useful because in real data sets, there are usually separate files for every 10 minute sample. If a gust detection algorithm is applied over each file separately, then a gust rising in the end of a 10 minute sample can be easily missed.

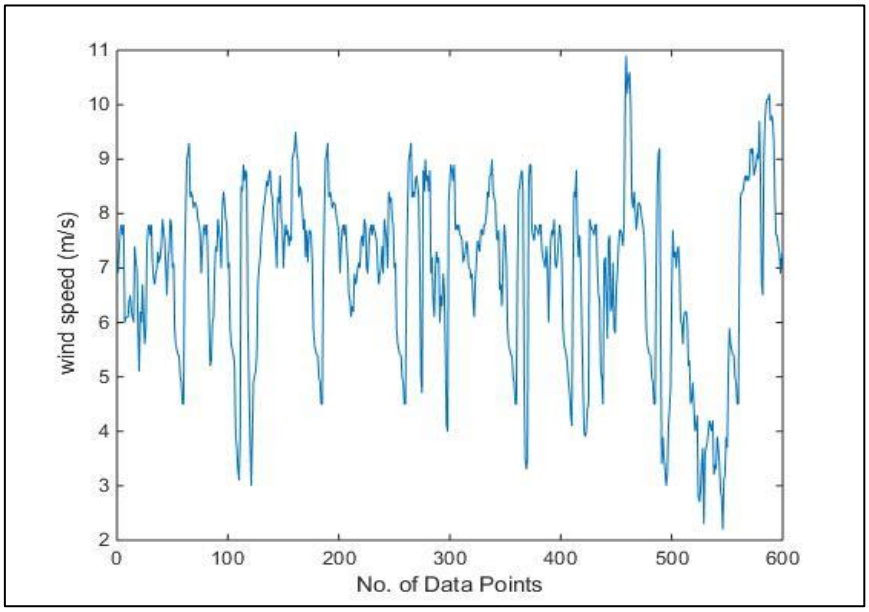

Figure 24: The entire test data combined into a single file

It is important to be aware of the fact that when similar codes are used for the actual data sets (for e.g. the reference data set from OWEZ), the single combined file (as shown in Fig. [24]) would become very large. Due to the limitations of computer memory, such file combinations are separately made for every month for the results and analysis performed within section [10].

As mentioned earlier, the peak over threshold and acceleration over threshold methods for gust detection require precise criteria for defining a gust. For this test data set, these threshold values are listed in Table [3]. The size of the moving window is taken as 5 seconds for the peak to peak and velocity increment methods.

S. No.	Parameters	Symbols	Values
1	Frequency	f	1 Hz
2	Gust threshold criteria	x	8 m/s
3	Gust min. duration criteria	d	5 seconds
4	Gust max. duration criteria	d_{max}	15 seconds
5	Characteristic time	τ	1 seconds
6	Acceleration criteria	a_t	2 m/s^2
7	Size of moving window	$e = \tau \times d$	5 seconds

Table 3: Gust defining parameters for test data set.

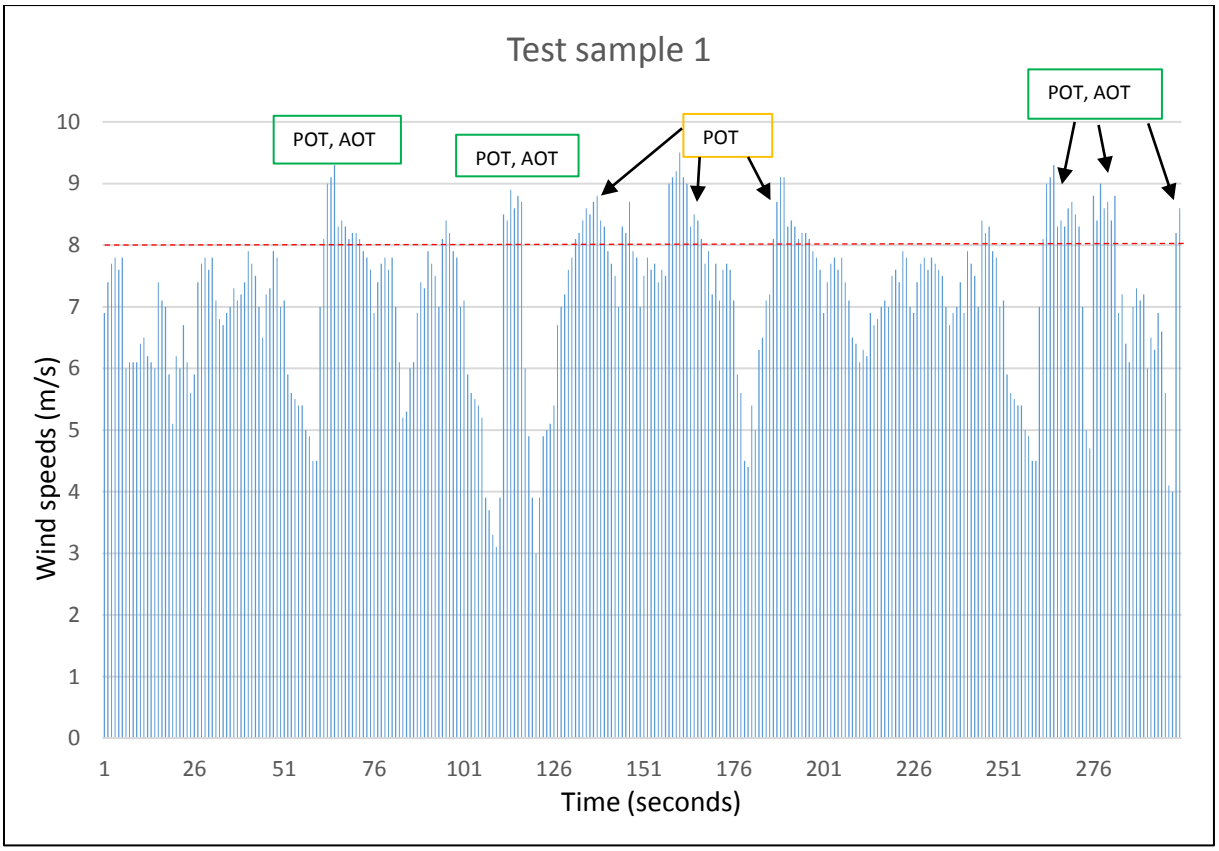

Figure 25: Test Data Set (Sample 1)

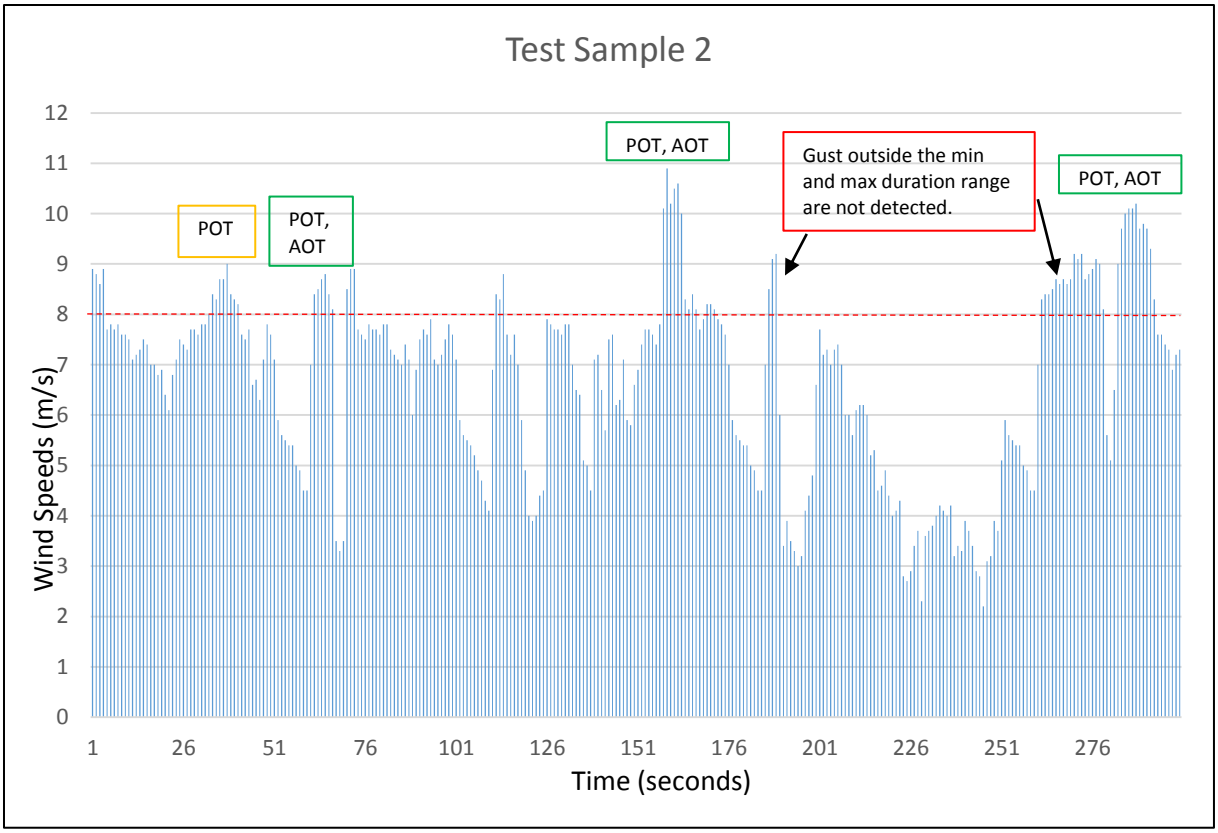

Figure 26: Test Data Set (Sample 2)

Fig. [25], [26] shows the two test samples separately for the purpose of clarity. From the visual inspection of this time series, the following observations can be made.

I. As per the POT criteria defined in Table [3], the sample 1 contains 7 and the sample 2 contains 4 wind gusts. There is 1 wind gust at the end of sample 1 extending into sample 2 (total no. of gusts detected= 13).

II. As per the AOT criteria defined in Table [3], the sample 1 contains 4 and the sample 2 contains 3 wind gusts. There is 1 wind gust at the end of sample 1 extending into sample 2 (total no. of gusts detected= 8).

III. The small scale fluctuations as well as the sustained high wind speeds for durations longer than the gust threshold should be neglected.

TEST DATA SET RESULTS

Peak to Peak Method

Fig. [27] shows the magnitudes of gusts computed at each simulation step for sample 1 and sample 2 of the test data set. While the gusts are calculated at each simulation step, the "maximum gusts" calculated for the test samples 1 and 2 are **5.4 m/s** and **5.8 m/s** respectively.

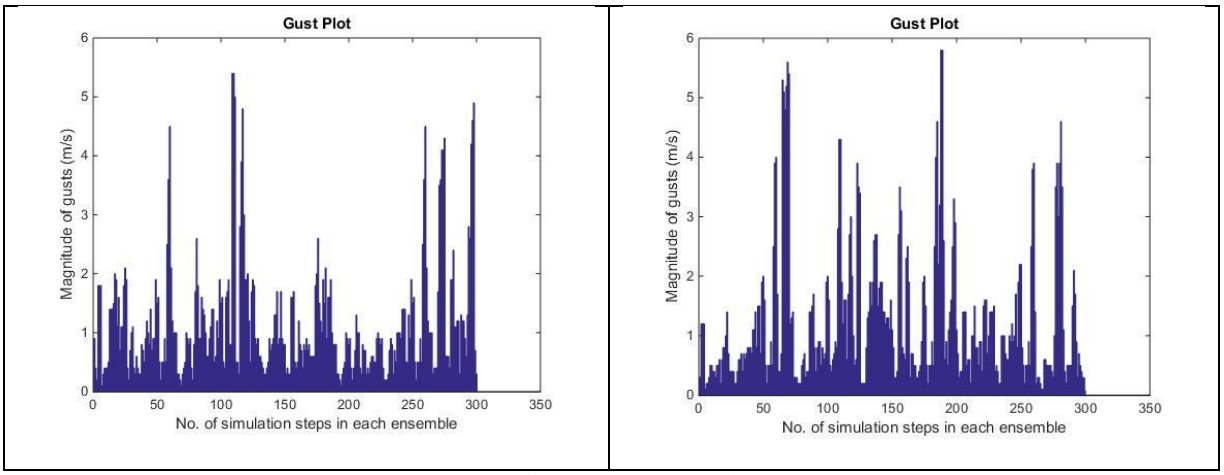

Figure 27: Gusts calculated at each step of the test data set (peak to peak method).

Velocity Increment Method

Fig. [28] shows the magnitudes of gusts computed at each simulation step for sample 1 and sample 2 of the test data set. The maximum gusts calculated for the test samples 1 and 2 are **5.3 m/s** and **5.7 m/s** respectively.

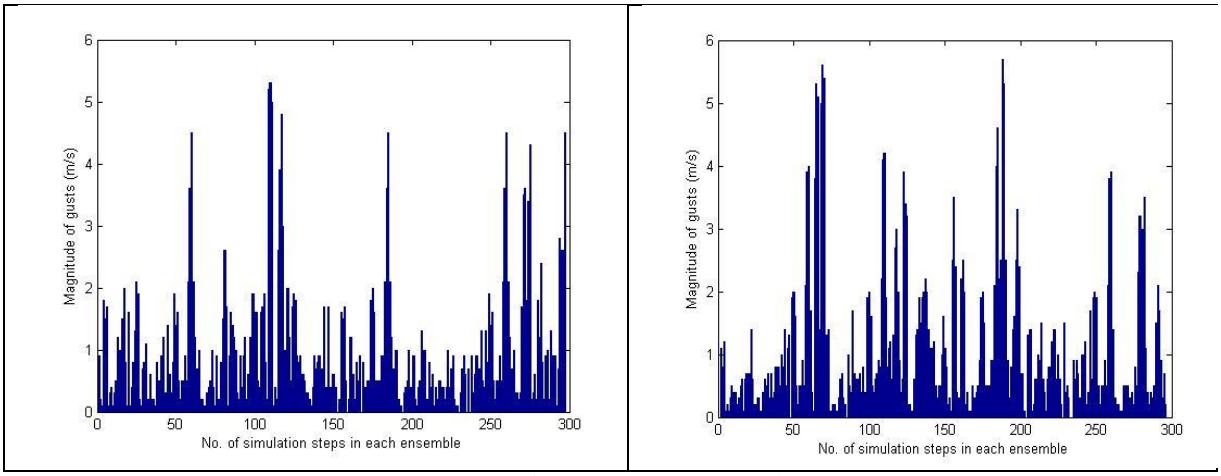

Figure 28: Gusts calculated at each step of the test data set (velocity increment method).

The total number of "maximum gusts" detected would be equal to the number of separate sample files present within the data set. For instance, in the case of wind data for one year, provided in the format such that there is a separate file for each ten minute sample, the total number of maximum gusts detected would be $6 \times 24 \times 365 = 52560$.

For the test data set, it is worth mentioning that both peak to peak method and velocity increment methods are predicting the maximum gust at nearly the same positions for each of the sample. Furthermore, the magnitudes of these maximum gusts are also almost comparable. Depending upon the real wind data, this behavior might change.

POT & AOT Method

The Matlab codes for POT and AOT when applied over the test data set, reproduced the same results as observed from the visual inspection of data set in Fig. [25] [26]. Hence the accuracy of the coding technique was confirmed.

It should be noted that the gust plots for the test data may not be of any significance because they just represent random fluctuations above the gust threshold. The gust plots can be arranged in different ways,

1. Gusts Peaks Centered At t=0

2. Gusts Plotted As Soon As Detected
3. Gusts plotted for the Entire Duration

Fig [29-31] shows all three of these arrangements for the 13 wind gusts detected through POT method. A better way is to obtain a mean gust shape which will be discussed later in in this report.

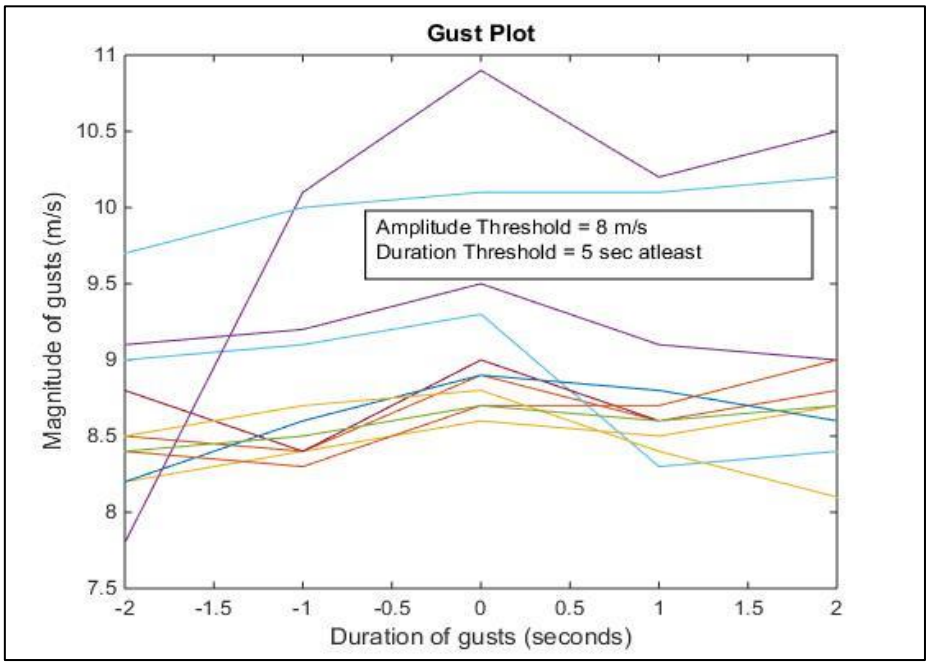

Figure 29: Gust plots with peaks centered at t=0. (POT Method)

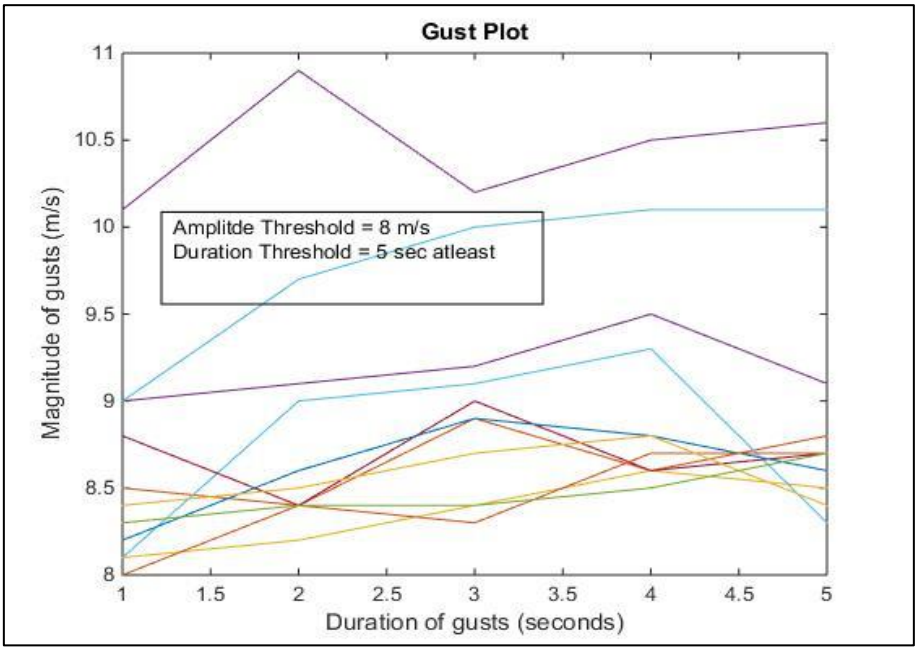

Figure 30: Gust plotted as soon as they are detected. (POT method)

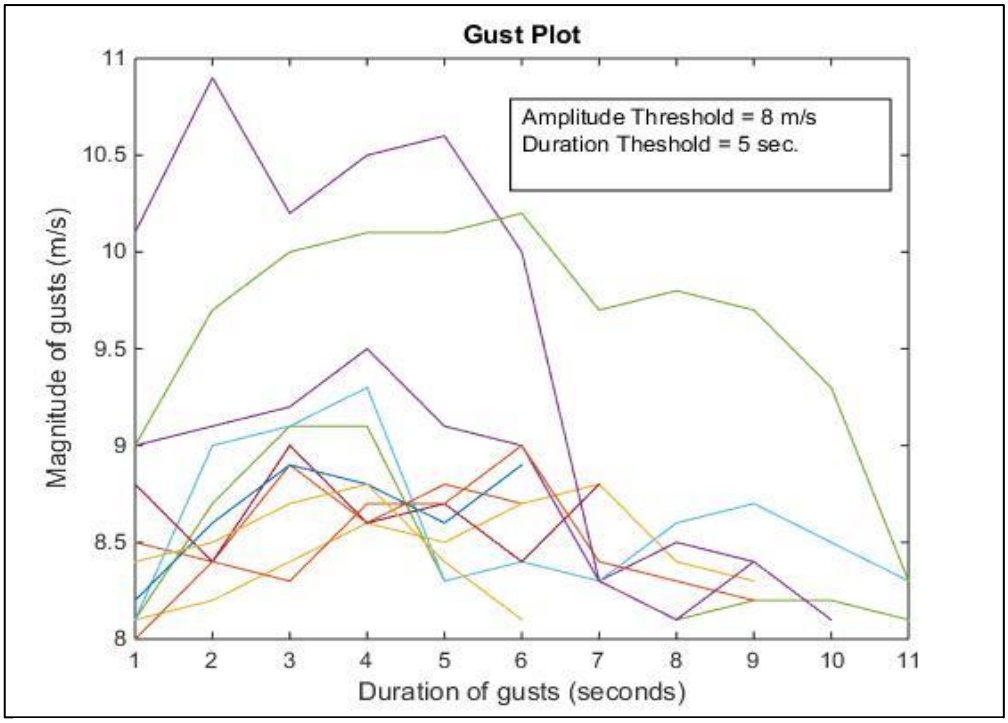

Figure 31: Gust plots for the entire duration. (POT method).

9.2 Verification through different programming techniques

Initially, the simulation time of running these gust detection algorithms was much longer when applied for the actual site data. This was true even for analyzing the wind data for durations lesser than a day.

Reduction in simulation time can also be achieved by reducing the user defined sampling frequency. However this may result in aliasing error as mentioned earlier in section [6] of this report and it is always recommended to use a high sampling rate data whenever it is possible.

In an effort to reduce the simulation times for different gust detection algorithms, many "vectorization techniques" have been utilized which are unique for each gust detection method. For example, the earlier versions of these codes involved the application of loops for moving the time window across the time series while the modified vectorization techniques utilizes the setting up of large matrices and then performing simple matrix operations over them without using any for loops.

Hence by using these vectorization techniques, the simulation times were significantly reduced for the test data set and this effect was even more pronounced when the similar techniques were applied over the actual wind data sets of 1 year duration.

A secondary incentive of experimenting with different programming techniques is the "**repeatability**" of the same results which ensured confidence in the theoretical as well as the coding aspects of different gust detection techniques.

APPLICATION OVER REAL WIND DATA IN GRADUAL STEPS

After the successful application and verification of gust detection algorithms for the test data set, the 1 year OWEZ data set, which was chosen as a reference data set for setting up the gust detection algorithms, was tested in gradual steps. A complete analysis of the OWEZ site wind data would form part of the results and analysis in section [10] of this report. From the perspective of verification of gust detection algorithms, the methodology used involved the gradual increment of the data samples in the following way,

1.	Small data set with 150/300 data points. Similar to the test data set.	Visual Inspection of individual gusts parameters is possible
2.	Six hour wind data	General plots/ trends could be inspected. Simulations could be completed and compared for different programming techniques using loops and alternate "vectorization" techniques.
3.	One Month Data	Simulations could only be completed with the most efficient "vectorization" techniques. General processing time and memory usage issues could be resolved here in this step before analyzing the full 1 year data.

Table 4: Gradual increments in the size of the data set from the verification perspective.

SIX HOURS WIND DATA RESULTS (OWEZ Site, July 2007)

Detailed results and plots for the gradual increments in the size of data samples have been presented in the preliminary progress reports from time to time. Here a period of six hours wind data is chosen to briefly demonstrate the following two aspects of the data analysis,

Mean Gust Shapes

These mean gust shapes can be obtained by two different techniques.

1) Mean gust shapes based on the mean wind speed (based on the method of bins).
2) Mean gust shapes based on the Autocorrelation function (ACF).

So far the concentration is on plotting mean gust shapes as a function of mean wind speed. Here the mean wind speed is assumed to be the mean wind speed for each 10 minute sample. Fig. [32] [33] show the mean gust shapes.

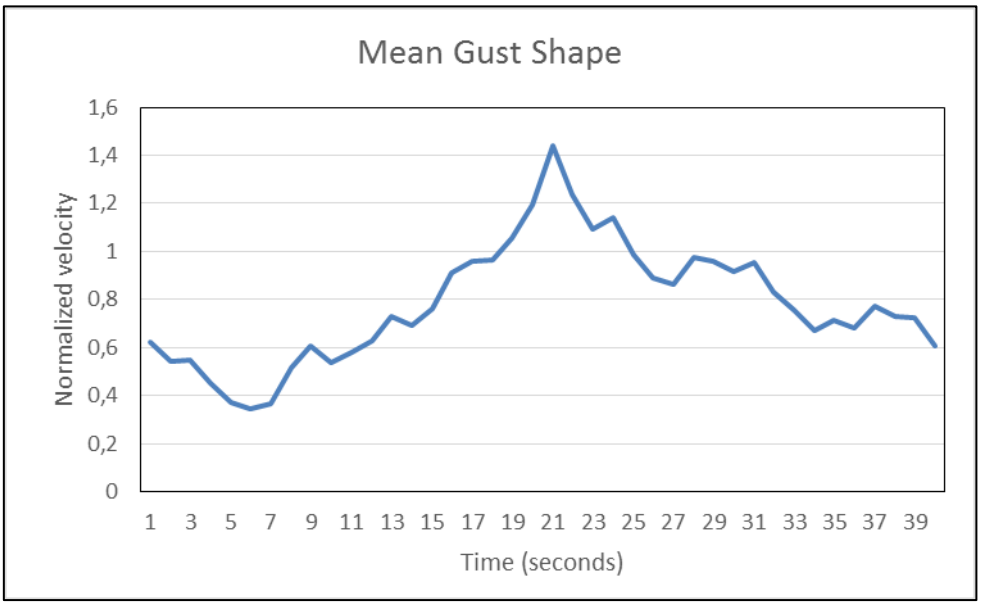

Figure 32: Mean gust shape for OWEZ six hour data (POT Method)

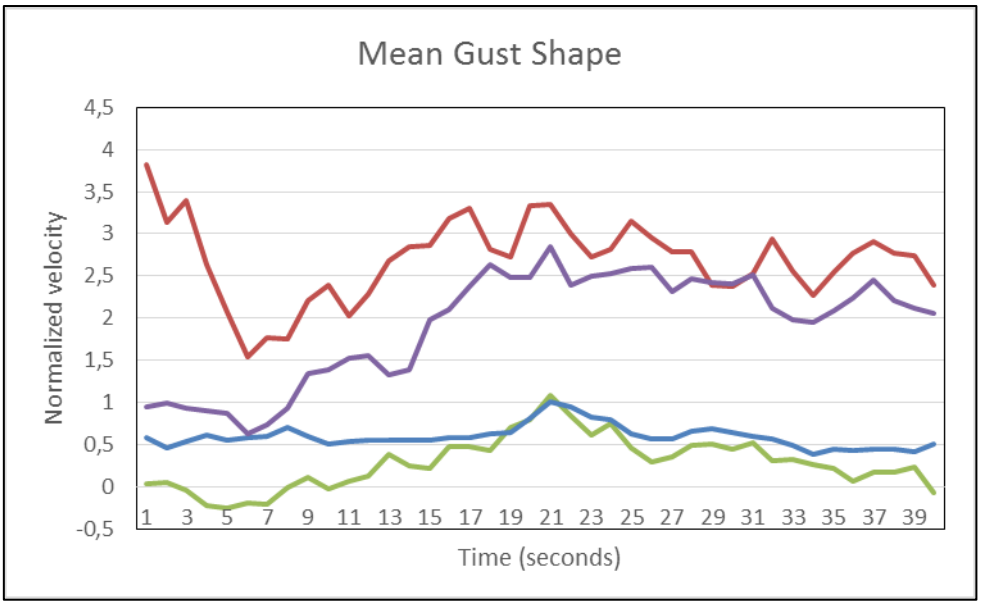

Figure 33: Mean gust shape (POT method). Velocity normalized at different mean wind speed bins.

Table [5] shows various gust parameters that have been used to compile the results. Depending upon the wind data, these parameters could be altered.

S. No.	Parameters	Symbols	Values
1	Frequency	f	4 Hz
2	Gust threshold criteria	x	13 m/s
3	Gust min. duration criteria	d	5 seconds
4	Gust max. duration criteria	d_{max}	15 seconds
5	Characteristic time	τ	1 seconds
6	Acceleration criteria	acc	1 m/s^2

Table 5: Gust defining parameters for OWEZ six hour data.

Calculation Estimates

The OWEZ data set contains data sampled at 4 Hz and comprises of separate csv files for every 10 minute sample.

No. of relevant data values in each file = 4 X 60 X 10 = 2400.

No. of files in 1 year data set = 6 X24 X 365 = 52,560

No. of relevant data values in 1 year data set = 2400 X 52,560 = **126,144,000**

This represents the number of relevant data values that needs to be combined into a single file before the execution of the gust detection code. However the actual number is usually a bit smaller due to the missing data values.

It is also worthwhile to note here that this format is unique for the OWEZ data set. Later on, for IJmuiden and Cabauw, the number of data values in each files and the total number of files in 1 year would be different but the method of compiling and making a single file would be the same.

9.3 Treatment of missing data values

Fig. [34] shows the velocity plots for 1 month data (July 2007) at OWEZ site.

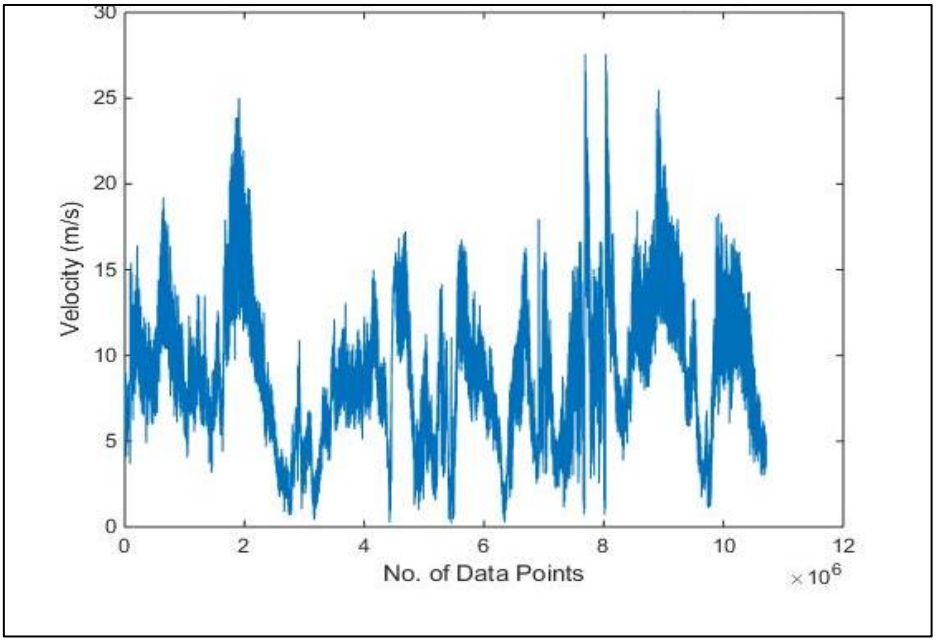

Figure 34: Velocity plot for 1 month data (July 2007) at OWEZ site.

Here the missing data is not shown because the designed codes for all the gust detection methods, automatically removes the non-existent values (shown in the mat file as Nan values) as soon as they combine the data into a single file. A closer inspection of the time series sometimes indicates sudden jumps as shown in Fig. [35].

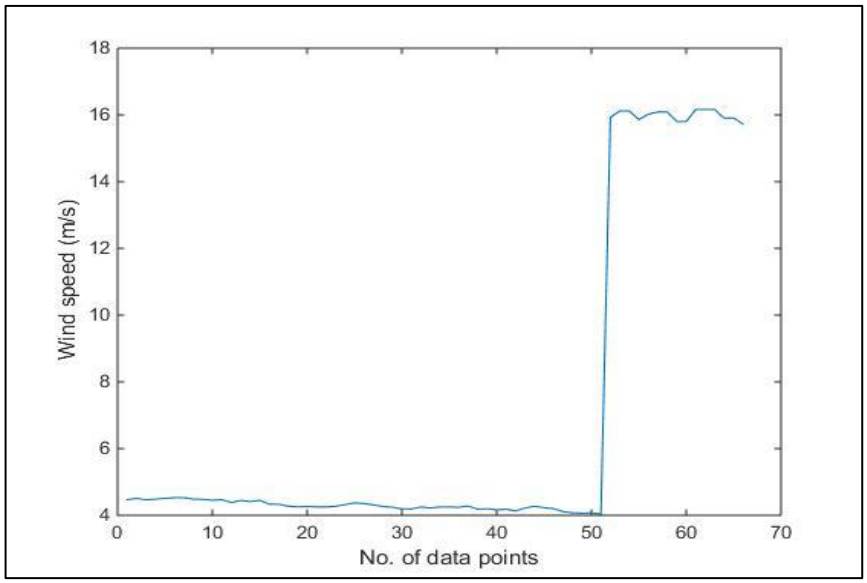

Figure 35: Sudden jumps encountered in time series.

Therefore it is important to verify if such occurrences are genuine sudden wind speed changes or they might be a consequence of some data handling technique like, for instance, merging of two non-adjacent 10 minute sample files in the case of missing data values in between.

In order to avoid the detection of such false gusts, a separate user defined function has been written to detect the locations (within the data set) of all the incidents where the two non-adjacent 10

minute periods are combined. In case, if these locations matches with the starting locations of any of the gusts, such gusts are interpreted as “false gusts” and are disregarded.

9.4 Tower Shadow Effects

Sometimes sudden peaks in the wind speed values can be detected which can be attributed to the tower shadow effects. Figure [36] shows such incidents within the time series.

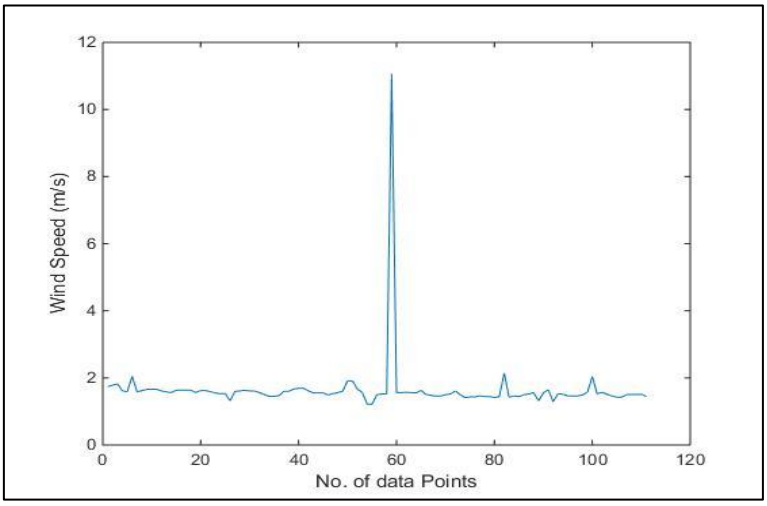

Figure 36: Sudden peaks encountered in time series.

A detailed discussion has been made under section [4] of this report regarding the selection of wind measurements considering the tower shadow effects.

For the OWEZ data set, the wind direction data is completely available. Ref. [7] provides some basic guidelines regarding the selection of sensors on either of the three booms (NW, NE and S). Fig [6] in section [4] shows six wind speed zones. Depending upon which of the six zones, the resultant of the wind direction belongs to, a corresponding sensor or a combination of sensors is chosen.

For the purpose of clarity, table [6] below shows various sensors or combination of sensors for which data can be retrieved form the data sets. Based on the recommendations from ref [7], and the discussion under section [4] of this report, wind speeds are selected from either of the six columns marked with blue. Hence for all the data points given in this table, either one of the values in blue is taken from each row. The choice of zone from 1 to 6, depends upon the resultant wind direction “WD (res)” which is also shown in red in Table [6].

NW (u)	NW (v)	NW (w)	NW (res)	NE	S	NW & NE	NW & S	NE & S	WD (NW)	WD (NE)	WD (S)	WD (res)
X	X	X	X	X	X	X	X	X	X	X	X	X
X	X	X	X	X	X	X	X	X	X	X	X	X
X	X	X	X	X	X	X	X	X	X	X	X	X

Table 6: Method for selecting the wind speed measurements incorporating tower shadow effects due to resultant wind direction.

Later on for IJmuiden data set, the wind direction data is not explicitly given. A technique using longitudinal and lateral wind speed components to determine the wind direction is used. This is based on the assumption that the orientation of the sensor is perfectly aligned with the boom.

9.5 Unreliable Data Values

In the analysis of IJmuiden data set, some unreliable data values have been detected as well. Constant wind speed values were found for the entire 10 minute time period as shown in Fig [37] below. This resulted in the standard deviation and turbulence intensity to become zero which in principle is not possible. Since this situation occurred only a few times during the month of May (2012), these entire 10 min segments were removed and treated in the same way as Nan values or missing data values.

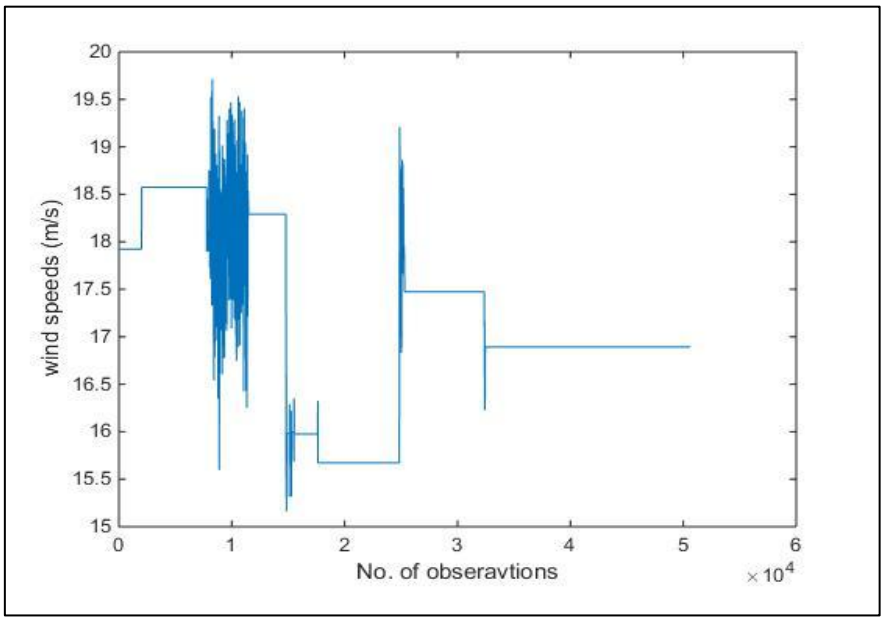

Figure 37: Various intervals of constant wind speed within a turbulent time series.

10. RESULTS AND ANALYSIS

In this section, the detailed 1 year analysis for three different data sets is presented. Various gust parameters discussed in section [7] have been identified through each of the gust detection methods listed in Section [8] of this report.

For each of the data set, the following aspects have been studied using different gust detection techniques.

1. Monthly gust distributions (To show seasonal variations)
2. Full 1 year results
3. Effect of change in characteristic time of an algorithm (OWEZ data set only)
4. Alternate mean gust compilations (OWEZ data set only)

Comparisons between different methods have been made during each of the sections while the overall analysis will be presented in the Section [11].

10.1: OWEZ 1 YEAR RESULTS

1) PEAK OVER THRESHOLD METHOD

The peak to peak to peak method (POT) and the acceleration over threshold method (AOT) requires the user to define the gust criteria. Table [7] below shows the criteria used throughout this section for the 1 year data sets of OWEZ, IJmuiden and Cabauw. The characteristic time is only used for the AOT method to calculate the acceleration values. The calculated acceleration values are used to compare against the acceleration threshold criteria "a_T".

S. No.	Parameters	Symbols	Values
2	Gust threshold criteria	x	20 m/s
3	Gust min. duration criteria	d	5 seconds
4	Gust max. duration criteria	d_{max}	15 seconds
5	Characteristic time	τ	1 seconds
6	Acceleration criteria	a_T	0.5 m/s^2

Table 7: Gust criteria used for POT and AOT methods (1 year data sets).

The detailed results for different gust parameters are saved separately. Wind speed values for +/- 5 seconds around the gust amplitude have been saved which were used for plotting the mean gust shapes. Table [8] shows different parameters like the absolute gust amplitude, rise time, lapse rate, duration and the mean value above the threshold. These are just the average values for the total number of gusts detected during that period (i.e. one month in this case). A total number of **9306** gusts have been detected using data for the entire year (2008) at OWEZ.

The last three columns in this table shows the average wind speed, standard deviation and turbulence intensity of the 10 minute samples. These values do not have any direct significance for the wind gusts but they have been calculated and shown here just to give an idea about the wind patterns for each specific month. Furthermore, they are also required for the alternate compilations for mean gust shapes.

Month	GUSTS counts	Amplitude	Rise Time	Lapse rate	Duration	Mean	AVERAGE	STD	TI
Jan	2921	22.48	3.74	4.76	8.5	21.24	13.19	0.82	0.05
Feb	1612	22.46	3.86	4.72	8.58	21.24	9.62	0.59	0.04
Mar	2176	22.52	3.76	4.86	8.62375	21.28	11.38	0.82	0.06
Apr	13	21.67	3.94	3.25	7.19	20.82	7.84	0.55	0.05
May	0	-	-	-	-	-	-	-	-
June	38	21.73	3.39	4.3	7.7	20.86	6.9	0.5	0.06
July	59	21.33	3.15	5.06	8.22	20.65	7.52	0.59	0.06
Aug	650	21.96	3.83	4.55	8.38	20.98	9.26	0.66	0.06
Sept	233	21.6	3.6	4.77	8.37	20.8	7.98	0.65	0.07
Oct	812	22.32	3.9	4.79	8.69	21.15	9.73	0.69	0.06
Nov	786	22.43	3.78	4.67	8.46	21.21	10.08	0.755	0.07
Dec	6	21.78	3.83	4.2	8.04	20.8	8.95	0.65	0.06

Table 8: Monthly distribution of different gust parameters as calculated through POT method.

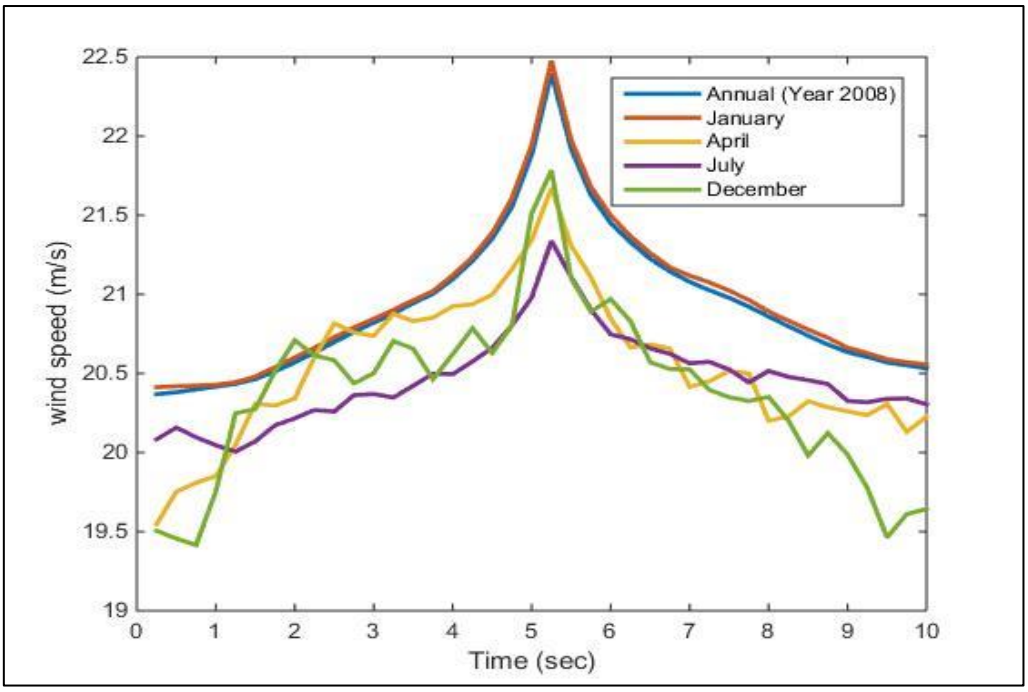

Figure 38: Monthly Distribution of mean gust shapes (POT method).

2) ACCELERATION OVER THRESHOLD METHOD

Table [9] shows the results using AOT method for the same gust parameters. The AOT method uses additional criteria for defining the wind gusts. As expected, the number of gusts detected reduced significantly to **4777** for the entire year. The threshold criteria for acceleration was selected arbitrarily through trial and error. A value of **0.5 m/s2** has been selected such that significant number of gusts could be detected for the same amplitude and duration criteria as what was previously used for the POT method. A better estimate for acceleration values would eventually be determined through peak to peak and velocity increment methods. Fig [39] shows the number of gusts detected through POT and AOT methods at OWEZ throughout the year 2008.

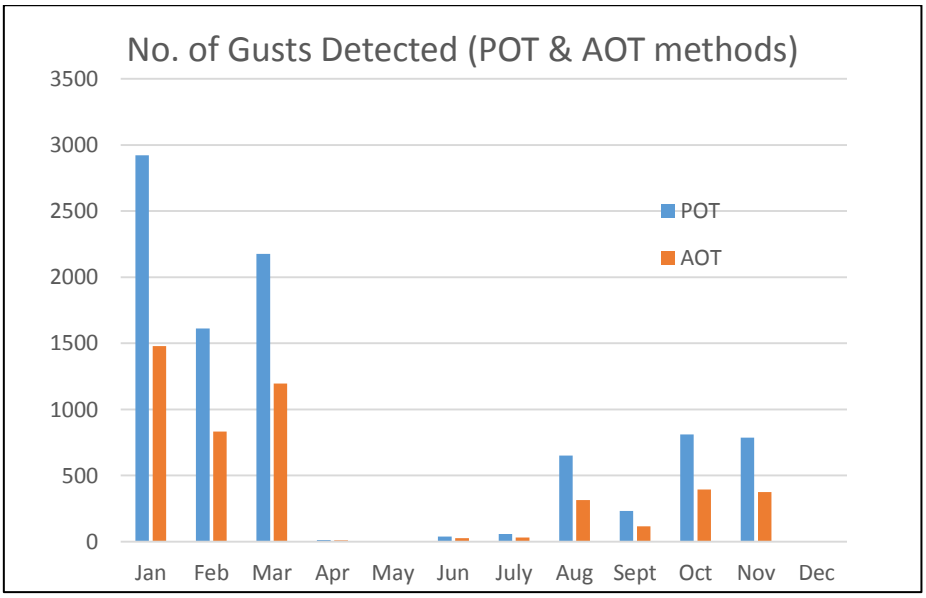

Figure 39: Number of gusts detected for each month through POT and AOT method.

Fig. [40] shows the mean gust shapes for different months obtained through AOT method.

Month	GUSTS counts	Amplitude	Rise Time	Lapse rate	Duration	Mean	AVERAGE	STD	TI
Jan	1478	22.45	3.58	4.81	8.4	21.23	13.19	0.82	0.05
Feb	833	22.45	3.7	4.83	8.53	21.25	9.62	0.59	0.04
Mar	1195	22.48	3.612	4.9	8.52	21.26	11.38	0.82	0.06
Apr	9	21.4	3.8	3.55	7.36	20.84	7.84	0.55	0.05
May	0	-	-	-	-	-	-	-	-
June	26	21.81	3.35	4.05	7.41	20.91	6.9	0.5	0.06
July	32	21.32	3.16	4.64	7.81	20.62	7.52	0.59	0.06
Aug	314	22	3.67	4.7	8.37	21	9.26	0.66	0.06
Sept	116	21.66	3.26	5.17	8.43	20.82	7.98	0.65	0.07
Oct	394	22.21	3.7	4.93	8.64	21.1	9.73	0.69	0.06
Nov	375	22.42	3.68	4.83	8.52	21.21	10.08	0.755	0.07
Dec	5	21.72	3.6	4.2	7.8	20.78	8.95	0.65	0.06

Table 9: Monthly distribution of different gust parameters as calculated through AOT method.

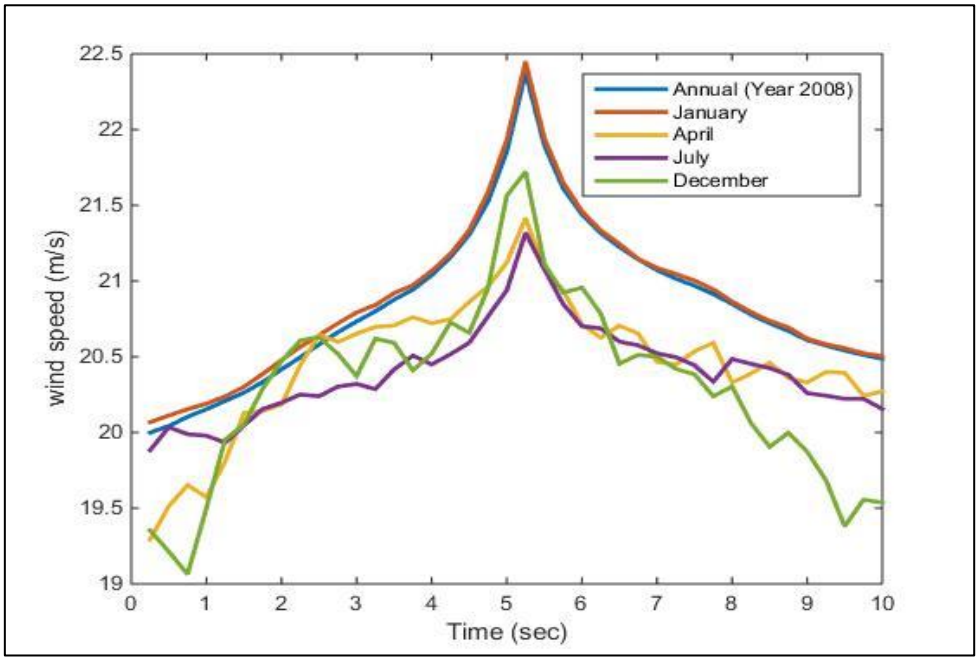

Figure 40: Monthly distributions of mean gust shapes (AOT method).

The following observations can be made from the results of the POT and AOT methods,

1. The occurrence of wind gusts is linked to the average wind speed values. Generally the occurrence of wind gusts is highest for the months when the average wind speed is also higher.
2. The rising time of wind gusts is found to be much smaller than its lapse rate in general which means, wind gusts takes lesser time to reach their peak value than to return back to their original average wind speeds values.
3. A comparison of Fig [38] and Fig [40] shows that the mean gust shapes obtained through both POT and AOT method shows similar patterns. Generally for summer months when the average wind speed is lower, lesser number of gusts were detected and gust peak were also much smaller in terms of magnitude.

3) PEAK TO PEAK METHOD

The peak to peak method and the velocity increment method are based on the moving window technique. These methods are particularly suited for detecting the velocity changes happening over small scale. As discussed earlier in Section [5] of this report, the size of a moving window can be related to the characteristic time of the algorithm.

The step change size may also be set differently in order to move the window along the time series. For maximum accuracy, a step change size of 0.25 seconds (limited by the frequency of the data set, 4 Hz) is recommended in the case of OWEZ. A larger step change size like 0.5 or 1 second could speed up the processing of the algorithms at the loss of some accuracy because it would skip some of the turbulent peaks occurring within 1 second. The results presented below are compiled using the following values,

- Characteristic time of the algorithm (τ) = 1 second.
- Step change size = 0.25 seconds

The detailed results for different gust parameters are again saved separately for every 10 minute sample because the peak to peak method and the velocity increment method, as per definition, detect a maximum gust for each 10 minute sample.

Wind speed values for +/- 5 seconds around the location where this maximum gust occurs are also recorded for every 10 minute sample. These values were used for plotting the mean gust shapes.

Table [10] shows different parameters like the maximum relative gust amplitude and the maximum acceleration occurring during the 10 minute period. These are just the average values for all the 10 minute samples during that period (i.e. one month in this case). Just like the POT and AOT methods, the last three columns in this table shows the average wind speed, standard deviation and turbulence intensity of the 10 minute samples on average.

Month	No. of 10 minute samples	GUSTS counts	Relative Amplitude (m/s)	ACCEL (m/s2)	AVERAGE	STD	TI
Jan	4356	4356	2.28	3.27	13.19	0.82	0.05
Feb	4112	4112	1.59	2.29	9.62	0.59	0.04
Mar	4271	4271	2.05	2.97	11.38	0.82	0.06
Apr	4090	4090	1.46	2.11	7.84	0.55	0.05
May	4417	4417	2.11	3.08	7.47	0.73	0.08
June	4254	4254	1.22	1.75	6.9	0.5	0.06
July	4330	4330	1.46	2.13	7.52	0.59	0.06
Aug	4345	4345	1.6	2.28	9.26	0.66	0.06
Sept	4228	4228	1.6	2.34	7.98	0.65	0.07
Oct	4291	4291	1.61	2.31	9.73	0.69	0.06
Nov	2741	2741	1.81	2.62	10.08	0.755	0.07
Dec	3618	3618	1.66	2.46	8.95	0.65	0.06

Table 10: Monthly distributions of different gust parameters as calculated through peak to peak method. (τ=1sec)

Fig. [41] shows the mean gust shape obtained through peak to peak method for the OWEZ data set during the entire year (2008).

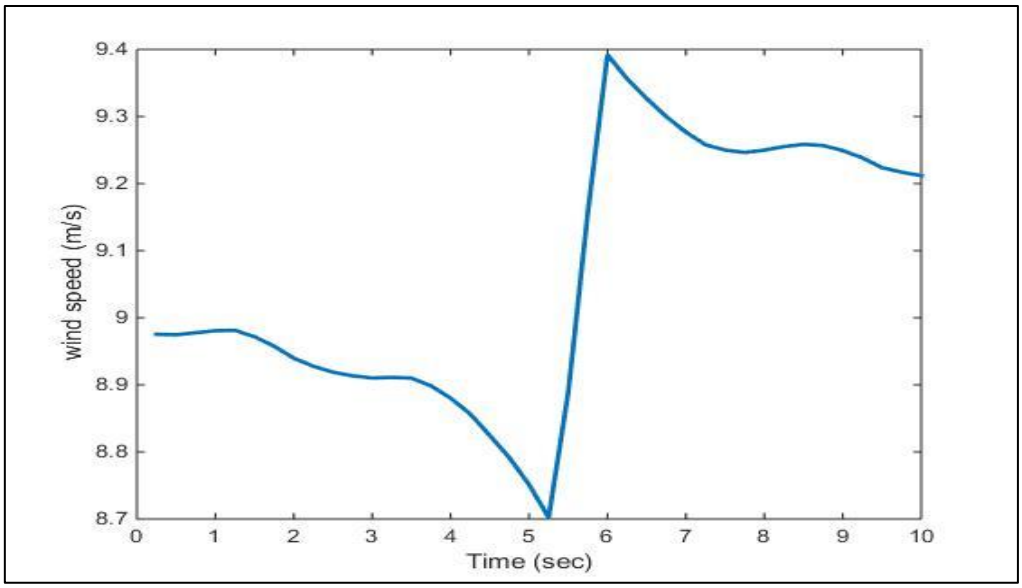

Figure 41: Mean gust shape, point of maximum fluctuation for every 10 minute sample. (Peak to peak method)

4) VELOCITY INCREMENT METHOD

Table [11] shows the results using velocity increment method (VIT) for the same gust parameters as identified through peak to peak method. In this study, the acceleration values computed were identical to the relative gust amplitude because the size of the moving window "τ" is 1 second and the relative gust amplitude has also been defined as the maximum change in velocity happening over the starting and ending points of the moving window.

Month	No. of 10 minute samples	GUSTS counts	Relative Amplitude (m/s)	ACCEL (m/s2)	AVERAGE	STD	TI
Jan	4356	4356	2.26	2.26	13.19	0.82	0.05
Feb	4112	4112	1.58	1.58	9.62	0.59	0.04
Mar	4271	4271	2.04	2.04	11.38	0.82	0.06
Apr	4090	4090	1.45	1.45	7.84	0.55	0.05
May	4417	4417	2.08	2.08	7.47	0.73	0.08
June	4254	4254	1.21	1.21	6.9	0.5	0.06
July	4330	4330	1.45	1.45	7.52	0.59	0.06
Aug	4345	4345	1.58	1.58	9.26	0.66	0.06
Sept	4228	4228	1.59	1.59	7.98	0.65	0.07
Oct	4291	4291	1.6	1.6	9.73	0.69	0.06
Nov	2741	2741	1.79	1.79	10.08	0.755	0.07
Dec	3618	3618	1.65	1.65	8.95	0.65	0.06

Table 11: Monthly distributions of different gust parameters as calculated through VIT method. (τ=1sec)

Fig. [42] shows the mean gust shape obtained through the VIT method for the OWEZ data set during the entire year (2008). Monthly comparisons between peak to peak method and the velocity increment method is shown in Fig. [43].

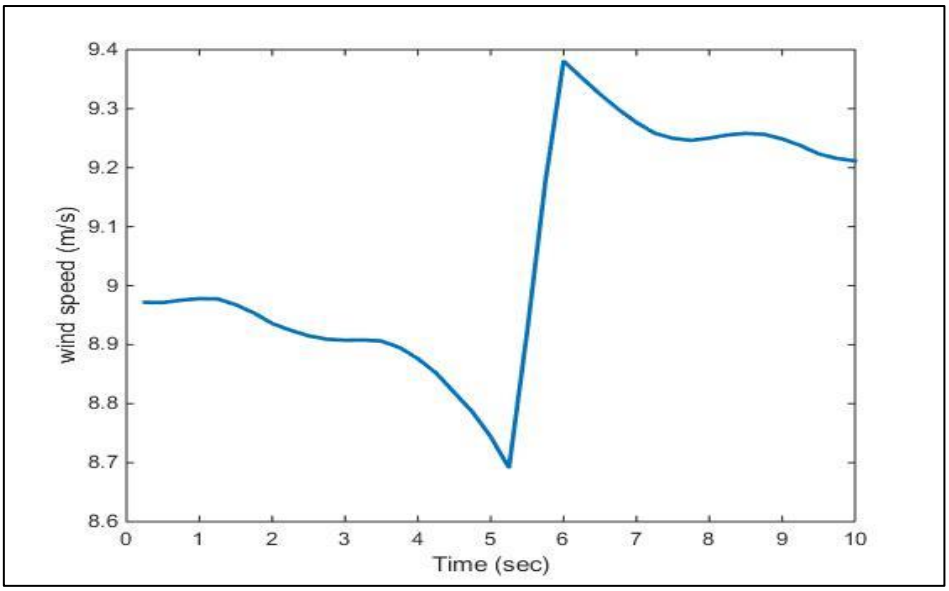

Figure 42: Mean gust shape, point of maximum fluctuation for every 10 minute sample. (VIT Method).

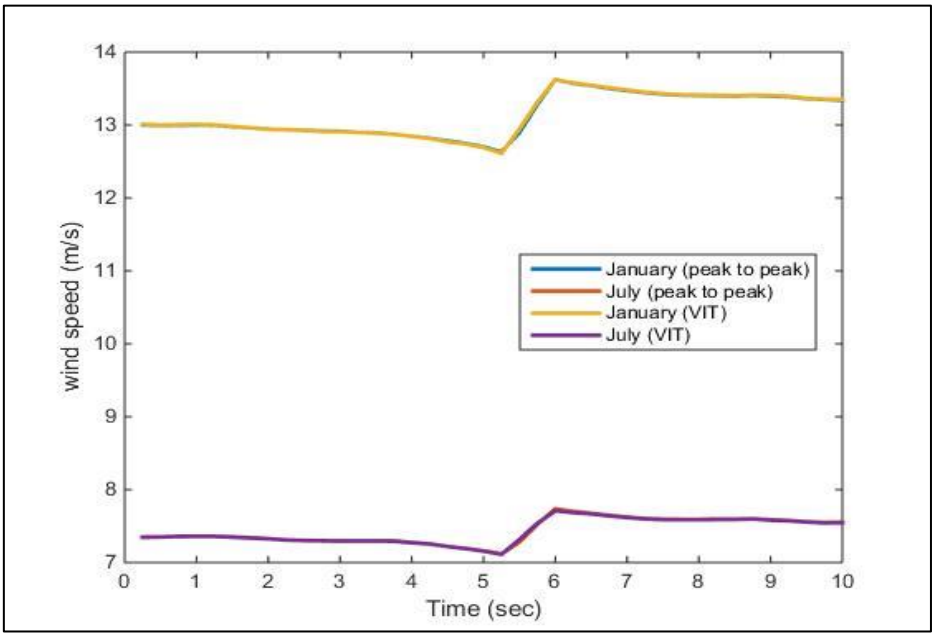

Figure 43: Comparison between peak to peak and velocity increment methods for different months.

Following observations can be made from the results of the peak to peak and velocity increment methods.

1. On average, the maximum gusts for 10 minute wind samples are accompanied by acceleration values much greater than 0.5 m/s^2 (hence the acceleration threshold criteria used for AOT method was much smaller). However this may not be potentially dangerous depending upon the application under consideration because of the very low wind speeds at which these changes in velocities takes place.
2. The acceleration values calculated for velocity increment method are much lower than peak to peak method because it computes the velocity difference only at the starting and the ending points of the moving window. A much greater change in velocity over a time period shorter than "τ" might take place within the moving window which will be detected by peak to peak method but missed by the VIT method.

3. Both the peak to peak method and the VIT method show that the maximum relative gust amplitude and the maximum acceleration occurring for each 10 minute sample is generally higher when the average wind speeds were higher as well.

COMPARASONS OF RESULTS FOR DIFFERENT TIME SCALES

In section [5] of this report, some guidelines have been provided for selecting the appropriate length of a moving window. While different values for "τ" can be used for a more comprehensive study, the following analysis has been performed to highlight the impact of different lengths of moving window.

The analysis has been performed keeping the step change size of 0.25 seconds for maximum accuracy.

3 SECONDS GUSTS

PEAK TO PEAK METHOD

Month	No. of 10 minute samples	GUSTS counts	Relative Amplitude (m/s)	ACCEL (m/s2)	AVERAGE	STD	TI
Jan	4356	4356	3.09	1.47	13.19	0.82	0.05
Feb	4112	4112	2.15	1.05	9.62	0.59	0.04
Mar	4271	4271	2.8	1.33	11.38	0.82	0.06
Apr	4090	4090	1.96	0.98	7.84	0.55	0.05
May	4417	4417	2.8	1.37	7.47	0.73	0.08
June	4254	4254	1.66	0.82	6.9	0.5	0.06
July	4330	4330	1.96	0.98	7.52	0.59	0.06
Aug	4345	4345	2.17	1.06	9.26	0.66	0.06
Sept	4228	4228	2.18	1.06	7.98	0.65	0.07
Oct	4291	4291	2.21	1.07	9.73	0.69	0.06
Nov	2741	2741	2.49	1.19	10.08	0.755	0.07
Dec	3618	3618	2.24	1.14	8.95	0.65	0.06

Table 12: Monthly distributions of different gust parameters as calculated through VIT method. (τ=3sec)

VELOCITY INCREMENT METHOD

Month	No. of 10 minute samples	GUSTS counts	Relative Amplitude (m/s)	ACCEL (m/s2)	AVERAGE	STD	TI
Jan	4356	4356	2.26	2.26	13.19	0.82	0.05
Feb	4112	4112	2.03	0.68	9.62	0.59	0.04
Mar	4271	4271	2.65	0.88	11.38	0.82	0.06
Apr	4090	4090	1.85	0.62	7.84	0.55	0.05
May	4417	4417	2.65	0.88	7.47	0.73	0.08
June	4254	4254	1.57	0.52	6.9	0.5	0.06
July	4330	4330	1.86	0.62	7.52	0.59	0.06
Aug	4345	4345	2.05	0.68	9.26	0.66	0.06
Sept	4228	4228	2.07	0.69	7.98	0.65	0.07
Oct	4291	4291	2.09	0.7	9.73	0.69	0.06
Nov	2741	2741	2.36	0.77	10.08	0.755	0.07
Dec	3618	3618	2.11	0.70	8.95	0.65	0.06

Table 13: Monthly distributions of different gust parameters as calculated through VIT method. (τ=3sec)

5 SECONDS GUSTS

PEAK TO PEAK METHOD

Month	No. of 10 minute samples	GUSTS counts	Relative Amplitude (m/s)	ACCEL (m/s2)	AVERAGE	STD	TI
Jan	4356	4356	3.42	1	13.19	0.82	0.05
Feb	4112	4112	2.4	0.75	9.62	0.59	0.04
Mar	4271	4271	3.12	0.91	11.38	0.82	0.06
Apr	4090	4090	2.18	0.65	7.84	0.55	0.05
May	4417	4417	3.09	0.92	7.47	0.73	0.08
June	4254	4254	1.88	0.55	6.9	0.5	0.06
July	4330	4330	2.19	0.64	7.52	0.59	0.06
Aug	4345	4345	2.43	0.71	9.26	0.66	0.06
Sept	4228	4228	2.44	0.71	7.98	0.65	0.07
Oct	4291	4291	2.5	0.74	9.73	0.69	0.06
Nov	2741	2741	2.8	0.79	10.08	0.755	0.07
Dec	3618	3618	2.49	0.76	8.95	0.65	0.06

Table 14: Monthly distributions of different gust parameters as calculated through peak to peak method. (τ=5sec)

VELOCITY INCREMENT METHOD

Month	No. of 10 minute samples	GUSTS counts	Relative Amplitude (m/s)	ACCEL (m/s2)	AVERAGE	STD	TI
Jan	4356	4356	3.17	0.63	13.19	0.82	0.05
Feb	4112	4112	2.21	044	9.62	0.59	0.04
Mar	4271	4271	2.9	0.58	11.38	0.82	0.06
Apr	4090	4090	2.01	0.4	7.84	0.55	0.05
May	4417	4417	2.87	0.57	7.47	0.73	0.08
June	4254	4254	1.73	0.35	6.9	0.5	0.06
July	4330	4330	2.03	0.41	7.52	0.59	0.06
Aug	4345	4345	2.25	0.45	9.26	0.66	0.06
Sept	4228	4228	2.26	0.45	7.98	0.65	0.07
Oct	4291	4291	2.32	0.46	9.73	0.69	0.06
Nov	2741	2741	2.6	0.52	10.08	0.755	0.07
Dec	3618	3618	2.3	0.46	8.95	0.65	0.06

Table 15: Monthly distributions of different gust parameters as calculated through VIT method. (τ=5sec)

For different values of τ, fig. [44] [45] shows the plots for mean gust shapes obtained for peak to peak and VIT methods respectively.

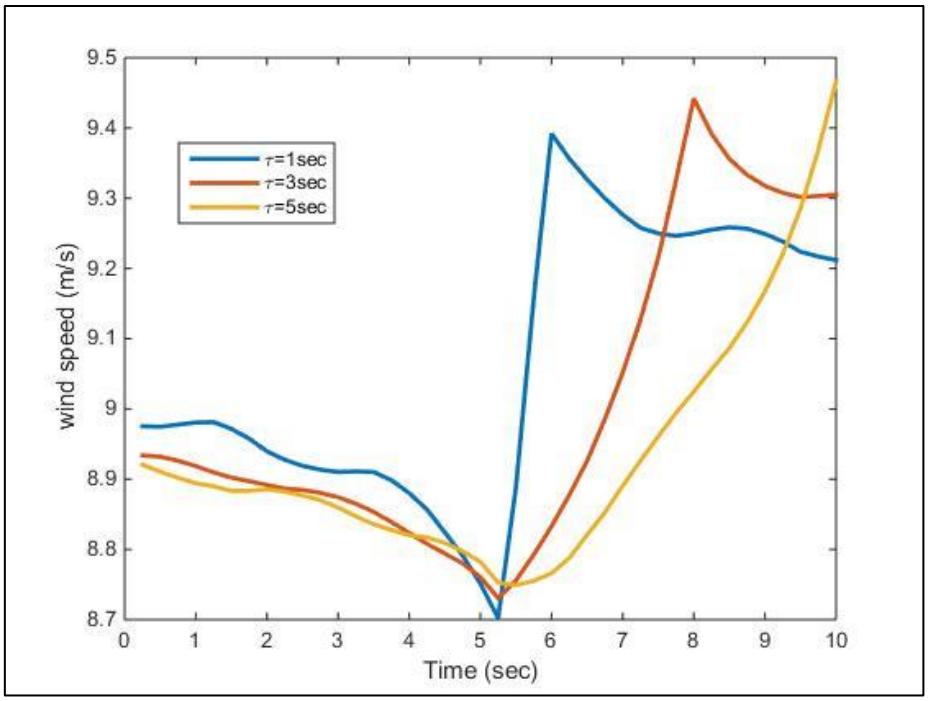

Figure 44: Mean gust shapes for different values of τ (peak to peak method).

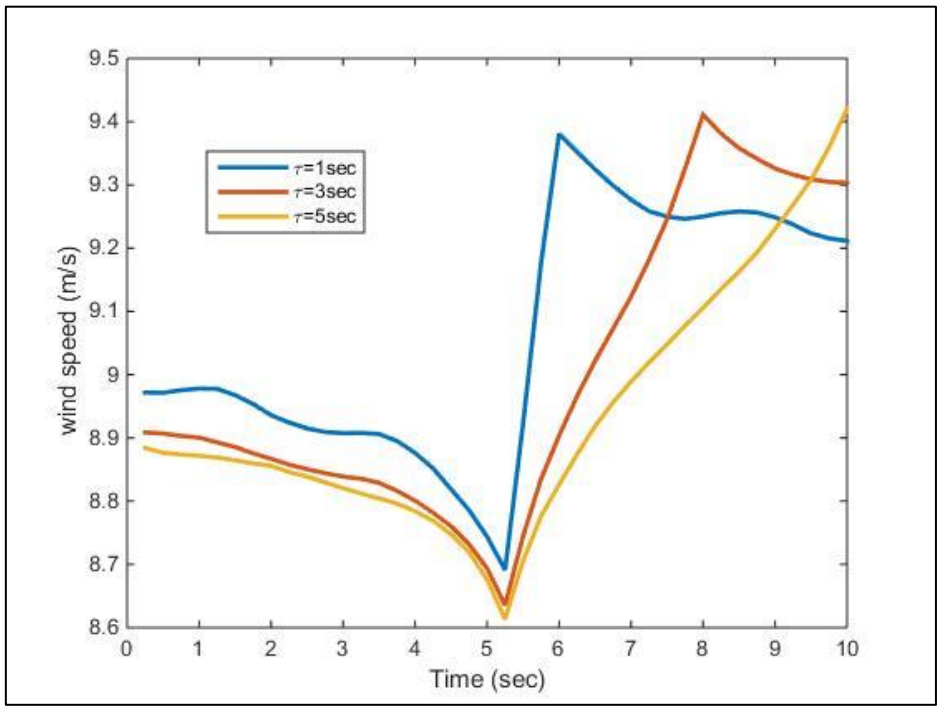

Figure 45: Mean gust shapes for different values of τ (VIT method).

The following observations can be made from the results of the peak to peak and velocity increment methods.

1. For the increasing values of τ, the difference between the maximum and minimum wind speed value (in case of peak to peak) and the first and last wind speed value (in case of VIT) generally increases slightly. This is because the window size is increasing (based on the value of τ).
2. This difference between extremes is spread over a larger time period, hence the curve becomes more horizontal.

3. The slight increase in gust amplitude with the increasing values of τ is also accompanied with the increase in time interval over which these velocity changes are recorded. Hence the resulting acceleration values for the maximum 10 minute gusts drops.

An important outcome of this parametric study for the variation of "τ" is the estimate about the acceleration threshold criteria used for the AOT method. Earlier, the threshold of 0.5 m/s^2 was chosen arbitrarily and the initial estimates using peak to peak and VIT method (with τ = 1 sec) suggested that the maximum gusts for 10 minute are usually accompanied with acceleration values greater than 0.5 m/s^2. However, with the increasing values of τ, we can observe a decreasing acceleration value for an average maximum 10 minute gust as shown in Table [12] to Table [15].

This is also expected, based on the understanding that the size of the moving window increases with the increasing characteristic time. As a consequence, the difference between maxima and minima (in case of peak to peak method) or the first and the last value (in case of VIT method) of the moving window is defined over a larger period of time. Therefore the computed acceleration values for maximum 10 minute gusts would become smaller. In short,

Depending upon the selected criteria for the characteristic time "τ" based on the ACF of the atmospheric turbulence, we can define a suitable acceleration threshold for the AOT method.

For example, in the analysis presented above in Table [14] [15], in general, for a maximum 10 min wind speed fluctuation, the accompanied acceleration would usually be somewhere between 0.5 to 1 m/s^2. Hence a threshold criteria greater than 1 m/s^2 for AOT method would not be of much use, as it will only serve to significantly reduce the number of gusts detected.

ALTERNATE MEAN GUST COMPILATIONS

For the purpose of clarity, the mean gust shapes can be plotted in different ways. For instance, gusts can be distinguished based on the average wind conditions of the environment in which they occur. Hence the average 10 minute statistics may be utilized to highlight different type of gusts. The peak over threshold (POT) method has been used for the following presentations of different mean gust compilations.

GUSTS AT DIFFERENT 10 MINUTE AVERAGE WIND SPEEDS

The gusts corresponding to different 10 minute wind speed intervals are presented here. With POT method, a total no. of **9306** gusts have been identified earlier. Since all of these gusts occurred randomly throughout the year 2008 at OWEZ site, we have different 10 minute wind speed averages corresponding to the occurrence of individual gusts.

Three different wind speed categories have been defined in Table [16]. The criteria used for defining these categories is the visual inspection of the individual time series for each month of year 2008 at OWEZ. It is found that the occurrence of wind gust during the 10 minute sample with an average wind speed of lower than 15 m/s is extremely rare. This situation is due to the threshold criteria for POT method as specified in Table [7].

S. No.	Wind Speed Category	10 minute AVERAGE	No. of occurrences (2008)
1.	High wind gusts	>20 m/s	5354
2.	Medium wind gusts	15 – 20 m/s	3951
3.	Low wind gusts	<15 m/s	1

Table 16: Different categories of wind speeds for distinguishing gusts.

Fig. [46] shows the results for the mean gust shapes obtained for each wind speed category.

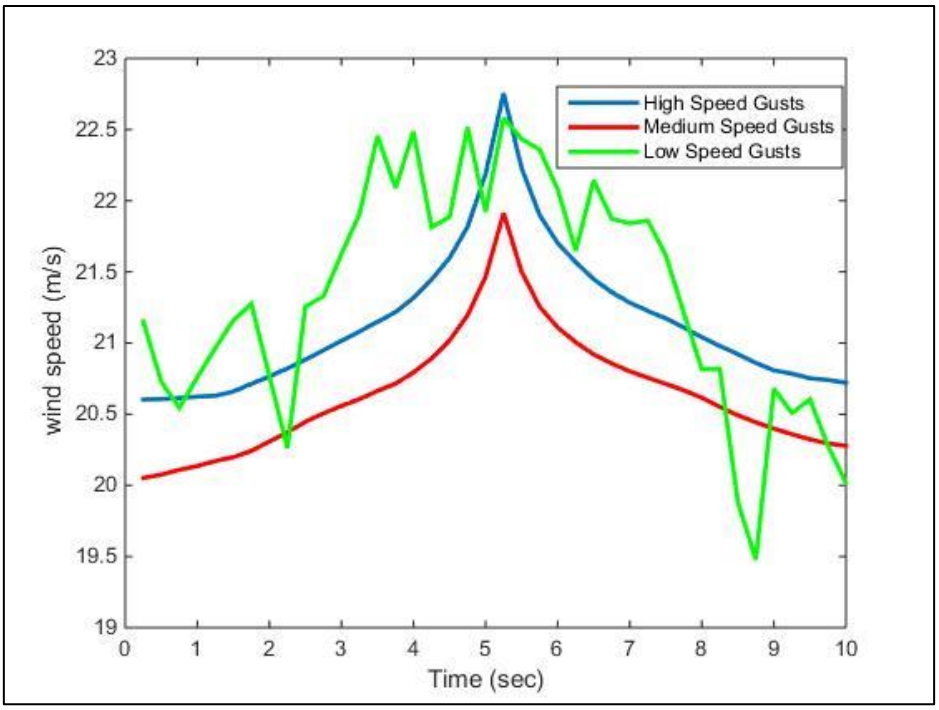

Figure 46: Wind gusts occurring at different wind speed ranges (bins).

The following observations can be made based on the results,

1. The gusts occurring at high wind speeds are typically narrower in comparison to low or medium wind speed gusts which means that the difference between the maximum peak and the minimum wind speed value within the gust would also be larger for high speed gust.
2. The average difference is found to be **2.15 m/s** for high speed gusts and **1.86 m/s** for medium speed gusts.
3. This difference is not very large owing to the fact that the average wind speeds for high speed and medium speed gusts are also quite close here. Therefore a larger and noticeable difference is expected if low speed gusts have been compared with the high speed gusts.
4. Due to just a single occurrence of low speed gust, it is not possible to obtain a true representative mean gust shape for this category.

10.2: IJMUIDEN 1 YEAR RESULTS

The second data set analyzed for this research work is from the far offshore location of IJmuiden in the North Sea for the year 2012.

The preliminary analysis at IJmuiden was performed without taking into consideration, the tower shadow effects i.e. only the sonic wind speed data from the NW boom was taken. The analysis presented here in this section takes into consideration the tower shadow effects. Table [17] gives a brief comparison of the results obtained with or without tower shadow effects for the Ijmuiden data set.

Month	Gusts Detected (without tower shadow checks)	Gusts Detected (with tower shadow checks)
Jan	3575	3561
Feb	906	883
Mar	124	113
Apr	935	789
May	267	211
June	1092	958
July	-	-
Aug	246	273
Sept	128	128
Oct	302	292
Nov	980	883
Dec	4147	4005
Total	**12702**	**12096**

Table 17: Comparison between gusts counted with or without tower shadow effects. (POT method)

As it can be seen from the Table [17], a slightly smaller number of wind gusts are detected when appropriate tower shadow effects are incorporated. This is quite reasonable because sudden disappearance of a measuring sensor behind the tower might cause the measured wind speeds to fluctuate rapidly. These sudden fluctuations may be mistaken as a wind gust by the gust detection algorithms if appropriate tower shadow effects are not incorporated.

The number of gusts detected without considering proper tower shadow effects, would be higher.

With reference to the tower shadow effects, similar approach has been used as it was used for the OWEZ data set and the wind speeds are selected from the sensors of the relevant booms or a combination of booms based upon the direction of the incoming wind speed.

However, the difference is about the way in which wind direction is obtained. While the wind direction data is directly available in case of OWEZ, for IJmuiden, the two wind speed components present in the horizontal planes were resolved using basic trigonometry so that the angle for the resultant incoming wind can be calculated.

The results obtained from different gust detection algorithms for the 1 year data set of IJmuiden are presented below,

1. PEAK OVER THRESHOLD METHOD

In order to ensure the uniformity of comparison between different sites, the gust criteria defined for POT and AOT methods have been kept the same as mentioned in Table [7] with reference to the OWEZ data set.

Again the detailed results for different gust parameters were saved separately. Wind speed values for +/- 5 seconds around the gust amplitude have been saved which were used for plotting the mean gust shapes. Table [18] shows different parameters like the absolute gust amplitude, rise time, lapse rate, duration and the mean value above the threshold. A total number of **12702** gusts have been detected using the data set for the entire year (2012) at IJmuiden.

Month	GUSTS counts	Amplitude	Rise Time	Lapse rate	Duration	Mean	AVERAGE	STD	TI
Jan	3561	22.32	3.93	4.8	8.73	21.18	11.93	0.78	0.06
Feb	883	22.15	3.73	4.66	8.4	21.08	10.73	0.67	0.06
Mar	113	21.6	3.68	4.77	8.45	20.77	7.76	0.33	0.03
Apr	789	21.56	3.68	4.58	8.26	20.8	9.26	0.52	0.05
May	211	21.58	3.86	4.36	8.22	20.95	9.05	0.37	0.03
June	958	21.98	3.83	4.89	8.72	21.01	9.63	0.46	0.04
July	-						7.51	0.38	0.04
Aug	273	21.62	3.86	4.54	8.41	20.81	7.64	0.38	0.04
Sept	128	22.16	3.75	4.59	8.34	21.08	9.45	0.61	0.06
Oct	292	21.62	3.65	4.7	8.35	20.81	9.46	0.65	0.06
Nov	883	21.9	4.02	4.61	8.63	20.96	10.37	0.7	0.06
Dec	4005	21.98	3.8	4.77	8.58	21	11.94	0.81	0.06

Table 18: Monthly distribution of different gust parameters as calculated through POT method.

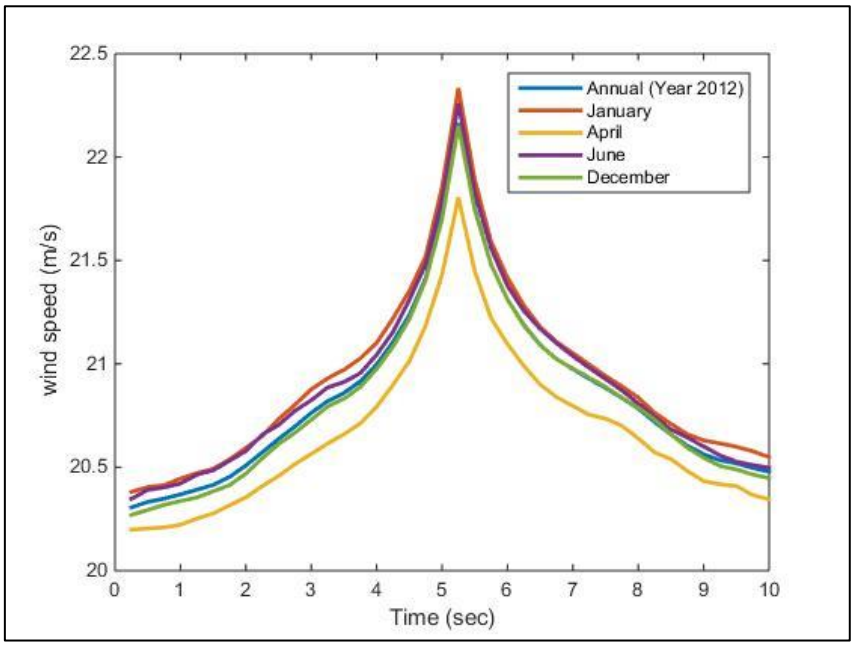

Figure 47: Monthly distributions of mean gust shapes (POT method).

2. ACCELERATION OVER THRESHOLD METHOD

Table [19] shows the results using AOT method for the same gust parameters. The AOT method uses additional acceleration threshold criteria for defining the gust. As expected, the number of gusts detected reduced to **6124** for the entire year. The threshold criteria for acceleration was kept the same as that for OWEZ. Fig [48] shows the number of gusts detected through POT and AOT methods while Fig. [49] shows the mean gust shapes for different months obtained through AOT method.

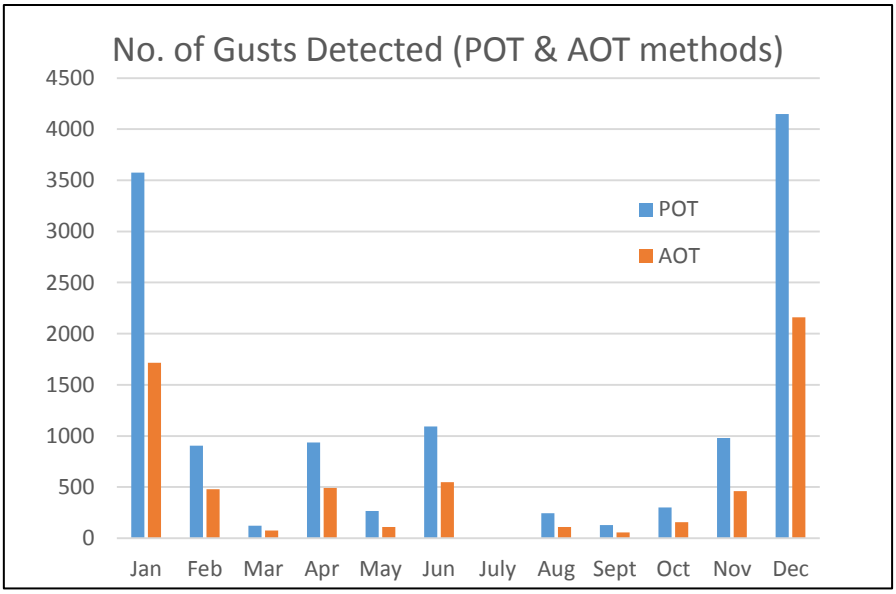

Figure 48: Number of gusts detected for each month through POT and AOT methods.

Month	GUSTS counts	Amplitude	Rise Time	Lapse rate	Duration	Mean	AVERAGE	STD	TI
Jan	1710	22.3	3.76	4.86	8.62	21.18	11.93	0.7	0.06
Feb	456	22.15	3.62	4.7	8.32	21.1	10.73	0.67	0.06
Mar	66	21.58	3.53	4.86	8.39	20.78	7.76	0.33	0.03
Apr	425	21.59	3.44	4.5	7.95	20.81	9.26	0.52	0.05
May	86	21.62	3.78	4.29	8.07	20.81	9.05	0.37	0.03
June	506	21.94	3.67	4.93	8.6	21	9.63	0.46	0.04
July	-	-	-	-	-	-	7.51	0.38	0.04
Aug	132	21.64	3.98	4.21	8.19	20.85	7.64	0.38	0.04
Sept	56	22.1	3.35	4.92	8.27	21.07	9.45	0.61	0.06
Oct	141	21.62	3.67	4.69	8.36	20.82	9.46	0.65	0.06
Nov	431	21.85	3.79	4.73	8.52	20.94	10.37	0.7	0.06
Dec	2115	22	3.66	4.86	8.52	21.02	11.94	0.81	0.06

Table 19: Monthly distribution of different gust parameters as calculated through AOT method.

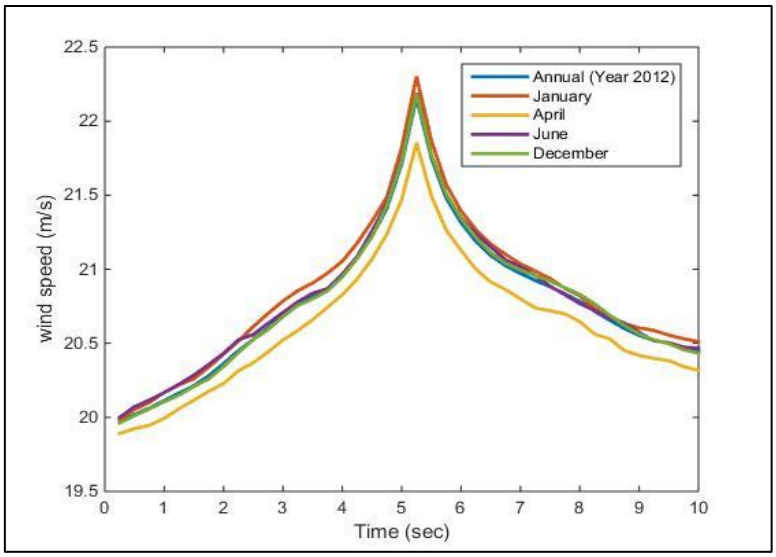

Figure 49: Monthly distributions of mean gust shapes (AOT method).

Similar observations can be made for the IJmuiden data set results as stated during the analysis of OWEZ data set. However two distinguishing observations can be made here,

- The far offshore location IJmuiden on average has higher wind speeds as compared to near offshore OWEZ site.
- The number of gusts detected through both POT and AOT methods is larger in case of IJmuiden which is expected.

3. PEAK TO PEAK METHOD

Just like the OWEZ data set, the wind speed values for +/- 5 seconds around the location where this maximum gust occurs were also recorded for every 10 minute sample. These values were used for plotting the mean gust shapes. Table [20] shows different parameters like the maximum relative gust amplitude and the maximum acceleration occurring during the 10 minute period. These are just the average values for all the 10 minute samples during that period (i.e. one month in this case). Just like the POT and AOT methods, the last three columns in this table shows the average wind speed, standard deviation and turbulence intensity of the 10 minute samples.

Month	No. of 10 minute samples	GUSTS counts	Relative Amplitude (m/s)	ACCEL (m/s2)	AVERAGE	STD	TI
Jan	4461	4461	1.8	2.54	11.93	0.78	0.06
Feb	3451	3451	1.6	2.27	10.73	0.67	0.06
Mar	3813	3813	0.79	1.08	7.76	0.33	0.03
Apr	4316	4316	1.11	1.54	9.26	0.52	0.05
May	4463	4463	0.89	1.25	9.05	0.37	0.03
June	4316	4316	1.1	1.53	9.63	0.46	0.04
July	4288	4288	0.86	1.2	7.51	0.38	0.04
Aug	4461	4461	0.83	1.15	7.64	0.38	0.04
Sept	4317	4317	1.35	1.91	9.45	0.61	0.06
Oct	4462	4462	1.39	1.96	9.46	0.65	0.06
Nov	4316	4316	1.47	2.07	10.37	0.7	0.06
Dec	4461	4461	1.81	2.58	11.94	0.81	0.06

Table 20: Monthly distribution of different gust parameters as calculated through peak to peak method.

4. VELOCITY INCREMENT METHOD

Table [21] shows the results using velocity increment method (VIT) for the same gust parameters as identified through peak to peak method. In this study, the acceleration values computed were identical to the relative gust amplitude because the size of the moving window "τ" is 1 second and the relative gust amplitude has also been defined as the maximum change in velocity happening over starting and ending points of the moving window.

Month	No. of 10 minute samples	GUSTS counts	Relative Amplitude (m/s)	ACCEL (m/s2)	AVERAGE	STD	TI
Jan	4461	4461	1.79	1.79	11.93	0.78	0.06
Feb	3451	3451	1.58	1.58	10.73	0.67	0.06
Mar	3813	3813	0.76	0.76	7.76	0.33	0.03
Apr	4316	4316	1.1	1.1	9.26	0.52	0.05
May	4463	4463	0.88	0.88	9.05	0.37	0.03
June	4316	4316	1.09	1.09	9.63	0.46	0.04
July	4288	4288	0.85	0.85	7.51	0.38	0.04
Aug	4461	4461	0.82	0.82	7.64	0.38	0.04
Sept	4317	4317	1.35	1.35	9.45	0.61	0.06
Oct	4462	4462	1.38	1.38	9.46	0.65	0.06
Nov	4316	4316	1.47	1.47	10.37	0.7	0.06
Dec	4461	4461	1.8	1.8	11.94	0.81	0.06

Table 21: Monthly distribution of different gust parameters as calculated through velocity increment method.

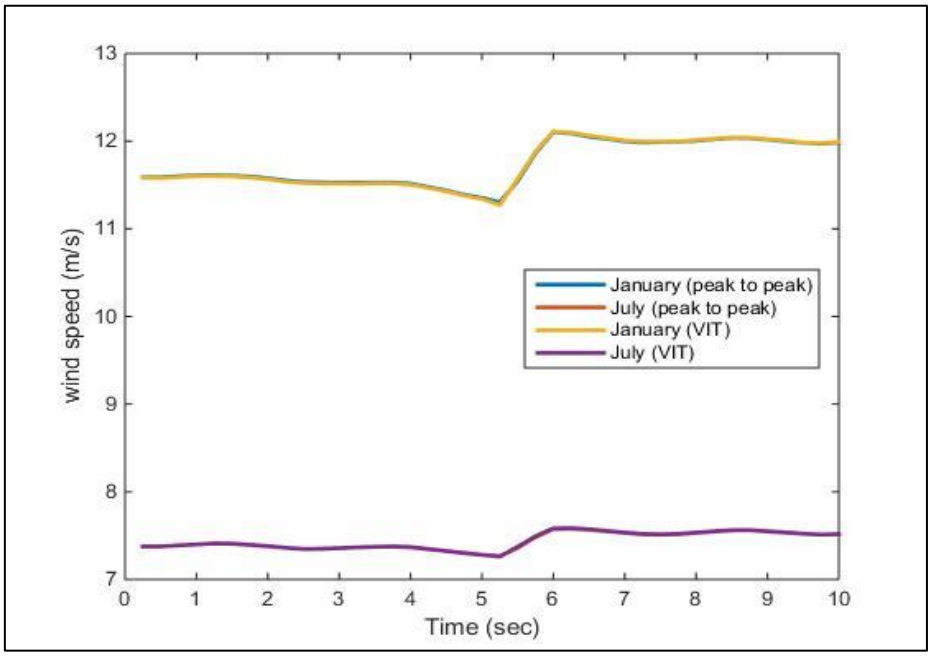

Figure 50: Comparison between peak to peak and velocity increment methods for different months.

A unique difference between OWEZ and Ijmuiden results is noticed for the winter month (January) where the occurrence of maximum 10 minute gust (on average) takes place at a higher wind speed for OWEZ.

10.3: CABAUW 1 YEAR RESULTS

The Cabauw data set is acquired from the CESAR database. It consists of sonic wind data measured at 10 Hz sampling frequency during the year 2012. A total of 194 days' data is completely available.

1. PEAK OVER THRESHOLD METHOD

In order to ensure the uniformity of comparison between different sites, the gust criteria defined for POT and AOT methods have been kept the same as mentioned in Table [7] with reference to the OWEZ data set.

Table [22] shows different parameters like the absolute gust amplitude, rise time, lapse rate, duration and the mean value above the threshold. A total number of **907** gusts have been detected using the data set for the entire year (2012).

Month	GUSTS counts	Amplitude	Rise Time	Lapse rate	Duration	Mean	AVERAGE	STD	TI
Jan	836	24.84	3.78	4.45	8.24	22.49	7.89	1.12	0.09
Feb	-	-	-	-	-	-	6.51	0.79	0.08
Mar	-	-	-	-	-	-	5.14	0.59	0.08
Apr	-	-	-	-	-	-	6.4	0.75	0.09
May	-	-	-	-	-	-	5.47	0.81	0.1
June	28	22.74	4.03	4.15	8.18	21.32	6.36	0.82	0.1
July	-	-	-	-	-	-	5.47	0.62	0.08
Aug	-	-	-	-	-	-	5.42	0.63	0.08
Sept									
Oct									
Nov									
Dec	43	23.5	3.78	3.87	7.48	21.65	8.33	0.88	0.09

Table 22: Monthly distribution of different gust parameters as calculated through POT method.

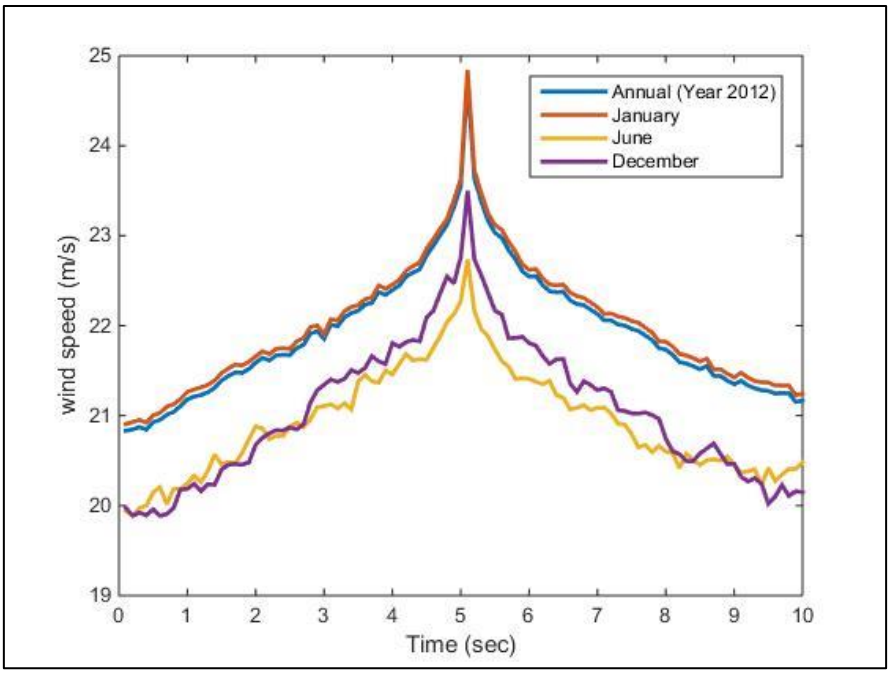

Figure 51: Monthly Distributions of mean gust shapes (POT) method.

2. ACCELERATION OVER THRESHOLD METHOD

Table [23] shows the results using AOT method for the same gust parameters. Just like the previous data sets of OWEZ and IJmuiden, the number of gusts detected reduced significantly in comparison to POT method due to the additional constraint used for AOT method. A total of **534** wind gusts are detected for the entire year of 2012. Fig [52] shows the number of gusts detected through POT and AOT methods while Fig. [53] shows the mean gust shapes for different months obtained through AOT method.

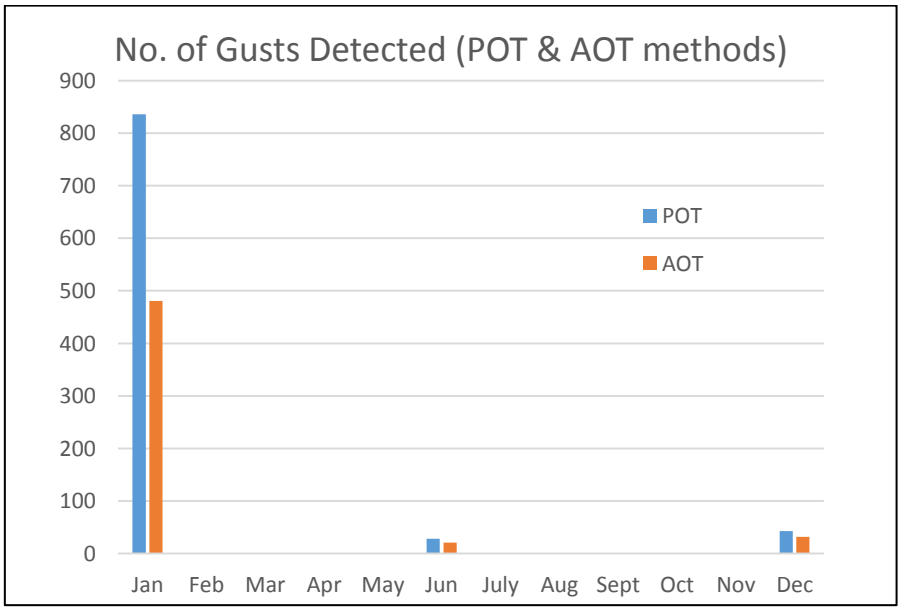

Figure 52: Number of gusts detected for each month through POT and AOT methods.

Month	GUSTS counts	Amplitude	Rise Time	Lapse rate	Duration	Mean	AVERAGE	STD	TI
Jan	481	24.91	3.74	4.46	8.2	22.53	7.89	1.12	0.09
Feb	-	-	-	-	-	-	6.51	0.79	0.08
Mar	-	-	-	-	-	-	5.14	0.59	0.08
Apr	-	-	-	-	-	-	6.4	0.75	0.09
May	-	-	-	-	-	-	5.47	0.81	0.1
June	21	22.74	3.9	4.28	8.19	21.3	6.36	0.82	0.1
July	-	-	-	-	-	-	5.47	0.62	0.08
Aug	-	-	-	-	-	-	5.42	0.63	0.08
Sept									
Oct									
Nov									
Dec	32	23.52	3.54	4.13	7.67	21.66	8.33	0.88	0.09

Table 23: Monthly distribution of different gust parameters as calculated through AOT method.

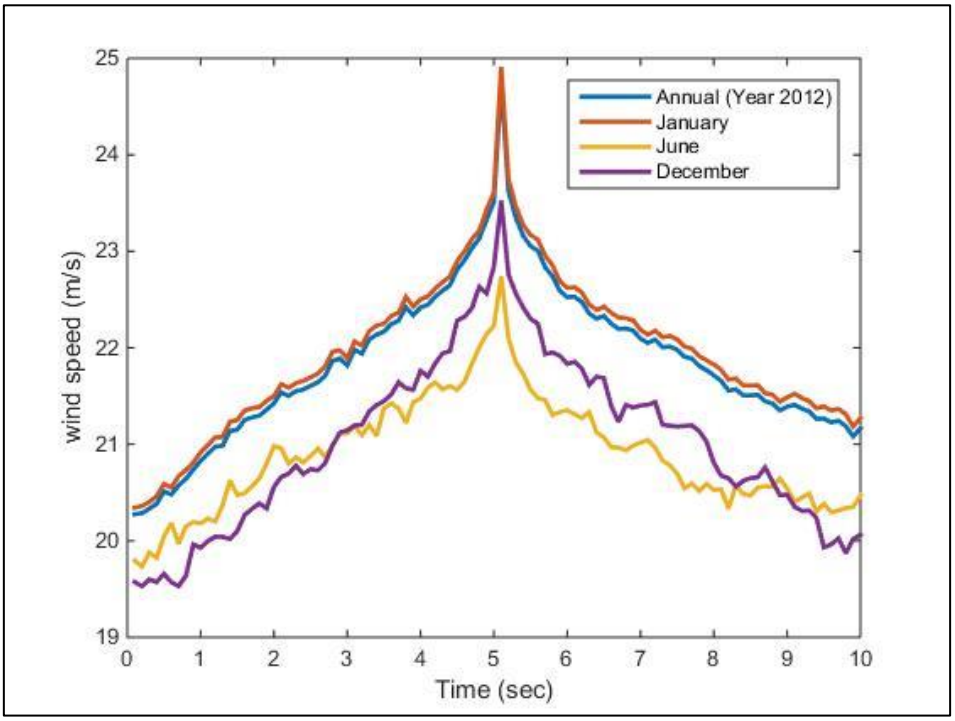

Figure 53: Monthly distributions of mean gust shapes (AOT method).

3. PEAK TO PEAK METHOD

Table [24] shows different parameters like the maximum relative gust amplitude and the maximum acceleration occurring during the 10 minute period. These are just the average values for all the 10 minute samples during that period.

Unlike, the OWEZ and IJmuiden data sets, the step change size in case of Cabauw data set is 0.1 seconds because the data is available at 10 Hz sampling frequency. Hence turbulent fluctuations of the wind speeds during each step of the moving window techniques can be recorded more accurately. The results presented below are compiled using the following values,

- Characteristic time of the algorithm (τ) = 1 second.
- Step change size = 0.1 seconds

Month	No. of 10 minute samples	GUSTS counts	Relative Amplitude (m/s)	ACCEL (m/s2)	AVERAGE	STD	TI
Jan	4440	4440	2.68	2.73	7.89	1.12	0.09
Feb	4172	4172	2.5	2.89	6.51	0.79	0.08
Mar	3453	3453	2.08	2.58	5.14	0.59	0.08
Apr	3861	3861	2.35	3.1	6.4	0.75	0.09
May	3583	3583	2.66	3.1	5.47	0.81	0.1
June	4171	4171	2.53	3.16	6.36	0.82	0.1
July	575	575	1.67	2.4	5.47	0.62	0.08
Aug	997	997	1.74	2.72	5.42	0.63	0.08
Sept	-	-	-	-	-	-	-
Oct	-	-	-	-	-	-	-
Nov	-	-	-	-	-	-	-
Dec	2586	2586	2.74	3.4	8.33	0.88	0.09

Table 24: Monthly distribution of different gust parameters as calculated through peak to peak method.

4. VELOCITY INCREMENT METHOD

Table [25] shows the results using velocity increment method (VIT) for the same gust parameters as identified through peak to peak method.

Month	No. of 10 minute samples	GUSTS counts	Relative Amplitude (m/s)	ACCEL (m/s2)	AVERAGE	STD	TI
Jan	4440	4440	2.71	2.71	7.89	1.12	0.09
Feb	4172	4172	2.41	2.41	6.51	0.79	0.08
Mar	3453	3453	1.98	1.98	5.14	0.59	0.08
Apr	3861	3861	2.25	2.25	6.4	0.75	0.09
May	3583	3583	2.58	2.58	5.47	0.81	0.1
June	4171	4316	2.43	2.43	6.36	0.82	0.1
July	575	575	1.59	1.59	5.47	0.62	0.08
Aug	997	997	1.66	1.66	5.42	0.63	0.08
Sept	-	-	-	-	-	-	-
Oct	-	-	-	-	-	-	-
Nov	-	-	-	-	-	-	-
Dec	2586	2586	2.66	2.66	8.33	0.88	0.09

Table 25: Monthly distribution of different gust parameters as calculated through velocity increment method.

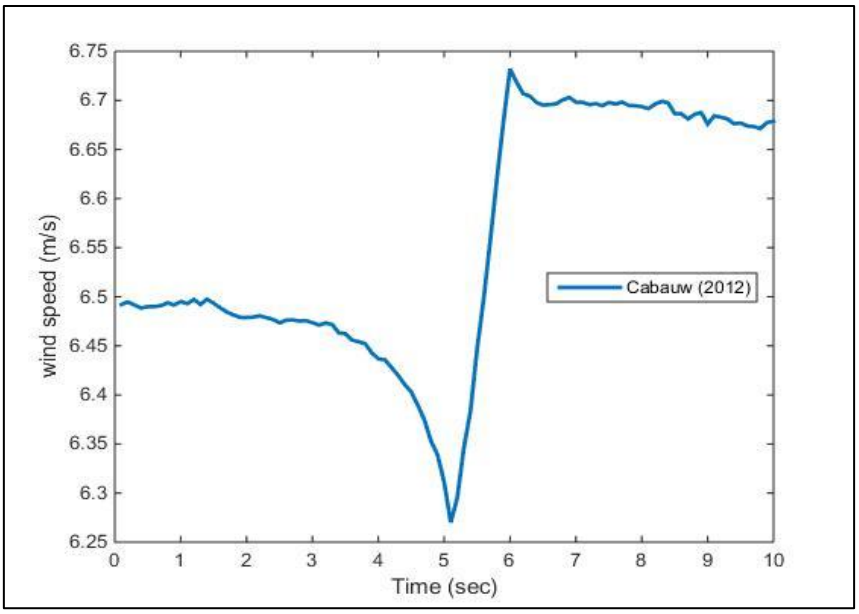

Figure 54: Peak to peak methods average gust shape for Cabauw (2012).

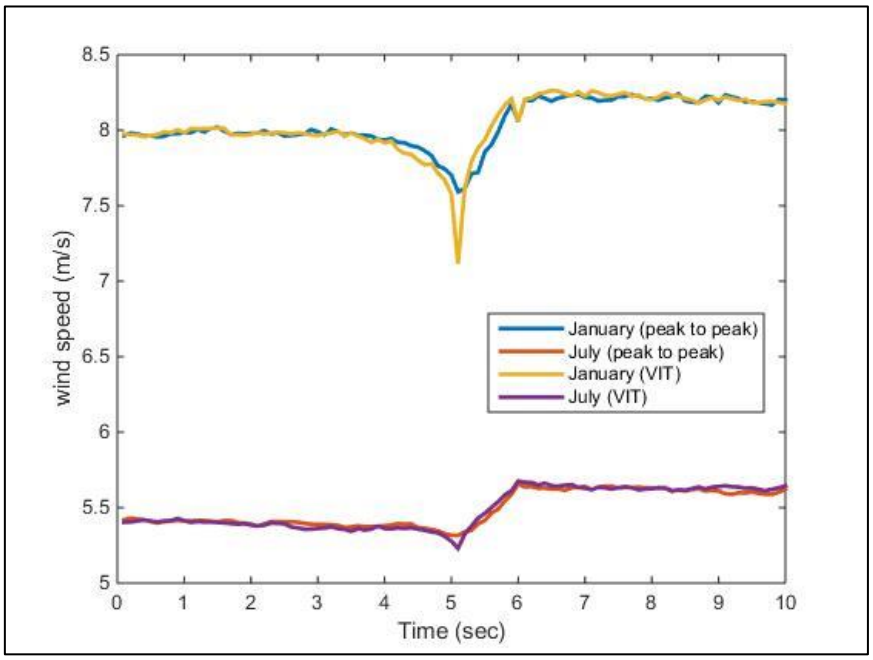

Figure 55: Comparison between peak to peak and velocity increment methods for different methods.

- The mean gust shapes obtained for both peak to peak and velocity increment methods in general contains more wiggle in case of the Cabauw data. This is due to the high sampling frequency for the wind data and as a result, more frequent oscillations have been captured around the maximum gusts.

EFFECT OF CHANGING SAMPLING FREQUENCY

The data set for Cabauw is sampled at 10 Hz frequency while the previous two data sets from OWEZ and Ijmuiden are sampled at 4 Hz frequency. In order to investigate any peculiar changes associated with the high sampling rate, the Cabauw data set is reduced to the sampling rate of 5 Hz. The gust detection analysis has been performed once again with the POT method and the results are compared with the 10 Hz. results.

PEAK OVER THRESHOLD METHOD

Table [26] shows different parameters like the absolute gust amplitude, rise time, lapse rate, duration and the mean value above the threshold. A total number of **948** gusts have been detected using the data set for the entire year (2012).

Month	GUSTS counts	Amplitude	Rise Time	Lapse rate	Duration	Mean	AVERAGE	STD	TI
Jan	871	24.5	3.66	4.66	8.32	22.32	7.89	1.12	0.09
Feb	-	-	-	-	-	-	6.51	0.79	0.08
Mar	-	-	-	-	-	-	5.14	0.59	0.08
Apr	-	-	-	-	-	-	6.4	0.75	0.09
May	-						5.47	0.81	0.1
June	28	22.53	3.63	3.9	7.52	21.2	6.36	0.82	0.1
July	-	-	-	-	-	-	5.47	0.62	0.08
Aug	-	-	-	-	-	-	5.42	0.63	0.08
Sept	-	-	-	-	-	-	-	-	-
Oct	-	-	-	-	-	-	-	-	-
Nov	-	-	-	-	-	-	-	-	-
Dec	49	23.37	3.64	4.05	7.69	21.6	8.33	0.88	0.09

Table 26: Monthly distribution of different gust parameters as calculated through POT method.

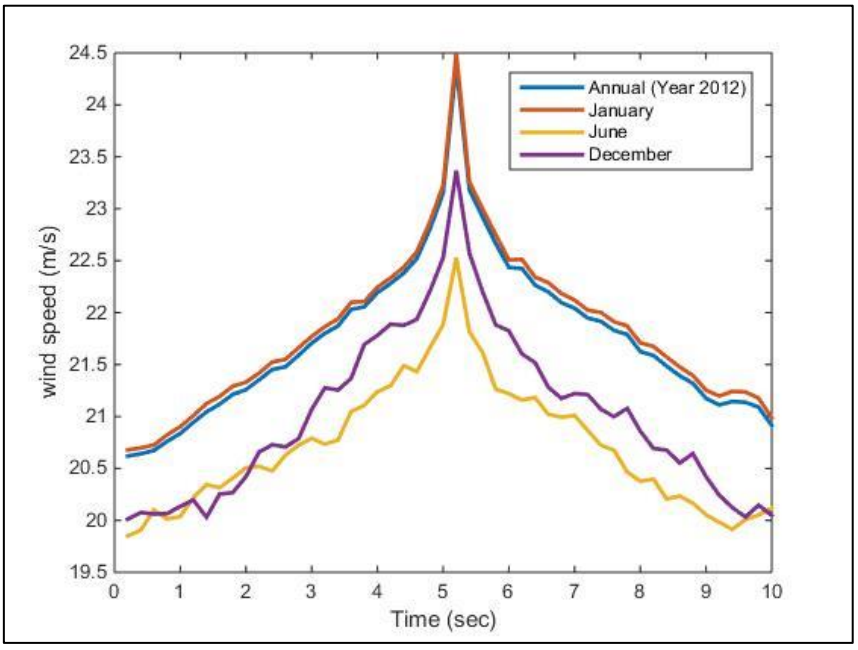

Figure 56: Monthly Distributions of mean gust shapes (POT) method. (5Hz)

In order to change the sampling frequency from 10 Hz to 5 Hz, alternate values from time series have been used. Hence there is some possibility that the lower value data points (within a region of high wind speeds) that could cause the high wind speeds not to be detected as gust, may have been missed in the alternate values of num5. Therefore,

- 5 Hertz sampling detects a slightly higher number of wind gusts.

The peaks for the mean gust shapes were found to be much narrower in case of Cabauw data set. The change in sampling frequency from 10 Hz. To 5 Hz, reduced the difference between the highest and the lowest value within the gust but the difference is not quite significant. Hence the mean gust shapes are still narrower for the Cabauw data set.

11. COMPARISONS

The Figure [57] shows the comparison of average monthly wind speeds for each of the sites during the entire year.

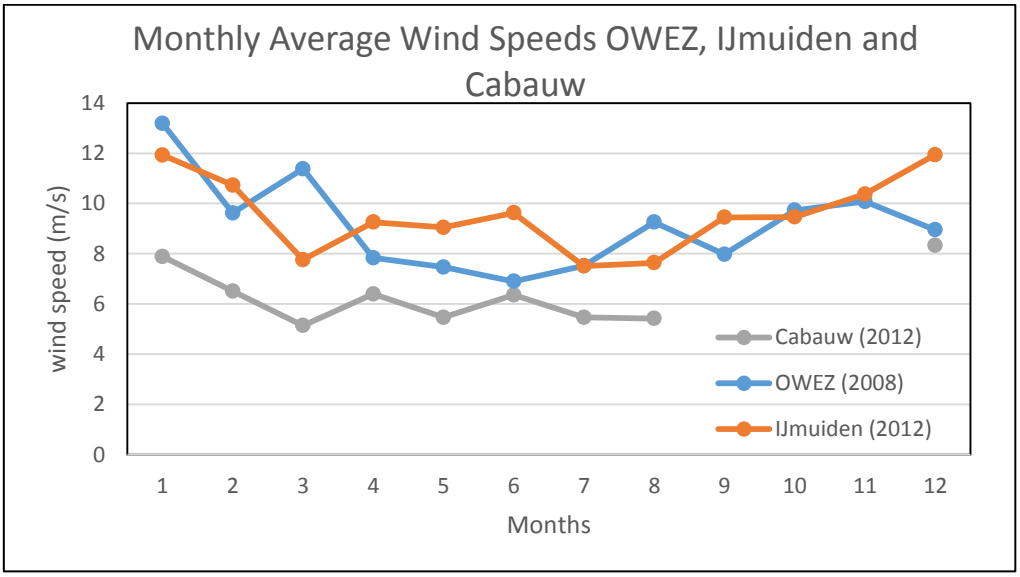

Figure 57: Average wind speeds at different locations over the entire 1 year period.

An important outcome of the research is the estimation of the seasonal distribution of the extreme wind gusts at different locations. Therefore, in POT and AOT methods, similar gust defining criteria (in terms of amplitude and direction) which are mentioned in Table [7] of this report have been used for all the sites. Fig. [58] shows the month wise occurrence of wind gusts for all three locations using POT method while Fig. [59] shows the similar distribution obtained through AOT method.

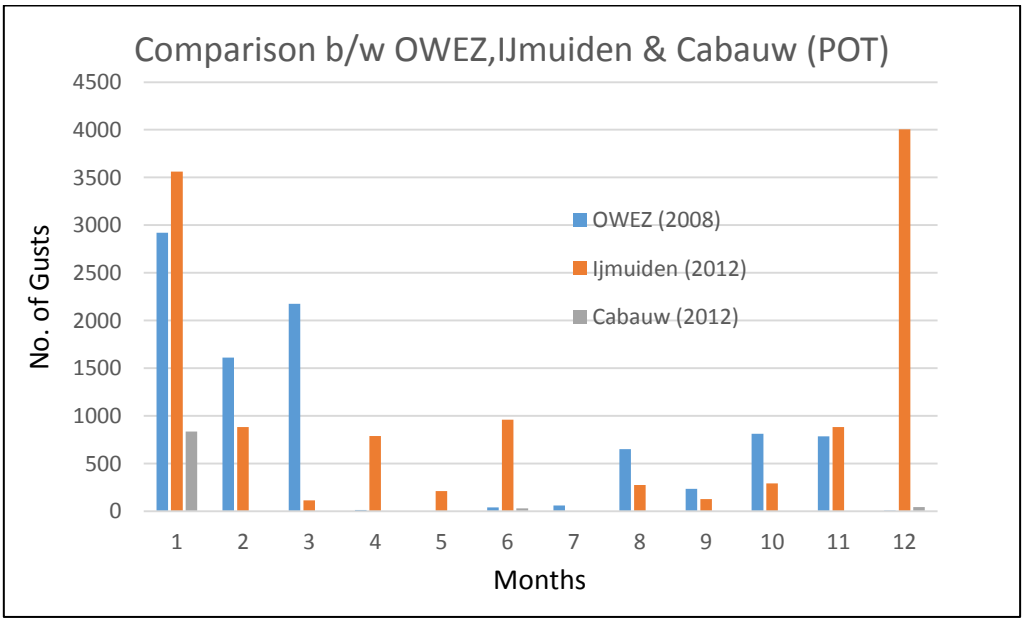

Figure 58: Number of gusts detected at different locations using POT method.

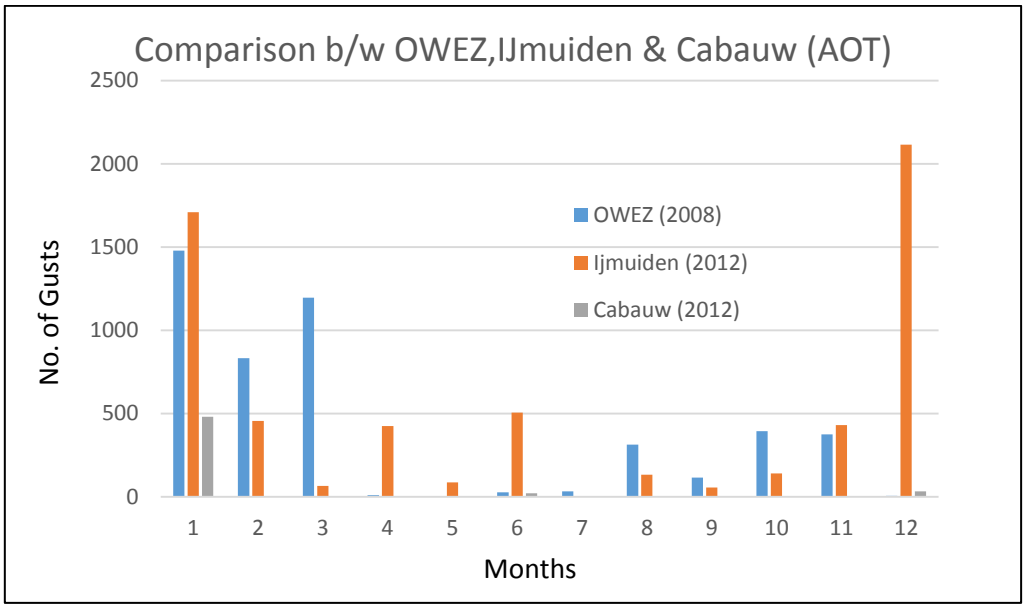

Figure 59: Number of gusts detected at different locations using AOT method.

For all the gust detection methods, the annual mean gust shapes have been plotted for different locations in Fig. [60] [61]. Based on the results, the following observations are made,

1. For peak over threshold (POT) method, a uniform threshold criteria regarding the amplitude and duration of wind gusts has been used for all three locations. The highest number of gusts were detected at the far offshore location of IJmuiden while the onshore location Cabauw had the lowest gust counts. This trend is maintained for almost every month throughout the year.
2. For the acceleration over threshold (AOT) method, the introduction of an additional acceleration threshold criteria typically reduces the number of detected gusts to half, irrespective of the location.
3. For all three locations, the highest number of gusts have been detected when the average wind speeds is also higher and, as expected, for the summer months, very few gusts are detected.
4. The mean gust shape for Cabauw site is much narrower and the difference between the maximum peak and the minimum wind speed value within the gust is also significantly larger as compared to OWEZ and IJmuiden. Fig. [62] [63] demonstrate this trend for P2P and VIT methods respectively.
5. Earlier during the alternate compilations of mean gust shapes at OWEZ, it has been identified that the gusts occurring at high wind speeds are typically narrower in comparison to low or medium wind speed gusts. This is in contrast to the observations noted for the Cabauw data set because in general at Cabauw, the wind speeds are much lower compared to OWEZ and IJmuiden, yet the mean gust shapes are much narrower in shape. The anomaly can be attributed to the high frequency resolution for the Cabauw data set.
6. The peak to peak method and the velocity increment method are defined in such way that they provide the values for maximum gust amplitudes and its acceleration for every 10 minute period. It is found that for all three locations, the higher the average wind speed, the larger would be the value for the 10 minute maximum gust amplitude and the associated acceleration.

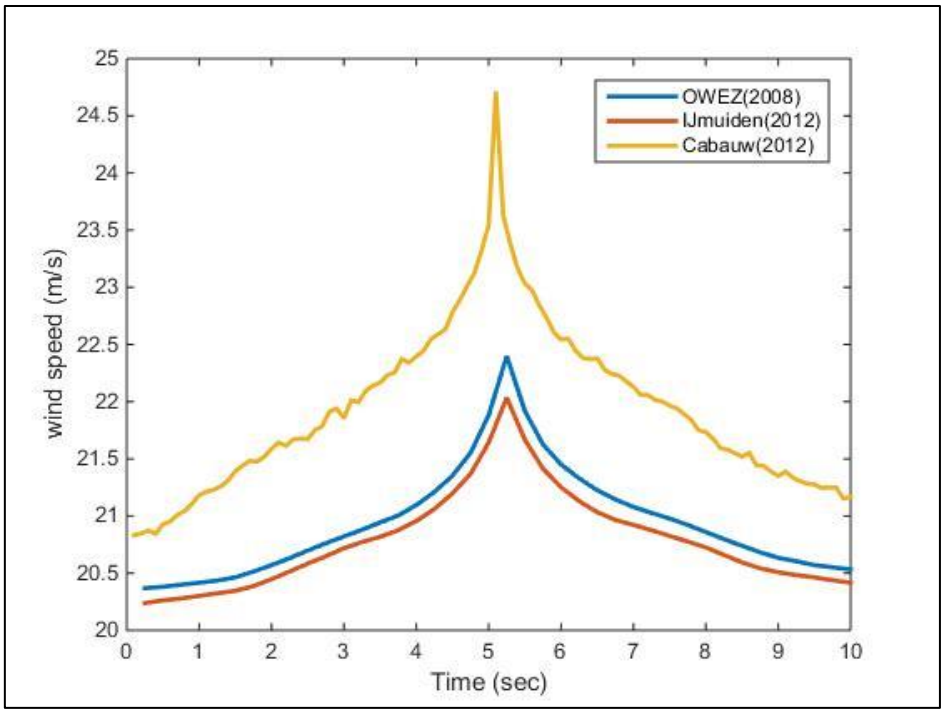

Figure 60: Annual mean gust shapes at different locations using POT method.

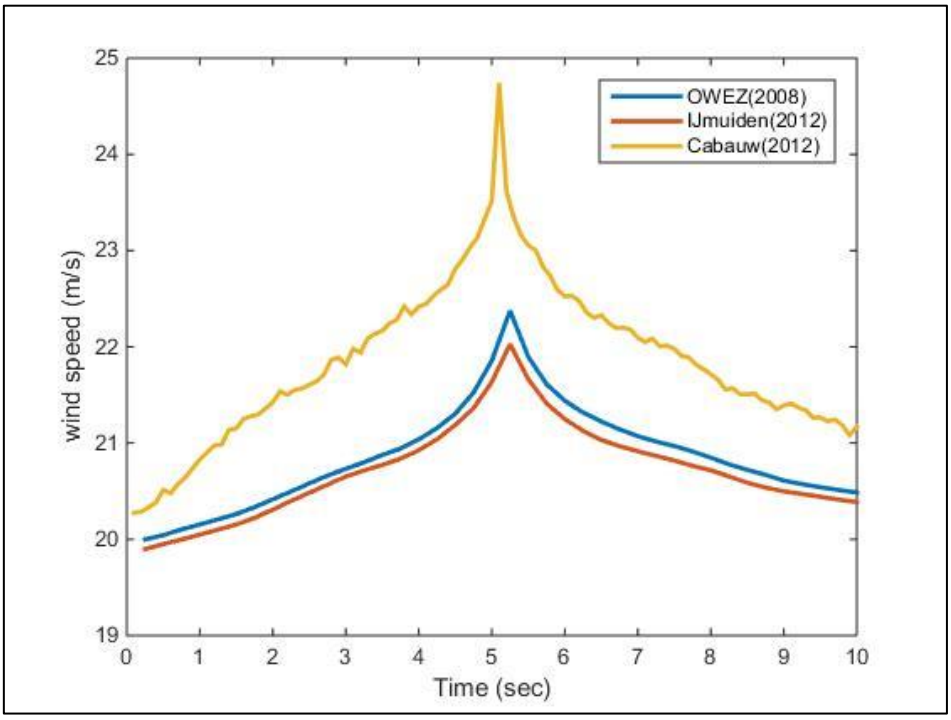

Figure 61: Annual mean gust shapes at different locations using AOT method.

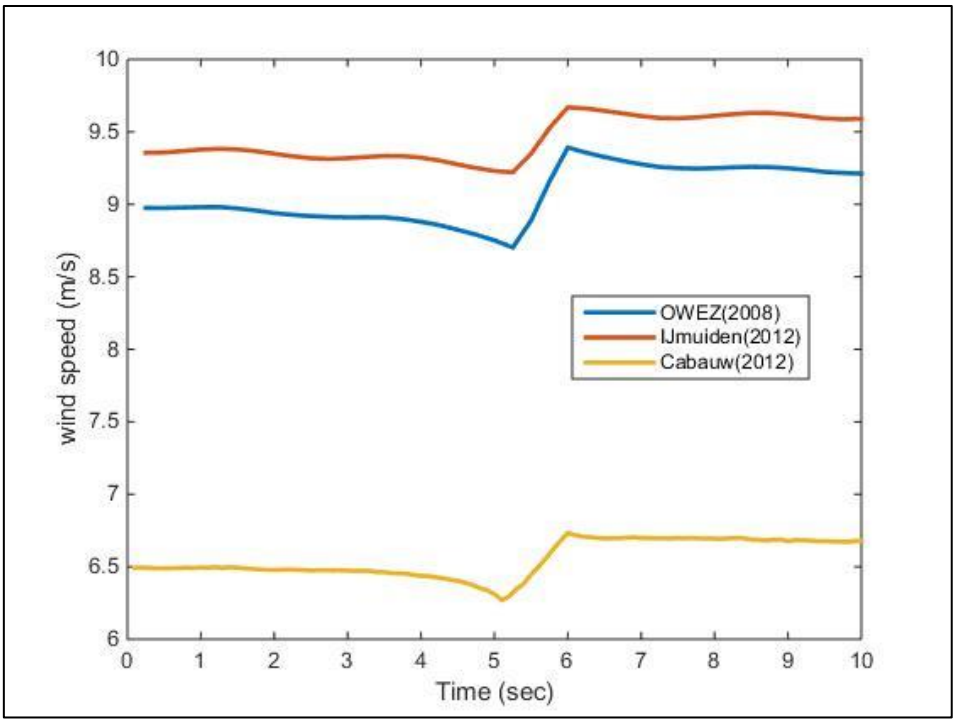

Figure 62: Annual mean gust shapes at different locations using peak to peak method.

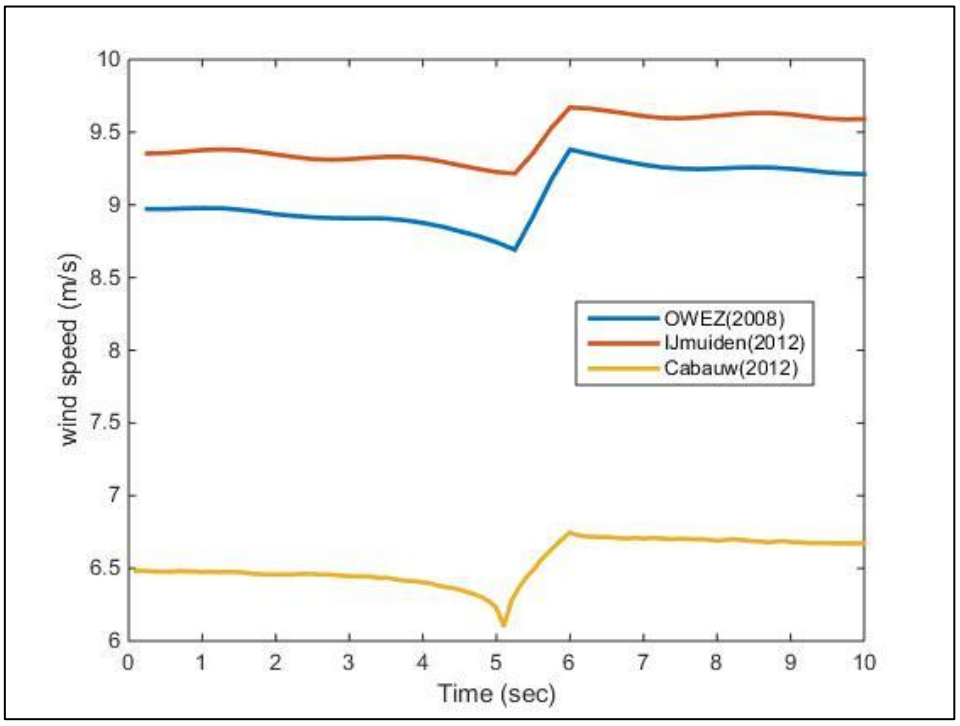

Figure 63: Annual mean gust shapes at different locations using VIT method.

12. APPROACH TOWARDS A MAXIMUM 50 YEAR WIND GUST AT DIFFERENT LOCATIONS

One of the aims of this research work is to provide a better estimate for the maximum wind gusts occurring at different geographical locations over a period of time.

With reference to the designing of wind farms or wind turbine, a crucial criteria is the estimation of maximum annual or maximum 50 year gust for the location under consideration. The IEC 61400 wind turbine standard provides an estimate for these values according to the following relations,

$$Reference\ wind\ speed = V_{ref} = 5 \times V_{avg}$$

$$Maximum\ 50\ year\ gust = V_{50} = 1.4 \times V_{ref} \left(\frac{z}{z_{hub}}\right)^{0.11}$$

$$Maximum\ annual\ gust = V_1 = 0.8 \times V_{50}$$

From the available data sets for OWEZ, IJmuiden and Cabauw, we can obtain the annual averages. Hence by using the annual average wind speeds for all these locations, the extreme wind events can be calculated to use for the above mentioned IEC 61400 standards. These calculated values are shown in Table [27].

Location	V_{avg} (m/s)	V_{ref} (m/s)	V_{50} (m/s)	V_1 (m/s)
OWEZ	9.16	45.8	64.12	51.3
IJmuiden	9.56	47.8	66.92	53.54
Cabauw	6.33	31.65	44.31	35.45

Table 27: Maximum wind speed values at different locations based on IEC 61400 standards.

The data sets for all three locations contain one year data only. Hence the maximum gusts are extracted for each month of the available 1 year data. Table [28] to [30] gives the values for the monthly maximum gusts (the gust containing the highest mean value for its entire duration is classified as the maximum monthly gust) for any particular location.

Month	Amplitude (m/s)	Mean (m/s)	Standard Deviation (m/s)
January	27.26	24.15	1.32
February	27.46	24.13	1.57
March	28.01	24.62	1.71
April	23.02	21.55	0.88
May	-	-	-
June	22.87	21.45	1

July	22.28	21.39	0.68
August	25.68	23.64	1.68
September	25.5	23.2	1.97
October	25.95	24.5	1.65
November	25.35	23.27	1.57
December	21.86	21.11	0.64

Table 28: OWEZ maximum monthly gusts (year 2008).

Month	Amplitude (m/s)	Mean (m/s)	Standard Deviation (m/s)
January	27.38	24.86	2.64
February	24.18	22.74	1.086
March	22.62	21.42	0.85
April	24.01	22.59	1.2
May	23.8	22.13	0.99
June	26.33	23.59	1.76
July	-	-	-
August	23.94	22.4	1.31
September	24.45	22.7	1.26
October	23.48	22.24	0.68
November	25.47	23.24	0.98
December	24.66	23.35	2.59

Table 29: IJmuiden maximum monthly gusts (year2012).

Month	Amplitude (m/s)	Mean (m/s)	Standard Deviation (m/s)
January	34.41	29.2	5.45
February	-	-	-
March	-	-	-
April	-	-	-
May	-	-	-

June	23.88	21.97	1.39
July	-	-	-
August	-	-	-
September	-	-	-
October	-	-	-
November	-	-	-
December	25.9	22.54	2.76

Table 30: Cabauw maximum monthly gusts (year 2012).

The amplitude and the mean value can be compared against the IEC 61400 standard calculated values in the Table [27].

Extreme Gust Shape

By averaging the monthly maximum gusts, an estimated shape for the extreme gust event is shown for each location from Fig. [64] to Fig. [66].

The shape of the extreme gust events is slightly different from the general mean gust shapes obtained for different sites using POT method as given in section [10] of this report. This is due to the fact that here an average of a fewer number of gusts (the maximum monthly gusts for each month only) has been taken. Hence the random fluctuations cannot be made smooth which could be the case if the average of a larger number of gusts is taken.

Therefore, a trend line may be added to these extreme gust shapes so that they can be compared with the standard IEC gust shapes like Extreme operating gusts (EOG) and Extreme Coherent Gusts (ECG) etc.

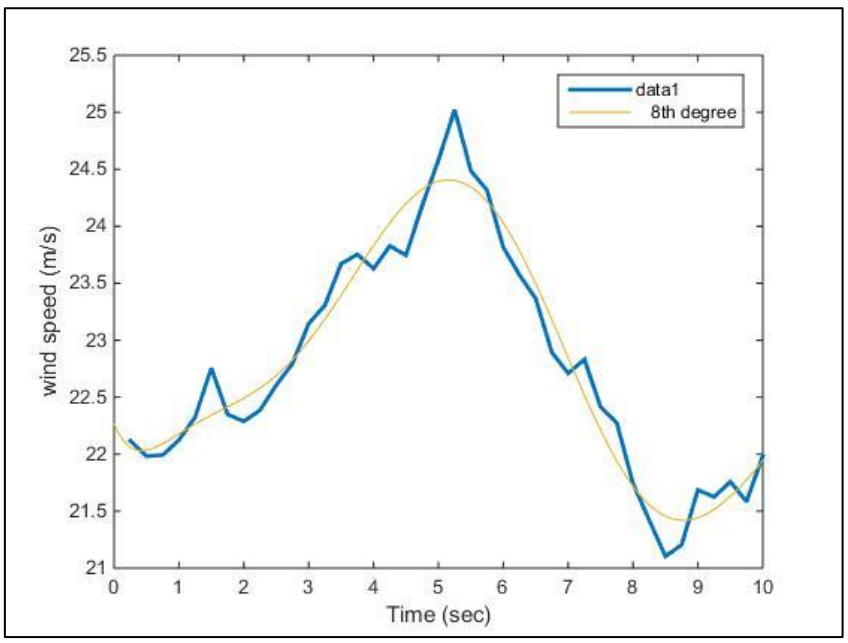

Figure 64: Extreme gust shape based on the monthly maximums (OWEZ).

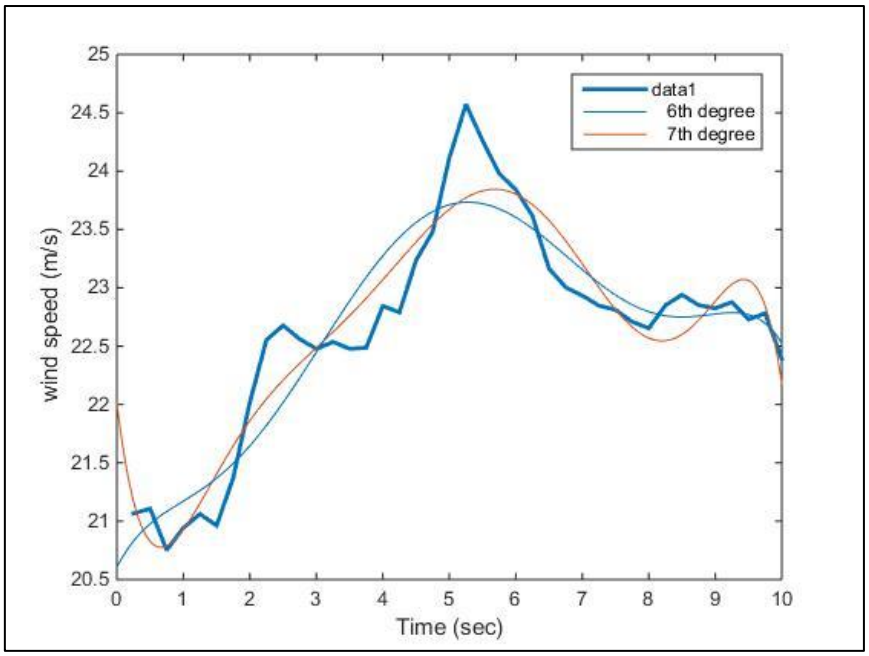

Figure 65: Extreme gust shape based on monthly maximums (Ijmuiden).

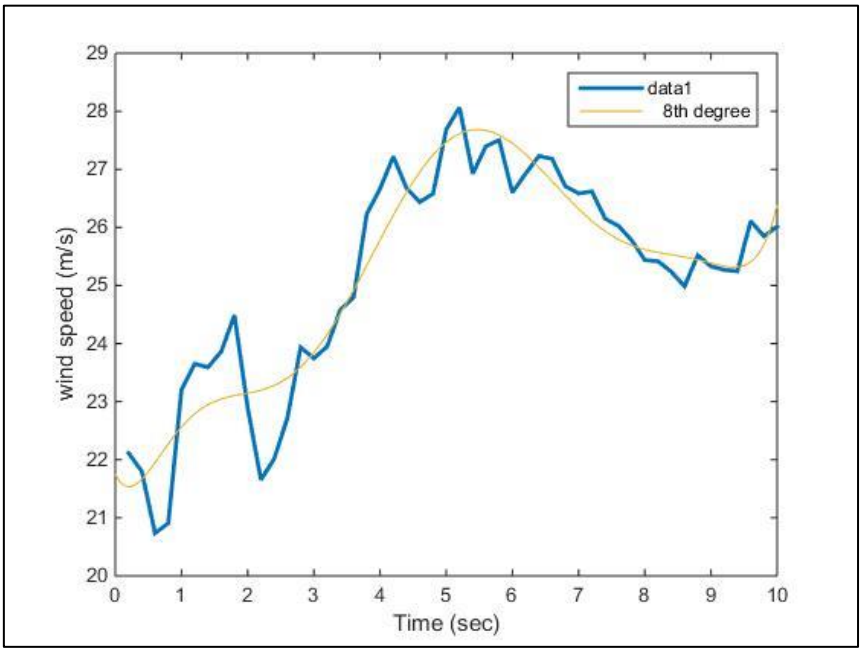

Figure 66: Extreme gust shape based on monthly maximums (Cabauw).

Fig. [65] and [66] shows the shape of the extreme gust shapes for IJmuiden and Cabauw sites respectively. It may be noted from the visual inspection of the trend lines that the mean wind speed tends to remain higher than the mean before the onset of the wind gust. This behavior resembles an ECG gust. However this trend could not be supported from the extreme gust shape for OWEZ. It can be further argued that the shape of the extreme gust event also depends upon the degree of polynomial used for fitting the trend line.

Similar approach may be adopted if data set for longer periods of time is available. For instance, in case of a 10 year data set, the annual maximums for 10 years maybe combined to give an extreme gust shape instead of monthly maximums.

The next step is to approach towards a more realistic estimate of extreme wind gusts based upon the analysis of the data sets during this research work.

The defining criteria for identifying wind gusts are same as mentioned in Table [7] of this report and the results from the POT method have been used for this exercise.

1. Extrapolation of Data

From the maximum gusts available for the given duration of time, we may assign probabilities to these maximum gust events depending upon how frequently they might be expected.

For example, if we have 11 years maximum gust events, we can plot a staircase function where the highest point of the stair case would represent the probability of non-occurrence (confidence interval) of the maximum of these 11 values and the lowest point in the stair case would be the probability of non-occurrence of minimum of these 11 gust values. On a probability scale which ranges from 0 to 1, we can assign the probabilities to all these values based upon the equation,

$$P = \frac{T-1}{T}$$

Where "T" represents the total points such that for the maximum of these 11 points, we get

$$P(Max.Gust) = \frac{11}{12} = 0.92$$

And for the minimum of these 11 points, we can write,

$$P(Min.Gust) = \frac{1}{12} = 0.08$$

It is based on the intuitive understanding that the maximum of these maximum values would be encountered more or less once in the entire 11 years period. Similarly, the minimum of these maximum values may be observed each year thus giving probability closer to zero.

If we plot the probability of non-occurrence of a maximum 50 year gust (on a scale of 0 to 1) against the maximum gust amplitudes, we may arrive at the conclusion that the maximum 50 year gust would have a confidence interval of **98%**.

$$P(Max.Gust)_{50\ year\ monthly\ data} = 1 - \frac{1}{50} = \frac{49}{50} = 0.98$$

For the purpose of understanding, we can take the maximum monthly gusts from OWEZ data set, where we have 11 maximum gust amplitudes (since no gusts, satisfying the defined threshold criteria were detected during the month of May, 2008).

First let us assume that these 11 data points represent annual maxima. Then the probability of the maximum and minimum of these 11 data points would be given exactly as mentioned in the above two equations. Hence these 11 data points representing the maximum gust amplitudes maybe plotted on the graph as shown in Fig. [67].

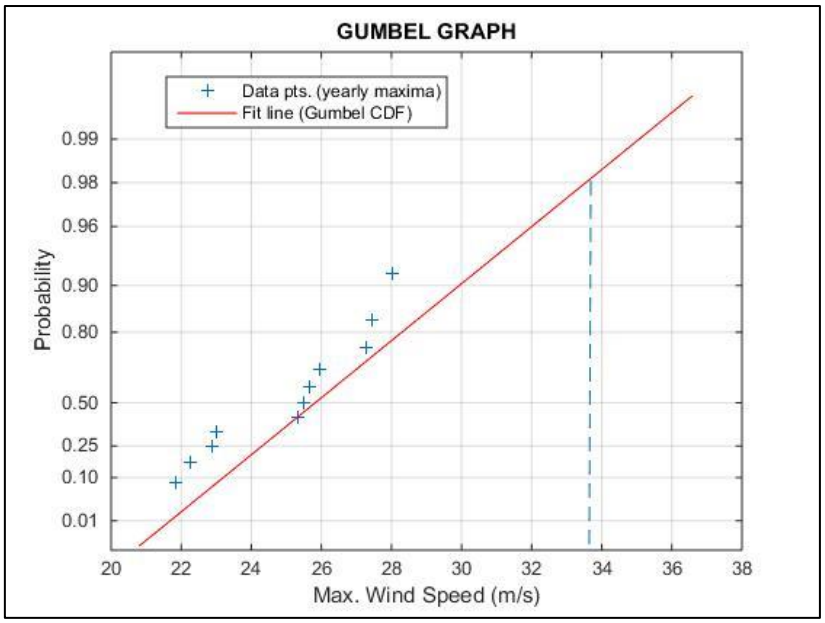

Figure 67: The probability of maximum 50 year gust (based on assuming yearly maximums)

As it can be seen in Fig. [67], by adding a trend line we can achieve a confidence interval of **98%** at wind speeds of about **33.5 m/s** (approx.) which may be taken as the amplitude for the maximum 50 year gust.

Now the actual data sets available are for the duration of 1 year only and the 11 maximum gust amplitudes taken from the OWEZ data set are basically monthly maximum gusts. Therefore, if we define the probability of non-occurrence of 50 year maximum gust based on availability of monthly maximum gusts, then by using the similar relation we obtain the confidence interval of **99.83%**.

$$P(Max.Gust)_{50\ year\ monthly\ data} = 1 - \frac{1}{(12\ X\ 50)} = \frac{599}{600} = 0.998$$

Fig. [68] shows the actual probability of the 11 maximum monthly gusts for OWEZ. Again a trend line can be fitted using the Gumbel CDF. The logarithmic scale defined on y-axis adjusts the value for probabilities closer to 1. Hence the value corresponding to 0.998 would provide us with the maximum gust amplitude for the 50 year time period. As it can be seen from fig. [68], this value is approximately **39.5 m/s** which is higher than 33.5 (the previous value obtained in case, if the 11 data points represented maximum annual gusts for 11 years)

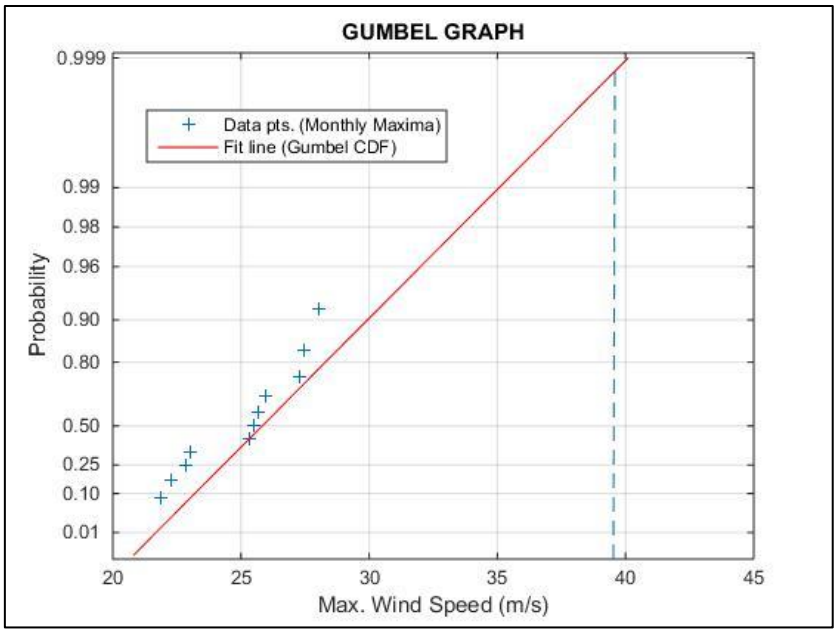

Figure 68: The probability of maximum 50 year gust (based on monthly maximums).

It is also worthwhile to mention here that the level of predictability for year to year wind speed variations is quite different from the seasonal or monthly variations and while for time scales shorter than a year, the seasonal or "synoptic" variations can be well characterized in terms of probability distributions [16], the annual wind speed changes remain hard to predict.

Nevertheless, the process has been explained in detail which can be used in case of the availability of data for larger duration of time.

2. Return Period of Wind Gusts

While searching for the maximum 50 year gust in the previous section, it is found that the predictability level is quite low due to the availability of only 1 year data for all the three locations.

Another approach that was considered during this study is to estimate the return period or frequency of the maximum gusts detected throughout the year at different locations. Again for the sake of uniformity, the same gust threshold criteria as listed in Table [7] for POT method has been selected for the detection of wind gusts.

As a test case, the Cabauw data set is selected here because at Cabauw, the results for the wind gusts have been compiled with POT method for different sampling frequencies in the previous sections.

It can be understood that the return period or frequency of the gusts may be calculated for each month by dividing the total number of gusts detected during that period by the total duration of the time series i.e. 1 month. However from taking the starting locations of the first and the last gusts within the time series for the entire month, an interesting observation has been made.

Regions for high wind speeds are found to be clustered within certain portions of the time series. Hence if we estimate the return period from the successive level crossings above and below the gust threshold, we may arrive at the conclusions that **during the periods of high wind speeds, each gust is followed by the occurrence of the next gust after a gap of a few minutes interval**. This is shown in Table [31] below.

	January	June	December
5 Hz.	1299 sec. (21.65)	1189 sec. (19.81 min)	1038 sec. (17.3 min)
10 Hz.	1352.1 sec. (22.54 min)	1256 sec. (20.93 min)	1186 sec. (19.77 min)

Table 31: Return periods for wind gusts at Cabauw during the periods of high wind speeds.

An analytical approach based upon the **random phase model** for a stochastic variable is also considered to predict the return period for the wind gusts. This approach, as discussed in detail in ref. [22] was previously utilized for the study of ocean waves.

The underlying concept for the probability distributions of a random phase model is that, if we add a large number of harmonic components at random phases with respect to each other (or in our case random turbulent fluctuations of wind speeds), we obtain a probability density function which resembles a Gaussian distribution. Thus restricting ourselves to the Gaussian distribution of a random variable (wind speed) and also using the assumption of a stationary time series, the frequency of occurrence of gusts or peak values above a certain threshold is given by an analytical relation as derived by Rice in 1944.

$$f_\eta = \frac{1}{T_\eta} = \sqrt{\frac{m_2}{m_0}}\, exp\left(\frac{-\eta^2}{2m_0}\right)$$

Where "m_0" is the zero order moment or variance (unit m^2) and "m_2" is the second order moment respectively. "f_η" is the mean frequency of the level crossings for the given threshold "η".

The above analytical expression provides reasonably accurate results as confirmed through various previous literature studies [22]. However, in order to obtain the values of different variables within this expression, we need to have the exact expression for the energy density spectrum (A spectrum showing the distribution of energy over different frequencies) of the time series. Some useful information about energy density spectrum has been included in the appendix [B] of this report.

In the present analysis, an attempt is made to predict the probability of occurrence or the return period of wind gusts from the analytical expression by Rice "T_0" and compare the results with the actual return period "Tz" as calculated from the time series available data. Table [32] gives a summary of this comparison. It should be noted that the actual return period "Tz" would be different and much longer than the return periods mentioned in Table [31] which are specific to the regions of high wind speeds only.

A reduced form of the above analytical expression (the Rice formula) is frequently used when the value of η is taken as the difference between the maximum threshold and the mean value of the time series. An advantage of this formulation is due to the fact that the second order moment term cancels out with the zero order moment term within the square root. Details are provided in ref. [22]. In simpler terms, we do not need to perform the integration of the energy density spectrum to obtain the second order moment and we are left with a much more simplified expression.

$$f_\eta = exp\left(\frac{-\eta^2}{2m_0}\right)$$

Therefore, for the values,

$\text{Threshold} = \eta = \text{Gust threshold} - \text{Monthly Avg. wind speed.}$

$\text{Variance} = m_0 = (\text{Calculated from the turbulent wind time series for each month}).$

$T_0 = \text{Return period as calculated from the reduced Rice formula.}$

$T_z = \text{Actual retrun period as calculated from the time series}$

Month	Average (m/s)	η (m/s)	m_0 (m2)	$exp\left(\frac{-\eta^2}{2m_0}\right)$	No. of gusts.	T_z (hours)	T_0 (hours)
January	7.89	12.11	11.85	0.00205	471	1.58	2.65
June	6.36	13.64	13.64	0.00109	28	25.71	31.17
December	8.33	11.67	13.46	0.0064	32	12.75	23.58

Table 32: Comparison of the return period of wind gusts based on anaalytical formulations and the time series analysis.

The return period analyzed from the actual time series "T_z" is somewhat comparable to the analytically calculated return period "T_o" (especially during the month of June). However, it is still not considered to be an accurate estimation of return period of wind gusts. While this topic remains to be explored for further research, some of the possible deficiencies within the current analysis that needs to be addressed are listed below,

1. Very often there are missing periods within a time series obtained through data sets. During the application of gust detection methods, the algorithms were designed to pick the location of discontinuities so that the detection of false gusts is avoided at the locations where the time series has missing data in between. However, during the calculation of return periods for the wind gusts, it has not been estimated how to account for the missing periods within the time series.
2. The return periods calculated through the Rice formula are highly sensitive to variance of the time series due to the presence of the exponential term within the expression. Since the estimates for variances have been obtained from the turbulent wind time series, it is also sensitive to the sampling frequency of the data set. This influence needs to be studied further in detail.

13. IMPORTANT ASSUMPTIONS & LIMITATIONS

Some of the limitations and underlying constraints have been summarized here in this section which might be useful for interested readers in order to conduct future research work within this field.

1. For different sites the booms are located at different heights. Data has been compared at the same height of 70 m for all the locations. For this purpose, simple logarithmic laws were used for scaling down the wind velocities. For example, from IJmuiden data set, the available sonic data at 86.5 m height has been scaled down to 70 m and for the Cabauw data set, the sonic data at 60 m height is scaled up to 70 m using the logarithmic wind profile assumptions which mainly requires neutral atmospheric conditions. Stability corrections (which are specially recommended for offshore conditions) have not been implemented during this study.
2. While the gust detection algorithms can be used for detecting wind gusts at any measuring height and location within the rotor plane, the results and analysis presented here is only conducted for a single point location at 70 m hub height.
3. For OWEZ and IJmuiden locations, the data sets are sampled at 4 Hz while the data set for Cabauw comprises of 10 Hz wind speed data. Hence the peak to peak method and the velocity increment method typically predicts higher 10 min gusts in case of Cabauw.
4. Furthermore, the data sets obtained for different locations are not from the same years. Ideally data sets for different locations from the same years should have been used.
5. Tower shadow effects could not be adequately addressed for the Cabauw data set because the high resolution sonic data is only available from the south east boom which is located at 130

degrees from North. Therefore, for the cases where the incoming wind direction is between 280 to 340 degrees from North, the sensors in the SE boom of the tower are in the wake of the tower and hence the reported wind speeds may not be reliable.

6. Tower shadow effects have been considered during the analysis of the OWEZ and IJmuiden data sets. Therefore wind speeds from the appropriate boom (or a combination of booms) of the met mast have been selected depending upon the wind speed directions. However, the wind directions have been acquired using a single boom data which is the NW boom of the met mast both in the case of OWEZ and IJmuiden data sets.
7. With reference to the tower shadow effects, a further assumption has been made for the IJmuiden site because the wind directions have not been recorded directly for this data set. It is assumed that the sensors in the different booms of the met mast are perfectly aligned with the North so that the wind speed components in the horizontal plane could be used for estimating the wind speed direction using basic trigonometry.
8. For moving window techniques like the peak to peak and the velocity increment methods, some better criteria for defining the step change size needs to be defined. For instance, in Cabauw data set when the step change size was reduced to 0.1 seconds (due to the high sampling rate of the data set), the amplitudes for maximum 10 minute gusts increased significantly.

14. RECOMENDATIONS FOR FUTURE STUDIES

As a follow up for this research, some of the recommended areas for further exploration have been outlined below,

1. Detailed load calculations needs to be performed for different wind turbine models with an aim to estimate most critical wind loads. These crucial wind loads would enable to outline some more realistic criteria to define a wind gust in terms of its duration and amplitude threshold.
2. With the increasing rotor sizes, the gusts sometimes do not affect the entire rotor plane equally. Thus subjecting the turbines to the unequal loads. For more extensive research, data should be analyzed at different heights to estimate the spatial extent of the wind gusts as shown in Ref [21].
3. One of the ambitious aims at the start of this research work is to design a computational code that can detect the wind gusts as defined by the user defined criteria by automatically analyzing the data set. This means, the code should be able to pick the relevant data from the data set and calculate all the relevant parameters automatically. This aim could not be achieved because the data sets from different locations were considerably different from one another, both in terms of format as well as their level of details.
4. An analytic formulations such as Rice formula for the estimation of return periods of the wind gusts has been presented in this research. The concept needs to be further explored and the results needs to be tested for different durations of time series.
5. Finally for the future research work, it is strongly recommended to be involved with the actual data acquisition from the met mast data loggers and program them in a more user friendly manner, using the computational codes developed during this research work.

15. CONCLUSIONS

The two primary research objectives set at the start of the project have been adequately addressed during this research work. Different gust detection techniques are explained, programmed into a

software code and successfully applied over different data sets. Due consideration has been given to the verification and testing of these gust detection algorithms.

A detailed comparison between different geographical locations has been made during this study. Using a well-defined and uniform threshold criteria for gust amplitude and duration, different methods have been utilized to detect wind gusts at three completely different geographical terrains which includes OWEZ (near offshore), IJmuiden (far offshore) and Cabauw (onshore) location. Based on the analysis of their respective wind data sets, the results obtained with reference to the occurrence of wind gusts generally follow the expected trends, where the highest number of gusts were detected for far offshore locations where the wind speeds are generally higher and also during the winter months when the wind speeds are expected to be higher.

On the basis of general trend of the maximum gusts in different months throughout the measuring periods, a shape for the extreme gust event is shown for all three locations. For Ijmuiden and Cabauw data sets, this shape somewhat resembles the ECG but the results from OWEZ do not follow this trend.

Some useful insight to the estimation of maximum 50 year gust is also provided. Two important aspects discussed in this regard are the extrapolation of wind data from the available data sets and using some analytical formulation to estimate the return period of wind gusts.

In addition to two primary objectives highlighted earlier, several sub questions mentioned in the research objectives have also been explored. A detailed explanation of the data sets and met mast considerations is provided and various aspects of atmospheric turbulence are discussed with reference to the calculation of appropriate characteristic time and sampling frequency etc.

The detailed theoretical analysis before the setting up of gust detection algorithms made it possible to select and define appropriate parameters for gust detection algorithms. Careful and systematic building up and testing of the gust detection programs resulted in obtaining meaningful results without taking any major restart.

In short this research work gives a detailed holistic view about the nature of wind gusts and provides some worthwhile input for better understanding the behavioral patterns of extreme winds.

APPENDIX

APPENDIX A: Programming Description and Pseudo codes.

The complete program set comprises of 3 levels of Matlab codes.

Level 1: location.m

This Matlab code extracts all the data from the csv/mat files present in the same folder and loads it into the Matlab workspace.

It stores the data in the form of "cell arrays". The size of the cell array would be automatically adjusted according to the number of csv/mat files in the folder.

$$N = cell(1, no.of\ files)$$

Each "pointer" inside this cell array refers to the data of a unique time sample (for example, 10 minute or 1 hour sample). The size of this time sample depends upon the format in which data has been provided. For example, in case of OWEZ reference data set, the data is available in separate time samples of 10 minutes. Hence, in order to analyze 1 year data for gust analysis, the number of files to be uploaded into this cell structure are, $6 \times 24 \times 365 = 52560$.

A separate structure is derived out of this cell array which contains the wind speeds from a specific height, measured through a specific instrument and in the dominant wind direction. The selection criteria for the dominant wind speed, choice of instrument and measuring height with reference to the OWEZ site has been discussed in section [4] of this report.

This structure could also be set to incorporate the average of the horizontal and vertical wind speeds in the dominant wind direction. A sample of this structure used for the OWEZ site is given below,

$$N2(1\ \ldots\ no.of\ files).velocity = N\{1, 1 \ldots \text{no. of files}\}.\text{OWEZ.h\_70m.sonic.NW.WS}$$

Level 2: gustdetection.m

This Matlab code should be run once the data is successfully loaded into the workspace through Level 1 code.

It asks the user input for the choice of gust detection method.

Depending upon the choice of the gust detection algorithm, it further asks the user input for the different parameters like the characteristic time of the algorithm (τ), sampling frequency (f), amplitude threshold (x), and the duration of the gust etc. This feature allows the users to define and analyze the gusts as per the unique requirements of their specific projects.

Some general guidelines for the selection of these parameters have been provided in section 4 of this report.

Once the values of these parameters have been obtained from the user, these are passed on as input arguments for functions corresponding to the specific gust detection algorithm.

Level 3: Gust Detection Algorithms

These Level 3 codes include functions which represents the individual gust detection algorithms as described in the section 8 of this report.

Once called upon by the Level 2 code, these functions performs the gust detection operations on the data uploaded through Level 1 code and returns the output arguments back to their main calling function i.e. Level 2 code.

Depending upon the individual requirements of the user, the type of output arguments, plots etc. can be adjusted here.

These level 3 codes are the most important part of this gust detection program set. Since they are required to read and process the entire data set uploaded through Level 1 code, hence the simulation time could considerably vary according to the way in which each gust detection method is applied.

The pseudo codes and flow charts for each type of code are given below,

Pseudo code 1: (Peak to Peak Method)

1. Take user input arguments for the characteristic time (τ) and frequency (f) from Level 2 code.
2. Read (<-) the no. of data points in the N2 structure uploaded through Level 1 code. For example, in case of OWEZ data set, it is $10 \times 60 \times 4 = 2400$ per file but it may vary depending upon the format of the provided data set.
3. Runs a loop for a number of times equal to the number of data files present in the work space. Again, for the OWEZ data set, it is $6 \times 24 \times 365 = 52560$ per year.
4. A nested loop inside this loop runs for 2400 times (or the number of data points in each individual file).
5. At each point, within this internal loop, it checks for the next 10 values. (10 could be different depending upon the characteristic time and frequency specified by the user).
6. Here it obtains the minimum value and the maximum value within this segment of 10 values, every time.
7. The difference between the maximum and the minimum value is recorded every time and denoted as gust for that step. Hence, approx. 2400 gust values are obtained during a "single run" of the outer loop out of which the maximum gust value is taken.
8. Consequently, the approx. 52560 gust values are obtained over the complete run of the outer loop i.e. 1 complete year.
9. Different parameters of these gusts are recorded (plots etc.) and passed on to the Level 2 code as the output arguments.

Note: The Pseudo code for the velocity increment Method is quite similar with minor alterations at step 6 of the above pseudo code.

Pseudo code 2: (Peak over Threshold method)

1. Take user input arguments for gust defining amplitude (x), duration (dt) and frequency (f) from Level 2 code.
2. Read (<-) the no. of data points in the N2 structure uploaded through Level 1 code. For example, in case of OWEZ data set, it is $10 \times 60 \times 4 = 2400$ per file but it may vary depending upon the format of the provided data set.
3. Runs a loop for a number of times equal to the number of data files present in the work space. Again for the OWEZ data set, it is $6 \times 24 \times 365 = 52560$ per year.
4. A nested loop inside this loop runs for 2400 times (or the number of data points in each individual file).
5. At each point, within this internal loop, it checks for the next 10 values. (10 could be different depending upon the duration specified by the user).
6. Here it obtains the minimum value and the value preceding this segment every time.
7. If the minimum value is above the gust threshold and the preceding value is also greater than the threshold, then no new gust is counted. It is simply the continuation of the previous gust.

8. If the minimum value is above the gust threshold and the preceding value is lesser than the threshold, then a new gust is counted. Different parameters of this gust are recorded (plots etc.) and passed on to the Level 2 code as the output arguments.

Pseudo code 3: (Velocity Increment with Acceleration method)

1. Take user input arguments for gust defining amplitude (x), duration (dt), characteristic time (τ), acceleration threshold (acc) and frequency (f) from Level 2 code.
2. Read (<-) the no. of data points in the N2 structure uploaded through Level 1 code. For example, in case of OWEZ data set, it is $10 \times 60 \times 4 = 2400$ per file but it may vary depending upon the format of the provided data set.
3. Runs a loop for a number of times equal to the number of data files present in the work space. Again for the OWEZ data set, it is $6 \times 24 \times 365 = 52560$ per year.
4. A nested loop inside this loop runs for 2400 times (or the number of data points in each individual file).
5. At each point, within this internal loop, it checks for the next 10 values. (10 could be different depending upon the duration specified by the user).
6. Here it obtains the minimum value, the maximum value and the value preceding this segment every time.
7. Acceleration is computed locally every time.
8. If the minimum value and the local acceleration value are above the defined threshold and the preceding value is also greater than the threshold, then no new gust is counted. It is simply the continuation of the previous gust.
9. If the minimum value and the local acceleration value are above the defined threshold and the preceding value is lesser than the threshold, then a new gust is counted. Different parameters of this gust are recorded (plots etc.) and passed on to the Level 2 code as the output arguments.

Note: The Pseudo code for the velocity increment Method with peak over threshold method is much similar with an additional constraint at step 8 and 9 of the above pseudo code.

Flow Chart 1: Peak to Peak Method

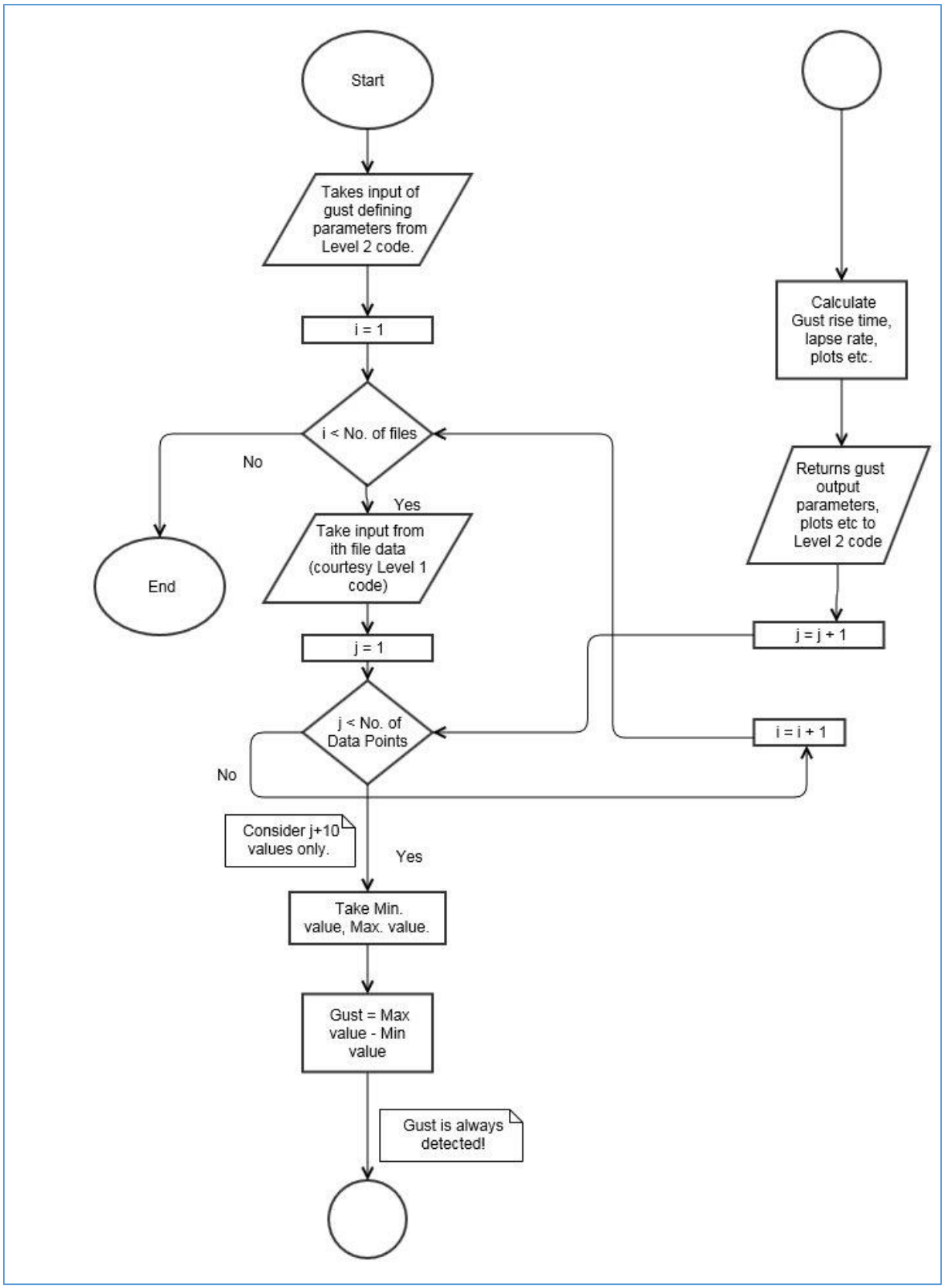

Flow Chart 2: Peak over Threshold Method

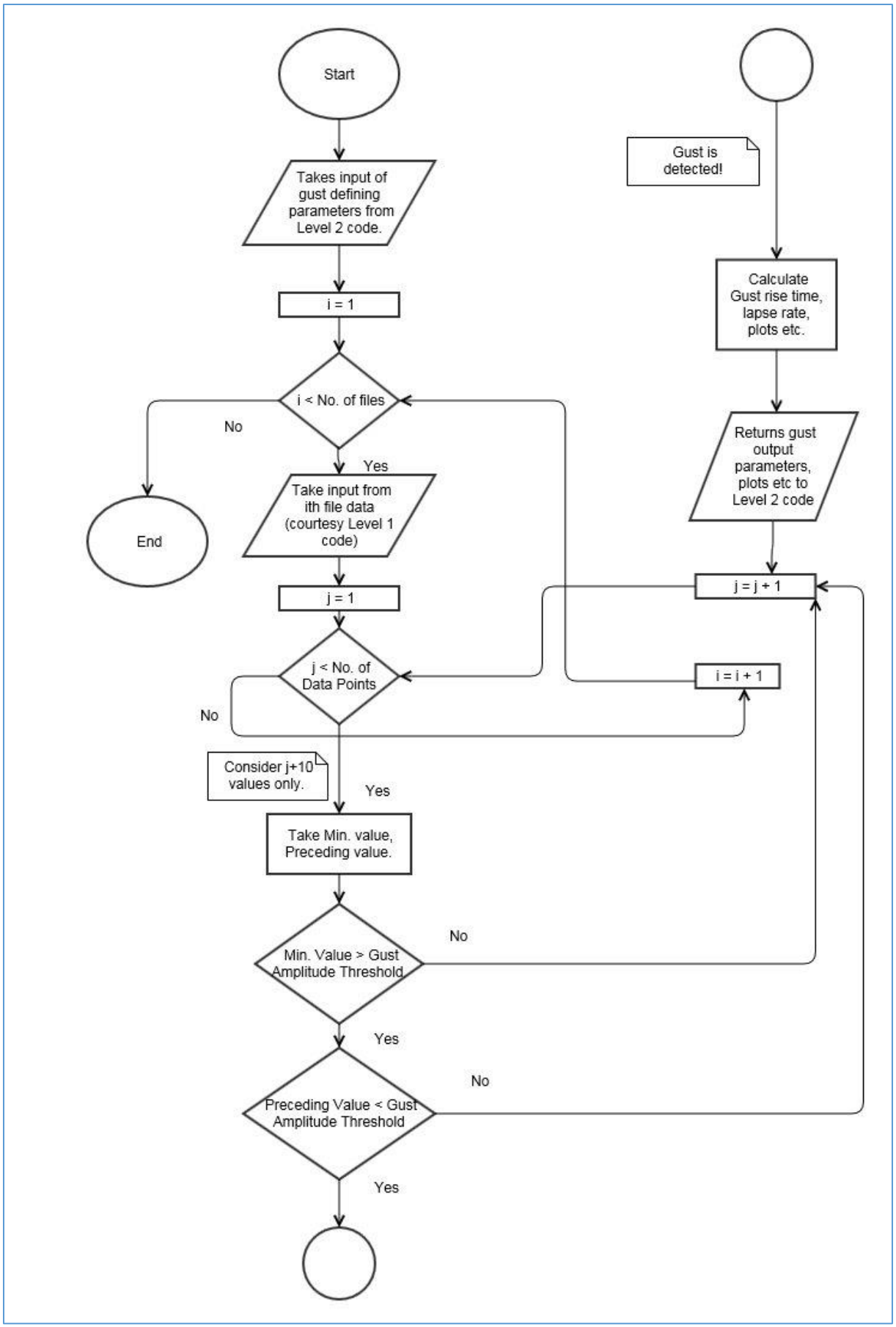
Start
Takes input of gust defining parameters from Level 2 code.
i = 1
i < No. of files
No
Yes
End
Take input from ith file data (courtesy Level 1 code)
j = 1
j < No. of Data Points
No
Consider j+10 values only.
Yes
Take Min. value, Preceding value.
Min. Value > Gust Amplitude Threshold
No
Yes
Preceding Value < Gust Amplitude Threshold
No
Yes
Gust is detected!
Calculate Gust rise time, lapse rate, plots etc.
Returns gust output parameters, plots etc to Level 2 code
j = j + 1
i = i + 1

Flow Chart 3: Peak to Peak Method

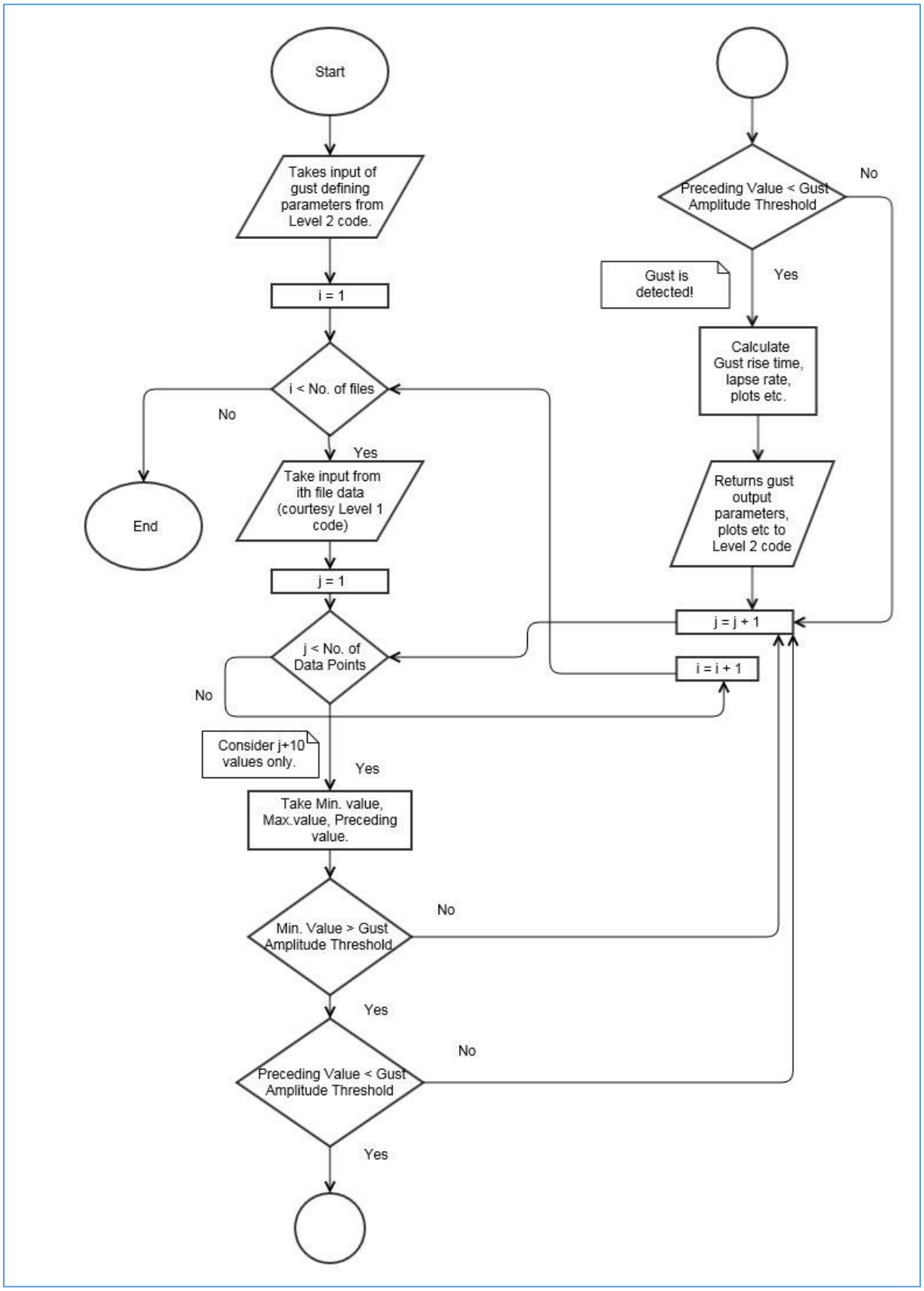

APPENDIX B: Additional Information Energy Density Spectrum.

In the random phase model, the frequency domain analysis of a random process is considered. An important consideration here is that the amplitude of the frequencies follow a Rayleigh distribution. This probability density function can be completely defined by a single variable i.e. "μ" which is the expected value of the amplitude "a_i" of a particular harmonic.

$$\mu_{amp} = E\{a_i\}$$

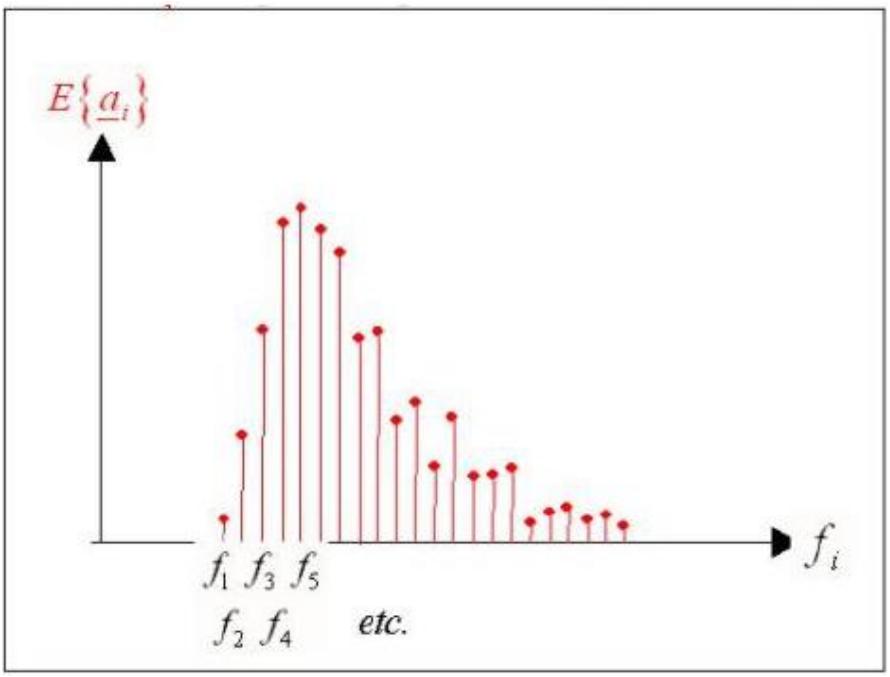

Figure 69: The amplitude spectrum of a random phase model.

Therefore, in **amplitude spectrum**, for each harmonic, we have the expected value of the amplitude. However, in practice, the **variance density spectrum** is more often used because the variance density can be more easily related to the energy content of the spectrum. Furthermore, from the amplitude spectrum, if we add the amplitude of the individual harmonics, we will not get the amplitude of the total wave. However if we have the variance density spectrum, the total variance of the signal is the summation of the variance of all the individual harmonics.

In order to arrive at the variance density spectrum, the variance of a single harmonic wave is given from the expected value of the amplitude by the relation,

$$Variance\ density\ of\ a\ single\ harmonic = E\left\{\frac{1}{2}{a_i}^2\right\}$$

And for the multiphase model of a random variable.

$$Variance\ density\ spectrum\ (discontinuous) = \frac{1}{\Delta f_i}\ E\left\{\frac{1}{2}{a_i}^2\right\}$$

$$Variance\ density\ spectrum\ (continuous) = \lim_{\Delta f \to 0} \frac{1}{\Delta f_i}\ E\left\{\frac{1}{2}{a_i}^2\right\}$$

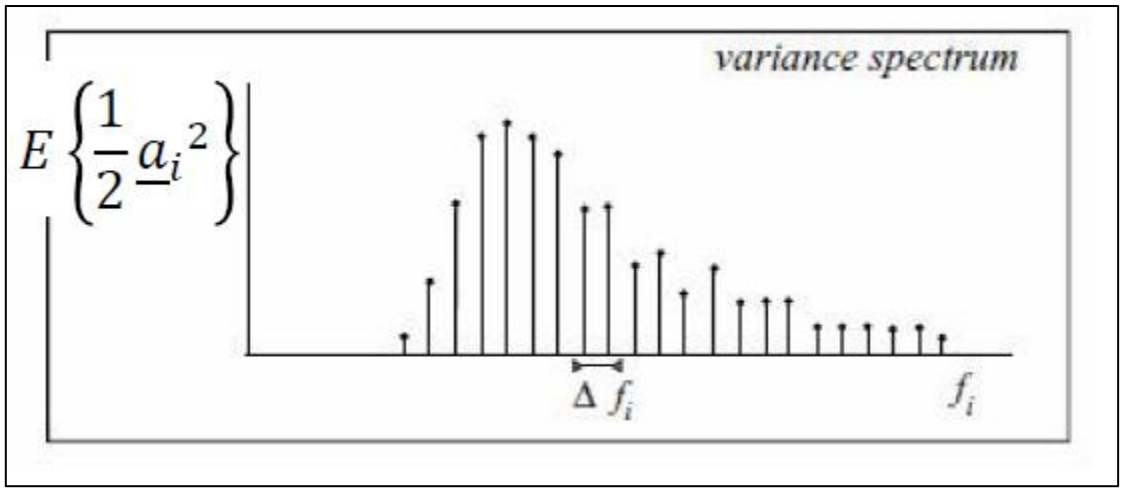

Figure 70: The variance density spectrum of a multiphase model.

The **energy density spectrum** is closely related to the variance density spectrum through the relation,

$$E_{energy}(f) = \rho g . E_{variance}(f)$$

The energy density spectrum of the time series can give some useful insight to the behavior of the stochastic process. Most importantly it shows the energy content associated with each harmonic within the time signal. Therefore it gives an idea about the shape of stochastic signal. For example, in case of a bichromatic wave signal, we just have two frequencies and their corresponding energy content is shown in fig. below.

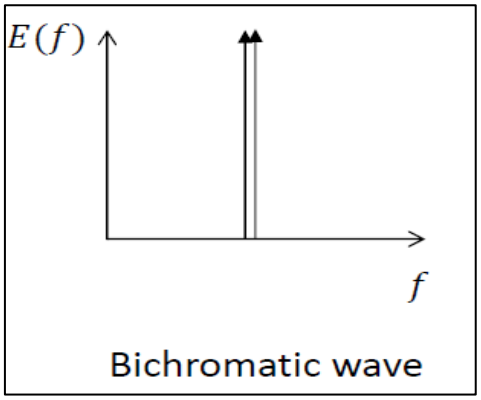

Figure 71: Energy density spectrum provides some useful information about the shape of the stochastic signal. Ref. [21]

Furthermore, the spectral analysis of the turbulent wind time series, gives us a clear picture of the different patterns of the diurnal and synoptic wind speed variations. Hence the energy associated with each of the peaks can be easily visualized.

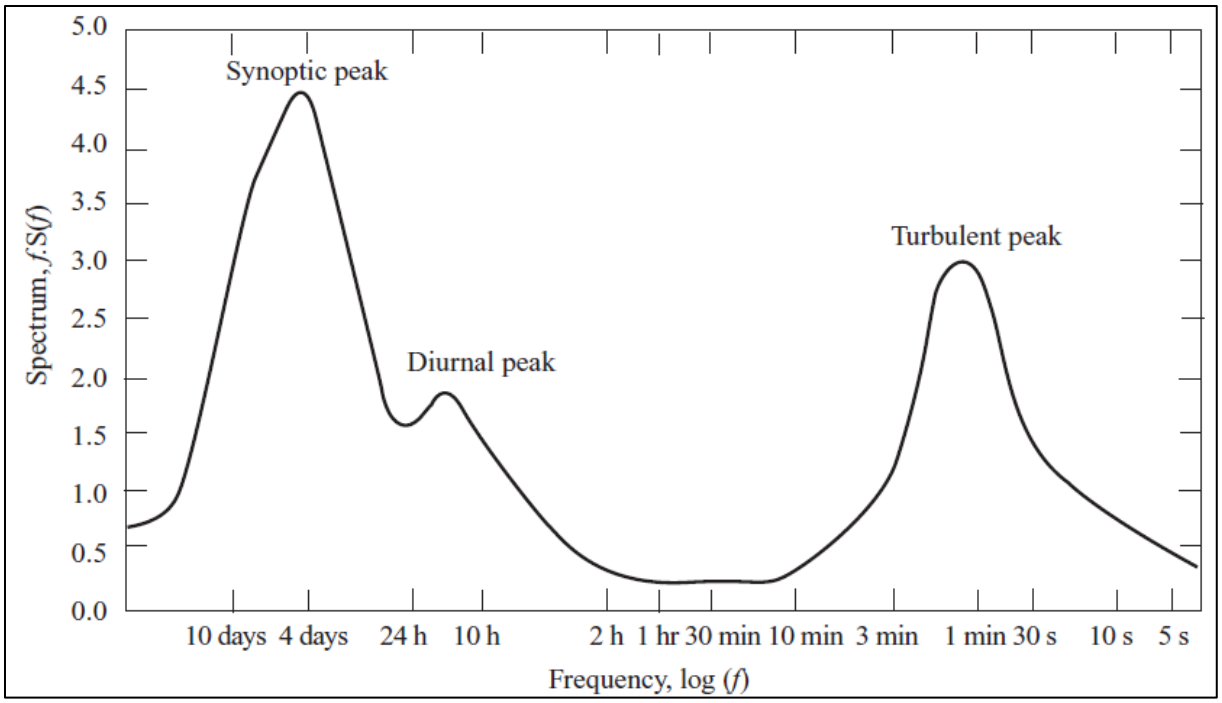

Figure 72: The energy density spectrum of the wind data. Ref. [11]

However, in comparison to the regular time series analysis, it has some limitations as well. Some of the limitations of this spectral analysis of the time series which are as follows,

1. Peak frequency switches depending upon the time series.
2. Also depends upon the number of blocks or frequency resolutions. If the frequency resolution is higher we can obtain more peak frequencies.
3. The more the number of frequency bands, the lesser will be the energy associated with each frequency.
4. As it is biased towards the higher frequencies (the spectral mean is somewhat different from the mean obtained through a regular time series analysis.

In short, the estimate of the return period depends upon the width of the spectrum.

REFERENCES

[1] J. Manwell, A. Rogers, Wind Energy Explained_ Theory Design and Explanations, Second Edition.

[2] Vlies, D., Wind Speed Measurements: An Elaboration on Different Methods. Delft University of Technology.

[3] Salzmann, C., Tempel, D. 2004. The Impact of Different Wind and Wave Data Sources on the Fatigue of Offshore Wind Turbines. Offshore Engineering Group, Delft University of Technology.

[4] Kouwenhoven, H. J., 2007. User Manual Data Files Meteorological Mast, NoordzeeWind, NZW-16-S-4-R03.

[5] Eecen, P. J., Meteorological Measurements at OWEZ: Half year report (1-07-2007 to 31-12-2007), Energy research Center of the Netherlands, ECN-E--08-061.

[6] Eecen, P. J., Branlard, E., The OWEZ Meteorological Mast: Analysis of Mast top displacements, Energy research Center of the Netherlands, ECN-E--08-067.

[7] Holtslag, M., OWEZ Data-Analyses, Tower Shadow effects (to be published).

[8] Werkhoven, E. J., Verhoef, J. P., ECN-Wind Memo-12-010: Offshore Meteorological Mast Ijmuiden_ Abstract of Instrumentation Report, 2012.

[9] www.cesar-database.nl

[10] Cabauw Experimental Site for Atmospheric Research (CESAR) – The Netherlands: An initial Gruan Atmospheric Profiling Station by R. Boers, F. Bosveld, W. Knap et al. February 2009.

[11] Steele, C. J., Dorling S. R., Bacon J., (2015). Modelling Sea Breeze climatologies and interactions on coasts in the southern North Sea: Implications for Offshore wind energy. *Quarterly Journal of the Royal Meteorological Society, (Vol. 141).*

[12] H. V. Storch, F. Zwiers, Statistical Analysis in Climate Research, (1st edition, 2003).

[13] V. Gupta, Fluid Mechanics and Its Applications (3rd Edition, 2012).

[14] Bierbooms, W., Larsen, G., 2003. Mean gust shapes, Riso National Laboratory, Roskilde, Denmark, Ris-R-1133(EN).

[15] Alexander D. Poularikas, The Transforms and Applications Handbook, (2nd Edition, 1996), CRC Press.

[16] N. Jenkins, T. Burton, Wind Energy Handbook, 2001.

[17] IEC standards 61400-1: Wind Turbines_ Design Requirements, 2005.

[18] National Weather Service Southern Region Headquarters, http://www.srh.noaa.gov/srh/dad/sfc/chapter2.pdf

[19] H.P. Waldl F. Boettcher, J. Pienke, On the statistics of wind gusts, Boundary Layer Meteorology (Vol. 108), August 2002.

[20] St. Barth F. Boettcher, Small and Large scale fluctuations in atmospheric wind speed, Jun. 2005.

[21] ECN Report_ Wind Energy: On the statistics of gusts and their propagation through a wind farm by Emmanuel Branlard, February 2009.

[22] Leo H. Holthuijsen, Waves in Oceanic Coastal Waters, 2007.